NASA

National Aeronautics and
Space Administration

Document No. TR-682-001
Date March 1, 1993

Test Report

APU Diaphragm Testing

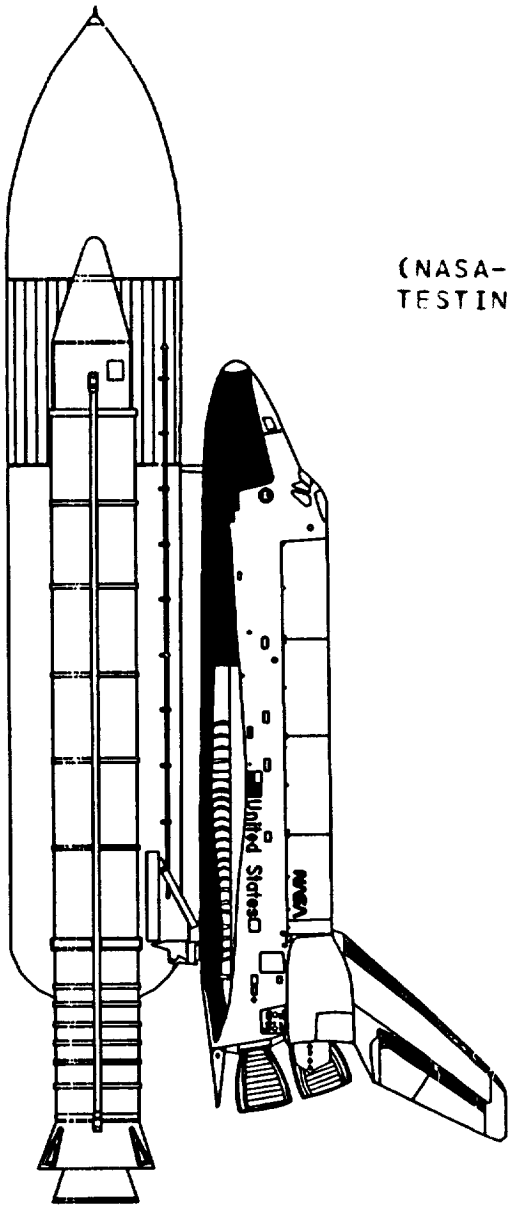

Lyndon B. Johnson Space Center
White Sands Test Facility
P. O. Drawer MM
Las Cruces, NM 88004
(505) 524-5011

Test Report

APU Diaphragm Testing

Issued By
National Aeronautics and Space Administration
Johnson Space Center
White Sands Test Facility
Laboratories Office

Prepared By: Richard Shelley
Richard Shelley
Lockheed-ESC

Prepared By: William L. Ross, Sr.
William L. Ross, Sr.
Lockheed-ESC

Concurred By: David W. Young
David Young
NASA Propulsion and Power Division

Reviewed By: David L. Baker
David L. Baker
NASA Laboratories Office

Approved By: David L. Baker for
Frank J. Benz, Chief
NASA Laboratories Office

Abstract

The Auxiliary Power Unit (APU) fuel (hydrazine) tanks were removed from the Columbia Shuttle during major modification of the vehicle, because of long-term hydrazine compatibility concerns. The three tanks had been in service for 11 years. As part of an effort to determine whether the useful life of the fuel tanks can be extended, examination of the ethylene propylene rubber (EPR) diaphragm and the metal casing from one of the APU tanks was required. NASA Johnson Space Center Propulsion and Power Division requested the NASA Johnson Space Center White Sands Test Facility to examine the EPR diaphragm for signs of degradation that might limit the life of its function in the APU tank and to examine the metal casing for signs of surface corrosion. No appreciable degradation of the EPR diaphragm was noted. A decrease in the tensile properties was found, but tensile failure is considered unlikely because the metal casing constrains the diaphragm, preventing it from elongating more than a few percent. The titanium casing showed no evidence of surface corrosion.

Contents

Contents, Continued

List of Tables

Glossary

A49197	Designation for APU tank that had only the hydrazine examined
A49198	Designation for APU tank that had hydrazine and materials of construction examined
AF-E-332	Compound designation of the EPR material under test
APU	Auxiliary Power Unit
a/o	Atomic percent
ASTM	American Society for Testing and Materials
C	Clockwise
D	Down
DI	Deionized water
EPR	Ethylene propylene rubber
EPR diaphragm	diaphragm made of EPR AF-E-332 material that had been exposed to hydrazine
ESCA	Electron spectroscopy for chemical analysis
EDS	Energy dispersive x-ray spectroscopy
HRC	Hardness on the Rockwell C scale
FTIR	Fourier transform infrared
JSC	Johnson Space Center
KHN	Knoop hardness number
OV	Orbiter vehicle
P/N	Part number
PPD	Propulsion and Power Division
PSI	Pressure Systems, Inc.
S/N	Serial number
σ_{n-1}	Sample standard deviation
T_g	Glass transition temperature
TGA	Thermogravimetric analysis
TMA	Thermomechanical analysis
Unexposed EPR	EPR AF-E-332 material made in 1984 that had not been unexposed to hydrazine and was used as a comparison with the EPR diaphragm
WSTF	White Sands Test Facility

1.0 Introduction

The Auxiliary Power Unit (APU) fuel (hydrazine) tanks were removed from the Columbia Shuttle (OV-102) during major modification of the vehicle, because of long-term hydrazine compatibility concerns. The three tanks were in service for 11 years.

As part of an effort to determine whether the useful life of the fuel tanks can be extended, examination of the ethylene propylene rubber (EPR) diaphragm and the metal casing from one of the APU tanks was required. The NASA Johnson Space Center (JSC) Propulsion and Power Division requested the NASA JSC White Sands Test Facility (WSTF) to examine the EPR diaphragm and the metal casing from one tank.

2.0 Objectives

The objectives were to examine the EPR diaphragm for signs of degradation that might limit the life of its function in the APU tank and to examine the metal casing for signs of surface corrosion.

3.0 Background

WSTF received the three tanks removed from OV-102. One tank was tested to determine any measurable degradation in the diaphragm material and any signs of surface corrosion in the metal casing.

The examination results are useful because the other orbiters have tanks that are generally newer than those from OV-102, and the tanks might not have to be replaced as soon as presently planned if insufficient signs of degradation are found in the OV-102 tank. Two OV-103 tanks are 7 years old and one tank (S/N 0004) is 14 years old (6 years of which it has been dry). The three OV-104 tanks are all 6 years old.

The diaphragm in the orbiter fuel tank has to be flexible, thus an elastomeric material was chosen. Several studies had been performed on different elastomers for their suitability for use with hydrazine (Coulbert, Cuddihy, and Fedors 1973; Martin and Sieron 1977; Repar 1970 and 1973; Sheets 1974; Takimoto and Denault 1969; Yee and Etheridge 1985). Takimoto and Denault (1969) found that elastomers containing carbon black increased degradation of hydrazine. Repar (1970, 1973) found that silica (SiO_2) fillers produced compounds that were more suitable for use in hydrazine. The base materials used in the test compounds were butyl and ethylene propylene terpolymer rubbers.

Sheets (1974) tested EPR AF-E-332, a newly developed polymer, that was based on an ethylene propylene terpolymer. This compound was found to be more resistant to hydrazine than the previously tested compounds.

Further testing of EPR AF-E-332 with hydrazine was performed (Coulbert, Cuddihy, and Fedors 1973; Martin and Sieron 1977; Yee and Etheridge 1985). These works tested for permeation of propellant, compression set of seal bead, swelling, and tensile property retention, as well as posttest appearance of the EPR diaphragm, potential leakage or pull-out

of different seal bead designs, pressure fluctuations, and chemical composition of the posttest propellant.

Lifetime predictions for EPR in hydrazine have been attempted using Arrhenius and Williams Landel Ferry models (Coulbert, Cuddihy, and Fedors 1973; Martin and Sieron 1977), but none has been thoroughly demonstrated as correlating and predicting long-term behavior. The diaphragm material is given a shelf life of up to 10 years (MIL-HDBK-695C 1985; MIL-STD-1523A 1984), although the shelf life is not based on scientific data (Boyum and Rhoads 1990). Reports indicate that EPR AF-E-332 is unaffected by up to 10 years of exposure to hydrazine (Gill 1986; Repar 1973). The nominal lifetime of the APU tanks was previously 10 years, but it has been extended by 2 years to 12 years.*

Aging of an elastomer material is usually caused by several mechanisms: chemical attack resulting in cross-linking or chain scission of the polymer chains, physical relaxation of the polymer arising from stress, and change in the compound when ingredients bleed to the surface or are leached out by contacting fluids.

Increased cross-linking has the reverse effect of chain scission; it causes the polymer to become harder, with a higher tensile strength and lower elongation (less flexible, more brittle). Relaxation of the polymer will increase compression set. Change in the compound changes the properties of the original compound; for example, removal of a plasticizer from an elastomer compound would result in a material with higher hardness, higher tensile strength, and lower elongation.

Because one of OV-103's tanks has been dry for six years, it is important to know whether significant diaphragm degradation occurs under ambient conditions. All the aging mechanisms except leaching could occur under ambient conditions as well as in hydrazine, so it is possible that the elastomer, if degraded by the hydrazine, could undergo similar degradation under ambient conditions. However, previous studies and case histories have shown that many elastomers (including EPR) either do not require a shelf life or do not age detectably under ambient conditions for up to 22 years (Bellanca and Harris 1967; Boyum and Rhoads 1990; House 1972; Rubber Manufacturer's Association 1966; Sullivan 1966; Young 1960).

The most important properties of the EPR diaphragm are compression set, hardness, specific gravity, tensile properties, and chemical content.

Compression set is important to the EPR diaphragm because it determines the sealing ability and therefore the ability of the seal bead to hold the hydrazine. Hardness is a sign of change in the elastomer properties caused by contact with the hydrazine. Specific gravity indicates changes in the elastomer ingredients. An elastomer compound consists of materials of different specific gravities. By knowing the amount and specific gravity of each ingredient in the compound, the compound specific gravity can be calculated fairly accurately. Any ingredients lost during exposure to hydrazine may result in a detectable change in specific gravity. Tensile properties are important to the EPR diaphragm because it is under tensile forces during use, but it is also constrained by the metal casing, making tensile failure

*Presentation by W. Scott. "OV-102 APU System Hardware Disposition." NASA, Propulsion and Power Division, May 1, 1991.

unlikely. Chemical content, like specific gravity, indicates changes in elastomer ingredients and thus changes in elastomer properties. To determine changes in elastomer ingredients another way, thermal analysis determines both ingredient change/loss and embrittlement or hardening.

The effect of hydrazine on metals and metal surfaces is generally analyzed by determining the corrosion product on the metal surface. Specifically for Ti-6Al-4V (the material from which the metal casing is constructed), titanium nitride, nitrogen, and ammonia usually would be deposited. Auger electron spectroscopy for chemical analysis (ESCA) studies on the sample surface could reveal some of these deposits. However, this detection technique has some inherent problems. The principle problem is that the Auger peaks for titanium, titanium nitride, and nitrogen overlap and are extremely difficult to decipher. Therefore, other surface techniques might need to be applied to determine the corrosion products.

For example, some metals are known to exhibit stress corrosion cracking when exposed to hydrazine for an extended period of time. To determine evidence of stress corrosion cracking, samples would need to be prepared for microstructure evaluation. Intergranular or transgranular cracking might be easily visible with this technique. Both corrosion of the metal surface and stress corrosion cracking can be observed by using optical and scanning electron microscopy.

4.0 Approach

The tank (APU A49197) found by X-ray to contain the most fluid of the three test tanks had the hydrazine from the gas side drained, analyzed and quantified. The tank with the most service cycles (A49198) was chosen for dissection and materials analysis on the EPR diaphragm and metal casing.

Testing of the EPR diaphragm was based on previous tests of materials immersed in hydrazine (Takimoto and Denault 1969; Repar 1970 and 1973; Sheets 1974; Coulbert, Cuddihy, and Fedors 1973; Martin and Sieron 1977; Yee and Etheridge 1985). Visual examination, microscopic analysis, thickness measuring, hardness testing, specific gravity measuring, tensile testing, chemical analysis, and thermal analysis were performed on the EPR diaphragm and on samples of EPR that had not been exposed to hydrazine (unexposed EPR).

Properties of the tested EPR diaphragm were compared with the tank manufacturer's compound property specifications, shown in Table 1, and also with the properties of unexposed EPR. Any changes were discussed in reference to the literature.

The metal casing was examined for any signs of surface corrosion. A complete visual examination (both outer and inner shell surfaces), hardness testing, thickness measurement and metallographic analysis (conventional, scanning electron microscopy [SEM], and ESCA) were performed on the samples. Samples taken included both base metal and weld seam locations in addition to any areas where anomalies were noted.

Test data were compared with both the data published by the manufacturer, Pressure Systems, Inc. (PSI 1977) and the applicable manufacturing specification (MIL-T-9047E, Comp. 6).

5.0 Experimental Materials

The system to be tested was APU Tank A49198 from OV-102, with an approximately 71-cm-diameter EPR diaphragm and a metal casing manufactured by PSI.

5.1 EPR

The EPR AF-E-332 compound is based on ethylene-propylene terpolymer rubber (Nordel 1635 EPT). The ingredients are listed in Table 2.

The following EPR materials were tested:

- **Unexposed EPR** (WSTF # 91-25134 and 91-25436). Two pieces of material were cut from P/N 80-228007, S/N 0071, which was molded in July 1984. Neither sheet had been exposed to hydrazine.
- **EPR diaphragm** (WSTF # 91-25361). This was the EPR diaphragm from the 11-year-old APU Tank A49198

The EPR materials were designated EPR AF-E-332 compound that meets MIL-R-83412A specifications (1977). Table 1 lists the manufacturer's design criteria of the diaphragm material. The mechanical properties of the unexposed EPR from the literature are given in Table 3 (Sheets 1974; Yee and Etheridge 1985).

5.2 Metal Casing

The metal casing of the OV-102 APU fuel tank is constructed of Ti-6Al-4V; this is an alpha beta titanium alloy typically containing 6-percent aluminum and 4-percent vanadium. Construction is of two hemispheres (equipped with inlet/outlet orifices at the poles) welded together at their circumferences. It is equipped with an internal ring located at the hemispherical circumference, which acts as

- A backing ring for the circumferential weld seam
- An element of the interior EPR diaphragm lip seal groove

The method of manufacture is generally closed-die hot forging to a hemispherical shape using wrought forging stock (billet). This is followed by heat treatment to achieve the specified physical properties. The heat treatment is composed of a solution treatment below the beta transformation temperature (typically 954.4° C), water quenching, and then aging at an intermediate temperature (typically 537.8° C). It is then machined to final shape after testing.

The chemical requirements of this alloy designation are shown in Table 4, which was taken from MIL-SPEC-T-9047E. These are similar to the chemical requirements of the current ASTM Designation B 381, Grade F-5.

Further details of the tank assembly construction are given in Table 5 and Figure H-1.

6.0 Experimental Procedures

The following tests were conducted on both the unexposed EPR (WSTF # 91-25134 and 91-25436) and the EPR diaphragm (WSTF # 91-25361).

6.1 Hydrazine

6.1.1 APU Tank A49197

Hydrazine from the gas side of APU Tank A49197 was removed, quantified, and analyzed for filtrate particle count and fuel purity. This tank was not further examined.

6.1.2 APU Tank A49198

X-ray had indicated little or no hydrazine remaining in this tank, so any hydrazine possibly remaining between the EPR diaphragm and the metal casing in APU Tank A49198 was measured by analyzing a measured deionized (DI) water rinse. The DI water rinse was also filtered and analyzed for particle count.

6.2 EPR

After the particle count was completed, APU Tank A49198 was cut in half to remove the EPR diaphragm.

6.2.1 Visual Examination

The EPR diaphragm was examined inside and outside for blemishes, cracks, discolorations, and any other distinguishing features. Cracks may have formed at or near the weld bead or at other places of high stress concentrations, or the material may have discolored on exposure to hydrazine. Color, frequency, size, shape, position, and any other noticeable characteristics of any distinguishing features were noted and photographed.

6.2.2 Sampling

Samples were cut from the unexposed EPR and the EPR diaphragm for all the tests as shown in Appendix A and Figures H-12 through H-14. The EPR diaphragm was partitioned into zones and laid out for sample preparation as shown in Figures A-1 and A-2. This zoning allowed a near-sample location retest in the event of a questionable test result. Samples of the unexposed EPR were taken as shown in Figures A-3 and A-4.

6.2.3 Microscopic Analysis

Sections of the EPR diaphragm were examined with a stereo microscope at magnifications of 10 to 15 times. Other sections of the EPR diaphragm were microtomed in liquid nitrogen and examined under a transmission bright field microscope to identify pigment and ingredient dispersion characteristics. The samples of the EPR diaphragm were compared with samples of the unexposed EPR.

6.2.4 Thickness Measurements

Thickness measurements were taken on the diaphragm seal lip to examine the change and uniformity of thickness around the circumference of diaphragm. These measurements provide information concerning the sealability of the diaphragm.

To calculate a range of thickness changes, 44 thickness measurements were taken around the seal bead of the EPR diaphragm (5 cm apart) and samples of the unexposed EPR and

percentage thickness change calculations were made, both according to ASTM D 395, sections 12 through 14. The original thickness of the material was obtained from historical records.

6.2.5 Compression Set Tests

Compression set testing also provides data relevant to the sealability of the elastomer. A higher value indicates a lower sealability. Compression set tests were performed on the unexposed EPR and the EPR diaphragm according to ASTM D 395 Method B, which is for constant deflection. Compression time was 22 hours at 70° C.

6.2.6 Hardness Tests

Hardness is an important measurement; seals usually will perform optimally only if in a specified hardness range. A change in hardness is often an indication of degradation. The type A durometer was used to perform hardness tests on samples of the unexposed EPR and on areas throughout the inside and outside of the EPR diaphragm according to ASTM D 2240.

6.2.7 Specific Gravity Measurements

Specific gravity changes can indicate loss of compound ingredients by comparing test values with values of original materials. Samples were measured for specific gravity by the water immersion method (ASTM D 792).

6.2.8 Tensile Tests

Tensile testing was performed because the diaphragm may be under tension during service. The diaphragm, however, is constrained by the metallic outer casing and is therefore subject, at most, to a few percent of strain. Although tensile failure is not considered a likely failure mode, tensile properties serve as a useful measure of comparison with original tensile properties.

Dogbone samples of unexposed EPR and the EPR diaphragm were tested for tensile strength. ASTM D 412 was used as the standard, with Die D defining the dogbone sample size. The grip separation rate was 500 mm/min. Tensile strength, elongation, and 100-percent modulus of samples of the EPR diaphragm were calculated according to the standard and compared with values from the unexposed EPR.

6.2.9 Chemical Analysis

The diaphragm material was analyzed for any chemical change that might have occurred as a result of exposure to hydrazine, for example, chemical modification of the chain or loss of plasticizer or other ingredients.

Material from the EPR diaphragm was microtomed to obtain samples at various distances from the surface in contact with hydrazine. These samples and samples of the unexposed EPR were then analyzed with Fourier transform infrared (FTIR) spectroscopy.

6.2.10 Thermal Analysis

Thermal gravimetric analysis (TGA) gives weight loss versus temperature. It indicates the quantity of, at what temperature, and which compound products are being lost by the material. Samples for thermal analysis were taken the unexposed EPR and from representative areas of the EPR diaphragm and were heated at 10° C per minute in ambient air to 700° C.

Material embrittlement was measured as a function of temperature using thermal mechanical analysis (TMA). The glass transition temperature (T_g) of EPR also changes as a function of the plasticizer content; the T_g's of the unexposed EPR and the EPR diaphragm were measured with TMA at subambient temperatures.

6.3 Metal Casing

6.3.1 Visual Examination

After dissection, the APU fuel tank casing was completely visually examined for any signs of surface corrosion, such as stains, discolorations, and cracks. Any such sign noted was photographed along with general interior views.

6.3.2 Sampling

Two base metal samples, 180° apart, were removed from each tank half. The two pairs were 90° out of phase with each other. In addition, two weld seam samples were removed from the gas-side half, 90° out of phase with the base metal pair taken from that half. One weld sample contained the weld start/stop point, which was the most unstable weld condition. The other weld sample, taken 180° away, represented the most stable weld condition. Sample locations are shown on the sample layout plan in Appendix G (Figure G-1).

All samples taken were documented in relation to several permanent punch marks made in the two casing halves, which corresponded to a notch in the EPR diaphragm. In this way, all metal sample locations could be related to a corresponding location on the EPR diaphragm. Location designations were given in inches measured clockwise (C) from the notch on the casing rim (or corresponding diaphragm lip) and down (D) from the respective center or rim of either hemisphere.

In addition, samples taken from any interior surface location containing noted surface anomalies were given location designations according to the above procedure.

The samples were cut with carbide cutters either flushed with sufficient inert coolant to prevent overheating or paced to prevent frictional heat buildup.

6.3.3 Metallographic Analysis

Samples taken were metallographically prepared (as required) and examined by optical microscopy. SEM was used to assist in further, more definitive analysis.

6.3.4 Hardness Testing

The hardness tests were performed on both the inner and outer surface of the metal casing at each location using a conventional Rockwell C-type tester for surface hardness determinations.

For microstructural analysis, Knoop microhardness measurements were taken at two locations in accordance with ASTM E 384, using a Wilson Tukon hardness tester model B240 manufactured by Wilson Instruments Inc., Binghamton, NY. These measurements were taken at two locations on the weld seam. One was located at the weld seam start/stop point and the other 180° from the first. These measurements were taken for the base metal, heat-affected zone, and weld (melted) material for both the shell and the corresponding attached backing ring at each location for comparison. While a meaningful comparison to the metal casing Rockwell C measurements cannot be made, this testing was performed to establish an indication of process uniformity.

6.3.5 Thickness Measurements

Thickness measurements were taken at selected locations on both halves. To facilitate readings, ultrasonic thickness measurement equipment was used. Care was taken to ensure readings were taken at locations where the inner and outer surfaces were parallel. All thickness measurements were compared with the published data for part number V070-465205-001 (PSI 1977).

7.0 Results

7.1 Hydrazine

7.1.1 APU Tank A49197

Tables 6 and 7 show the particle count and the fuel analysis, respectively. Three particles from the gas-side filtrates were analyzed and were found to contain the following elements:

Particle 1: Cr, Fe, Mn, Ni
Particle 2: Fe, Zn
Particle 3: Mo, S

7.1.2 APU Tank A49198

The DI water rinse particle count and filters are shown in Table 8 and Figure H-2 respectively. Five particles from the gas-side filtrates were analyzed and were found to contain the following elements:

Particle 1: Al, Si, Cl, K, Fe, Zn
Particle 2: Al, Si, S, Cl, K, Ca, Ti, Cr, Fe, Cu, Zn
Particle 3: Mg, Al, Si, K, Ca, Ti, Fe, Zn
Particle 4: Al, Si, S, Cl, Ca, Fe, Cu, Zn
Particle 5: Al, Si, S, Cl, Ca, Ti, Cr, Fe, Cu, Zn

Four particles from the fuel-side filtrates were analyzed and were found to contain the following elements:

Particle 1: Ti, Cr, Mn, Fe, Ni
Particle 2: Si, P, Cd, Ca, Ti, Cr, Mn, Fe
Particle 3: Si, Cr
Particle 4: Al, Si, Cd, Ca, Fe

7.2 EPR

7.2.1 Visual Examination

No cracks or mechanical damage were observed on the EPR diaphragm. The gas side of the EPR diaphragm remained unmarked. The fuel side was darker for approximately half the area; the other half was light brown (see Figures H-3 through H-5 in Appendix H). Local discolorations were recorded and are shown in Figures H-6 and H-7. Figures H-8 through H-11 show the diaphragm lip area. Particles from the dark grey areas on the EPR diaphragm were found to contain Fe, Ca, and Si; particles from the brown area were found to contain Ca.

7.2.2 Microscopic Analysis

No cracks were discernible in the microstructure using the transmission bright field or the stereo microscopes in the magnification range of 15 - 40 times. No marked surface phenomena were on the cross sections through the EPR diaphragm wall nor was any evidence of uneven pigment dispersion present, and no gross differences were evident between the unexposed EPR and the EPR diaphragm.

7.2.3 Thickness Measurements

The mean of the seal bead thicknesses was 0.361 cm. This mean corresponded to 94.4 percent of the original thickness (0.381 cm). The sample standard deviation (σ_{n-1}) for the data set was 0.015 cm. Figure H-8 shows the sealing bead in relation to the sealing configuration.

The minimum thickness measured was 0.33 cm (86.7 percent of the original). Comparison with PSI information showed that the lip was compressed between 12 - 15 percent (PSI 1977). The metal surface in contact with the EPR diaphragm lip was profiled with serrations to give more effective sealing. The original PSI tolerance for the seal lip thickness was $\pm$ 0.015 cm.

7.2.4 Compression Set Tests

The results are in Table 9. According to ASTM D 395, concerning the repeatability for a mean value of 13.7 percent compression, two results are considered significantly different if their difference as a percentage of their mean value is 1.67 percent compression.

7.2.5 Hardness Tests

A summary of the results is in Table 10, and further detailed results are given in Appendix B. According to ASTM D 2240, concerning repeatability and based on a 95-percent confidence interval, two results are considered significantly different if their difference as a percentage of their average exceeds 3.29 percent.

7.2.6 Specific Gravity Measurements

Table 11 gives the results of the specific gravity tests. ASTM D 792 states that, concerning repeatability, in comparing two mean values for the same material obtained by the same operator using the same equipment on the same day, the means should not be judged equivalent if they differ by more than the repeatability value (0.0153 was chosen in this instance).

7.2.7 Tensile Tests

A summary of the results is in Table 12, and further detailed results are given in Appendix C. ASTM D 412 gives information on repeatability for tensile properties in tension. Two single test results obtained under normal test procedures that differ by more than the repeatability value must be considered as derived from different or nonidentical sample populations; these values are 1.3 MPa (ultimate tensile strength), 17.8 percent (elongation), and 1.4 MPa (100-percent modulus).

7.2.8 Chemical Analysis

The FTIR peaks were assigned relative values as shown in Table 13. Appendix D contains the FTIR spectra for the samples.

7.2.9 Thermal Analysis

The results of the TGA testing are in Table 14, and the TGA traces and detailed additional data are in Appendix E. ASTM E 1131 gives guidelines for repeatability and reproducibility of testing by this method for medium volatile material (the percent EPR, polybutene, and PTFE in the compound). Repeatability is applicable here because all the tests were performed on one instrument by the same operator. Differences in averages exceeding 2 percent are considered significant (95-percent confidence interval). The repeatability figure for the total inorganic content is approximately 1.3 percent.

The results of the TMA testing are in Table 15. The TMA traces and further detailed results are in Appendix F. ASTM E 1363 states that repeatability (single analysis) should be 2.14° C. Two averages should be considered different if the temperature measurement difference is greater than 2.14° C.

7.3 Metal Casing

7.3.1 Visual Examination

No visual evidence of corrosion was observed on either the interior or exterior surfaces of the APU fuel tank metal casing. Several anomalies in the forms of stains, discolorations, and grind/polish marks were observed and photographed (see Figures H-15 through H-31). SEM analysis of the areas of stain, discoloration and grind/polishing disclosed no deleterious effects. Microscopy of the deep grind marks in the cross section revealed no evidence of either a sharp notch or crevice-type corrosion.

7.3.2 Metallographic Analysis

Metallographic analysis of the metal casing found no evidence of corrosion. The microstructure is a fine-grained alpha beta structure indicative of a traditional solution treatment below the beta transus followed by aging at an intermediate temperature. No evidence was observed of any stress corrosion cracking.

One anomaly observed was marks on the inner surface of the casing that translated into a mirror image of the EPR diaphragm rib arrangement, presumably caused by fuel drying. These marks were visible both visually and at higher optical magnifications. SEM coupled with energy dispersive X-ray spectroscopic (EDS) analysis revealed a trace amount of iron, estimated at 0.5 percent by weight. A follow-up analysis by ESCA indicated the presence of 9.27 atomic percent (a/o) of iron present in the discoloration. The discoloration is included in an oxide layer measured at approximately 800 Å thick. Normal surface oxide layers measure approximately 200 Å thick. A complete comparative analysis is in Table 16. The source of this iron is suspected to be the ancillary stainless steel support piping systems.

7.3.3 Hardness Testing

Results of the Rockwell C testing are summarized in Table 17, and results of the Knoop microhardness (KHN) testing are summarized in Table 18. As stated in the procedures, while a meaningful comparison of the Rockwell C measurements and the KHN measurements cannot be made, the KHN results are shown to establish an indication of process uniformity.

7.3.4 Thickness Measurements

The thickness measurements are in Table 19. These values were found to be in close conformance with the manufacturer's published results (PSI 1977).

8.0 Discussion

The analysis of hydrazine from APU Tank A49197 showed a slightly high particle count (see Table 6).* The purity, water content, isopropyl alcohol content, and CO_2 content were all out of specification per MIL-P-26536D. The high CO_2 level was indicative of exposure to air.

Both the brown and dark grey discolorations of the fuel side of the EPR diaphragm from APU Tank A49198 were evidently caused by a mechanism not present on the gas side. Chemical analysis showed that the brown discoloration was rich in calcium; this is most likely calcium oxide leached out from the EPR diaphragm. The dark grey areas were found to contain calcium as well as iron and silicon. The silicon could have come from the EPR diaphragm, and iron could have come from the trace amount of iron in the metal shell; it is more likely that the iron came from the construction materials of the feed systems. Particles found in the filtrate from the fuel side of APU Tank A49198 contained titanium, aluminum, and iron, obtainable from the casing material; silicon and calcium, obtainable from the diaphragm material; and chromium, manganese, nickel, phosphorus, and cadmium, all of which must be

*Smith, I. D. *Chemical/Cleanliness Requirements for WSTF Test Hardware and Facility Equipment.* NASA Spec 022, NASA Johnson Space Center White Sands Test Facility, NM, 1987.

from external sources. Particles from the filtrates of the gas side of both tanks were similar to the particles from the fuel sides, except that they usually contained zinc, which could have come from the diaphragm material. Microscopic analysis showed no difference near the fuel side that would mark ingredient depletion. The discoloration itself is not an indication of degree of degradation; it is a phenomenon, but the extent to which it affects properties is unknown.

The thickness measurements were made around the circumference of the EPR diaphragm to examine the uniformity and the thickness relative to the original thickness. According to PSI, the seal lip was compressed in the range of 12 - 15 percent. The average thickness measurement of 94.4-percent original thickness was well above this. The minimum thickness of 86.7-percent original thickness is in the 12 - 15 percent range. However, the serrations designed into the adjacent metal profile would cause some unevenness in thickness. PSI technical personnel indicated that this minimum thickness is not a problem when considering the seal design.

The original PSI tolerance on thickness variation was $\pm$ 0.015 cm about 0.381 cm. The variation in the measured thickness values was $\pm$ 0.031 cm about the mean; this was expected after the uneven compression that was applied to the seal lip.

More information on the sealability of the diaphragm material was obtained from the compression set testing. The lower the calculated compression set, the better the retained sealing force in the material. Both the unexposed EPR and the EPR diaphragm had compression set values within the specification value. The EPR diaphragm, in fact, had a lower compression set value than the unexposed EPR, indicating better sealability; the reason for the lower compression set value is unknown.

The hardness values for both the unexposed EPR and the EPR diaphragm were within the 90 $\pm$ 5 Shore A specification. The specific gravities for both materials were also close to the PSI comparison values.

The tensile testing showed that the unexposed EPR were within the PSI specification; the EPR diaphragm was within specification for the 100-percent modulus value. It was 97.4 percent of the minimum required ultimate tensile strength, and 86.5 percent of the minimum required elongation. The minimum required values set by PSI are arbitrary values set so the material can meet a required level of consistency in quality. In the application of an EPR diaphragm, the material is unlikely to be subjected to tensile strains greater than a few percent because it is constrained by the metallic casing. In the literature, Yee and Etheridge (1985) noted a decrease in tensile properties of 15 to 30 percent of EPR diaphragm material; they suggested that no loss of functionality would occur as a result of the decrease in tensile properties. Testing in this report showed a drop in tensile properties of only 14 to 24 percent when comparing the EPR diaphragm to unexposed EPR, less than that found by Yee and Etheridge. The drop in the ultimate tensile strength and elongation may thus be viewed as tolerable. The testing reported herein was unable to determine the time scale of decrease in the tensile properties (that is, whether the decrease occurred in the first few years or gradually over the life of the EPR diaphragm).

The FTIR results through cross sections of the EPR diaphragm wall showed no anomalies or signs of new peaks (corresponding to chemical reactions) when compared with the FTIR results from the unexposed EPR. Relative peak sizes were also similar. FTIR spectra of samples at various depths into the wall of the EPR diaphragm showed that the material near

the fuel side was not detectably different when compared with the sample in the center of the wall and on the gas side.

The TGA showed no gross differences in compound ingredients between the unexposed EPR and the EPR diaphragm. Both materials showed slightly low PTFE and slightly high inorganic residue contents when compared with the PSI compounding specification. The EPR diaphragm showed a slightly low CaO level.

The TMA results showed that the thermal transition measurements were similar for the unexposed EPR and the EPR diaphragm, indicating that the visco-elastic characteristics of the EPR diaphragm remained the same. While the T_g values were more or less independent of sample thickness in the experimental range, the modulus values were dependent of thickness; shape factor of rubbers determines modulus and is given by $R/2T$, where R is the radius of loaded area, and T is the thickness of sample (Freakley and Payne 1978). The standard deviations for the modulus values are consequently high because of the varying sample thicknesses.

The titanium alloy casing showed no evidence of surface corrosion attack. All other metallic properties examined (hardness, microstructure, etc.) appear to be in conformance with this alloy grade in the specified heat treatment condition.

The few anomalies observed proved to be harmless stains and polishing marks, confirmed by a thorough visual examination and both optical microscopy and SEM. An example was the observed markings on the fuel side of the metal casing, which were identified as corresponding to the EPR diaphragm ribs. The origin of these markings appears to be related to an interaction between the fuel, the EPR diaphragm, and the metal casing with a discoloration being deposited on both the EPR diaphragm and the metal casing selectively at the EPR diaphragm rib/casing contact points. The deposition mechanism may be associated with a drying out of the fuel-side contents (fuel and entrained contaminants). EDS and ESCA analysis indicated that iron had built up in the surface oxide layer of the fuel-side metal casing at the locations of these markings.

9.0 Conclusions

No appreciable degradation of the EPR diaphragm that might limit the life of its function in the APU tank was noted. A decrease in the tensile properties was found, but tensile failure is considered unlikely because the metal casing constrains the diaphragm, preventing it from elongating more than a few percent. The metal casing showed no signs of surface corrosion.

Table 1
Manufacturer's Compound Specifications for EPR AF-E-332

Property	Required Value	Standard Used For Testing
Compression Set	22% Max	ASTM D 395, Part B[a]
Hardness	90 ± 5	Shore A
Specific Gravity	1.07	Not Applicable
Tensile Strength	11.4 MPa (min.)	ASTM D 412[b]
Elongation	230% (min.)	ASTM D 412
100% Modulus	6.6 MPa (min.)	ASTM D 412
Tear Strength	525 N/cm (min.)	ASTM D 624[c]

[a]22 hours at 70°C
[b]Die D, 50.8 cm/minute
[c]Die B, nicked crescent

Table 2
EPR AF-E-332 Ingredients

Ingredients	Manufacturer	Parts by Weight	Specific Gravity
Nordel 1635 EPT	DuPont	100	0.86
Aerosil R972	Degussa	30 ± 1.5	1.95
B-3000 Resin	Dynachem Corp.	20 ± 1.0	0.90
Teflon Powder T-8A	DuPont	10 ± 0.3	2.15
Zinc Oxide Reagent	Baker	5 ± 0.2	5.57
Calcium Oxide Reagent	Baker	5 ± 0.2	2.20
Luper 101 Peroxide (Curing Agent)	Wallace and Tiernan	0.9 ± 0.2	1.00

Table 3
Mechanical Properties of EPR AF-E-332

Property	Value
Tensile Strength	12.4 MPa
Elongation	253%
Specific Gravity	1.08
Compression Set	17.3%

Table 4
Chemical Requirements of Metal Casing

Element	% Limit or Range
Nitrogen (max.)	0.05
Carbon (max.)	0.08
Hydrogen (max.)	0.015
Iron (max.)	0.30
Oxygen (max.)	0.20
Aluminum (max.)	5.50 - 6.75
Vanadium (max.)	3.5 - 4.5
Residuals, each (max.)	0.1
Residuals, total (max.)	0.4
Titanium	Remainder

Table 5
Manufacturer's Physical and Mechanical Properties of APU Metal Casing

Physical Property	Typically Reported	MIL-T-9047 Comp. 6
Tensile Strength	1100 - 1240 MPa	900 MPa (min.)
Yield Strength	970 - 1100 MPa	830 MPa (min.)
Percent Elongation	10-15	10 (min.)
Percent Reduction of Area	30-50	25 (min.)
Hardness	35 Rockwell C	
Microstructure	Equiaxed primary alpha grains in an aged, transformed beta matrix containing fine acicular alpha[a]	
Percent Primary Alpha	30	--
ASTM Grain Size	8-10	--

[a]Same for MIL-T-9047
-- indicates no data available

Table 6
APU Tank A49197 Particle Count[a]

Particle Diameter Range (μm)	Allowed (per 100 ml)[b]	Count (10 ml)
< 25	Unlimited	---
26-50	200	3
51-100	20	4
101-250	2	0
> 250	0	0

[a]Only the hydrazine from this tank was tested in this program.
[b]Smith, I. D. *Chemical/Cleanliness Requirements for WSTF Test Hardware and Facility Equipment.* NASA Spec 022, NASA Johnson Space Center White Sands Test Facility, NM, 1987.

Table 7
APU Tank A49197 Fuel Analysis[a]

Contents	Allowed[b] (weight percent)	Measured (weight percent)
Hydrazine	98.5	97.3
Water	1	2.6
Isopropyl alcohol	0.02	0.03
Carbon dioxide	0.003	0.02

[a]Only the hydrazine from this tank was tested in this program.
[b]Per MIL-P-26536D
Note: This data is slightly out of specification.
Note: The high carbon dioxide level is indicative of exposure to air.

Table 8
APU Tank A49198 Particle Count[a] (5 Micron Filter, DI Water Rinse #1)

Range	Gas Side	Fuel Side
< 200	109	51
200 - 400	2	2
400 - 600	0	0
600 - 800	0	0
800 - 1000	0	0
> 1000	0	0

[a]This tank and the hydrazine it contained were tested in this program.

Table 9
EPR Compression Set Data

Sample		Compression Set (%)	Standard Deviation
		WSTF # 91-25134, 91-25436[a]	
1		25.4	
4		17.04	
7		19	
	Median	19	
	Mean	20.48	4.4
		WSTF # 91-25361[b]	
2		7.97	
3		7.46	
5		13.79	
	Median	7.97	
	Mean	9.74	3.5
		AFE-332 specification	
	Median	22 max	
	Mean	22 max	

[a]Unexposed EPR
[b]EPR diaphragm

Table 10
EPR Hardness Test Data

Sample No.	Fuel Side Hardness Median	Mean	St. Dev., N	Gas Side Hardness Median	Mean	St. Dev., N
91-25134[a]	88	88	2, 15	89	88	1, 15
91-25436[a]	87	87	1, 30	87	87	2, 30
91-25361[b]	88	88	1, 24	88	88	1, 24
AFE-332 Specification		90 ± 5			90 ± 5	

[a]Unexposed EPR
[b]EPR diaphragm

Table 11
EPR Specific Gravity Data

Sample No.	Specific Gravity Mean	Standard Deviation[a]
91-25134 and 91-25436[b]	1.07	0.007
91-25361[c]	1.08	0.005
PSI Comparison Value	1.07	

[a]N = 8
[b]Unexposed EPR
[c]EPR diaphragm

Table 12
EPR Tensile Data

Sample No.	Data Type	Ultimate Tensile Strength (MPa)	Elongation at Break (%)	100% Modulus (MPa)
91-25134, 91-25436[a]	Median	15.0	250	10.1
	Mean	14.6	236.7	10.0
	St. Dev.[b]	0.9	23.5	0.2
91-25361[c]	Median	11.3	210	9.0
	Mean	11.1	199	8.6
	St. Dev.[d]	1.5[d]	53.8[d]	0.5[e]
AFE-332 Specification	Min. Required	11.4	230	6.6

[a]Unexposed EPR
[b]N = 12
[c]EPR diaphragm
[d]N = 10
[e]N = 9

Table 13
EPR FTIR Results

Sample	PEAKS 3641 cm^{-1} (OH)	2909 cm^{-1} (CH_2 Asymmetric Stretch)	2855 cm^{-1} (CH_2 Symmetric Stretch)	1640 cm^{-1} (Vinyl C=C)	1464 cm^{-1} (CH_2 Scissoring)	1375 cm^{-1} (CH_3 Symmetric Bending)	1350-1120 cm^{-1} (CF_2 & CH_2 Twist & Wag)	966 & 909 cm^{-1} (Vinyl)	720 cm^{-1} (CH_2 Rocking)	625 551 cm^{-1} (PTFE Char Band)
M1, M2, M3, M4, M5, M6[a]	w	s	s	w	m	m	s	w	w	w
M1, M5, M8[b]	w	s	s	w	m	m	s	w	w	w

Note: s = strong, m = medium, w = weak
[a]Unexposed EPR
[b]EPR diaphragm

Table 14
EPR TGA Data

Sample No.	EPR and Polybutene (%)	PTFE (%)	Total Inorganic Residue (%)	SiO_2 (%)	CaO (%)	ZnO (%)
T1-T6[a]	70.5	4.9	24.6	20.1	2.1	2.4
Standard Deviation[b]	1.0	0.8	1.1	0.8	0.1	0.2
TA4- TA10[c]	69.3	5.0	25.7	21.3	1.7	2.7
Standard Deviation[d]	0.7	1.1	0.5	0.7	0.1	0.2
EPR AFE-332 Specification	70-71.4	5.7-6.1	21.9-24.9	16.7-18.5	2.6-3.2	2.6-3.2

[a]Unexposed EPR
[b]N = 6
[c]EPR diaphragm
[d]N = 3

Table 15
EPR TMA Data

Sample No.	Tan δ Onset (T_{g1}) (°C)	Modulus Curve Drop Temperature (T_{g2}) (°C)	Storage Modulus at T_{g2} (MPa)	Storage Modulus at 20°C (MPa)
T1-T6[a]	-54.8	-50.6	20.9	1.9
St. Dev.[b]	1.7	1.1	9.6	0.9
TA4-TA10[c]	-55.8	-49.6	21.4	1.9
St. Dev.[d]	1.5	1.2	3.3	0.47

[a]Unexposed EPR
[b]N = 6
[c]EPR diaphragm
[d]N = 3

Table 16
ESCA Analysis of Rib Mark on Metal Casing

Surface Coating Thickness (Element)	Composition at 100 Å Deep (a/o) Normal Area 200 Å	Discolored Area 800 Å
Carbon	15.7	41.9
Titanium	34.2	11.2
Oxygen	43.0	36.6
Aluminum	4.7	0.1
Iron	2.3	9.27

Table 17
Metal Casing Hardness Measurements (HRC)

Location	Lowest (HRC)	Highest (HRC)
Fuel Side 0°	38.5	41.0
Fuel Side 180°	38.0	40.5
Gas Side 0°	38.5	41.0
Gas Side 180°	39.0	41.0
Polish/Grind	38.5	41.0
Grind (deep)	38.0	40.5
Rib Mark	32.0	35.0

Table 18
Metal Casing Weld Seam Microhardness Measurements (KHN)

Location	0° (KHN)	180° (KHN)
Base Metal	348 to 375	341 to 390
Heat Affected Zone	305 to 339	333 to 347
Weld (Melted) Material	324 to 381	335 to 382

Table 19
Metal Casing Thickness Measurements

Casing Half	Location Code[a,b]	Thickness (mm)
Fuel Side	C0.0 D1.25	3.84
	C0.0 D6	1.32
	C18 D18	5.38
	C22 D6	1.30
	C47 D6	1.30
	C67 D6	1.32
	C75 D11	1.30
Gas Side	C0.0 D5.5	1.24
	C0.0 D16.5	1.73
	C6 D6	1.27
	C20 D5.5	1.24
	C20 D15.5	1.40
	C41 D5.5	1.24
	C41 D15.5	1.37
	C64 D5.5	1.24
	C64 D15.5	1.40

[a]See Appendix G for the sample locations.
[b]Location Code: C = Clockwise from zero reference punch marks on rim
D = Down from rim

Acknowledgements

The authors wish to acknowledge the enthusiastic support of the following WSTF personnel who participated in this test program:

Chemistry Laboratory
Dennis Davis
Surender Kaushik

Defense Contracting Management Command (DCMC)
John Caruso

Design Group
Rollin Christianson
Jim Schadler

Metallurgy Laboratory
Robert Gomez
Paul Spencer
Brooks Wolle

Publications
Dana Hite

800 Area High-Flow Test Area (HFTA)
Ed Havenor
Ron Samaniego

References

ASTM B 381. *Titanium and Titanium Alloy Forgings.* American Society for Testing and Materials, Philadelphia, PA.

ASTM D 297. *Methods for Rubber Products--Chemical Analysis.* American Society for Testing and Materials, Philadelphia, PA.

ASTM D 395. *Rubber Property--Compression Set.* American Society for Testing and Materials, Philadelphia, PA.

ASTM D 412. *Rubber Properties in Tension.* American Society for Testing and Materials, Philadelphia, PA.

ASTM D 792. *Specific Gravity (Relative Density) and Density of Plastics by Displacement.* American Society for Testing and Materials, Philadelphia, PA.

ASTM D 2240. *Rubber Property--Durometer Hardness.* American Society for Testing and Materials, Philadelphia, PA.

ASTM E 384. *Standard Test Method for Microhardness of Materials.* American Society for Testing and Materials, Philadelphia, PA.

ASTM E 472. *Reporting Thermo-Analytical Data.* American Society for Testing and Materials, Philadelphia, PA.

ASTM E 1131. *Compositional Analysis by Thermogravimetry.* American Society for Testing and Materials, Philadelphia, PA.

ASTM E 1363. *Test Method for Calibration of Thermomechanical Analyzers.* American Society for Testing and Materials, Philadelphia, PA.

Bellanca, C. L., and J. C. Harris. *Literature Survey on the Effects of Long-Term Shelf Aging on Elastomeric Materials.* AFML-TR-67-235, Monsanto Research Corporation, April 1967.

Boyum, B. M., and J. E. Rhoads. *Elastomer Shelf Life: Aged Junk or Jewels?* Washington Public Power Supply System, Richland, Washington, 1990.

Coulbert, C. D., E. F. Cuddihy, and R. F. Fedors. *Long-Time Dynamic Compatibility of Elastomeric Materials with Hydrazine.* Tech Memo 33-650, NASA, JPL, September 1973.

Freakley, P. K., and A. R. Payne. *Theory and Practice of Engineering with Rubber.* Applied Science Publishers Ltd, London, 1978.

References (Continued)

House, P. A. "Age Control of Elastomers by ANA Bulletin No. 438." *Non-Metallic Materials Selection, Processing and Environmental Behavior.* Proceedings of the Fourth National Technical Conference and Exhibition, Palo Alto, CA, October 17-19, 1972 (A73-13001 03-18).

Gill, D. D. *Storability and Expulsion Test Program.* AFRPL TR-86-063, US Air Force Rocket Propulsion Laboratory, Edwards Air Force Base, CA, September 1986.

Martin, J. W., and J. K. Sieron. *A New Laboratory Procedure for Determining Compatibility of Positive Expulsion Elastomers with Liquid Propellants.* US Air Force Materials Lab, Dayton, OH, 1977.

MIL-HDBK-695C. *Standardization Handbook, Rubber Products: Recommended Shelf Life.* US Department of Defense, March 27, 1985.

MIL-P-26536D. *Propellant, Hydrazine.* US Department of Defense, May 23, 1969.

MIL-R-83412A. *Military Specifications of Rubber, Ethylene-Propylene, Hydrazine Resistant.* US Department of Defense, June 30, 1977.

MIL-SPEC-T-9047E. *Titanium and Titanium Alloy Bars (Rolled or Forged) and Reforging Stock, Aircraft Quality.* Comp. 6, US Department of Defense, June 15, 1970.

MIL-STD-1523A. *Age Controls of Age-Sensitive Elastomeric Material.* US Department of Defense, February 1, 1984.

MIL-T-9047E. *Military Specification for Titanium and Titanium Alloy Bars (Rolled or Forged) and Reforging Stock, Aircraft Quality.* US Department of Defense, June 15, 1970.

PSI. *Verification Program Report for Tank, Fuel, Diaphragm, Auxiliary Power Unit Subsystem (APUS) Part Number MC282-0084-0100.* Prepared for Space Division Rockwell International, Contract No. M5J7XMS-089100D, Pressure Systems, Inc., February 8, 1977.

Repar, J. *Flight and Experimental Expulsion Bladders for Mariner 69.* APCO Project Number 764400, JPL Contract No. 951939, January 1970.

Repar, J. *Rubber Compositions for Hydrazine Service.* PSI Project No. 7034000, JPL Contract No. 952864, Pressure Systems, Inc., California, April 1973.

Rubber Manufacturers' Association. *Effect of Long-Term Storage on O-ring Physical Properties.* March, 1966.

References (Continued)

Sheets, D. A. *Exploratory Development of Elastomeric Material*. LMSC Report No. AFRPL-TR-73-112, National Technical Information Service, VA, January, 1974.

Sullivan, J. J. *Evaluation of Materials and Equipment Recovered from the B-17E Aircraft "My Gal Sal."* AFML-TR-66-275, 1966.

Takimoto, H. H., and G. C. Denault. *Hydrazine Compatibility with Ethylene- Propylene Elastomers*. SAMSO, US Air Force, Los Angeles, California, February 28th, 1969: pp. 57-63.

Yee, R. N., and F. G. Etheridge. *Long-Term Hydrazine Storage Test Program*. Rockwell International Project 361, Task 36100, December 1985.

Young, C. B. *"Lady be Good" Hydraulic Components*. Report No. WWFESM-60-21 B-24-D, 1960.

Appendix A
EPR Samples Location

C = COMPRESSION SET SAMPLE
H = HARDNESS SAMPLE
M = MICROSCOPY SAMPLE
SG= SPECIFIC GRAVITY SAMPLE
T = THERMAL ANALYSIS SAMPLE

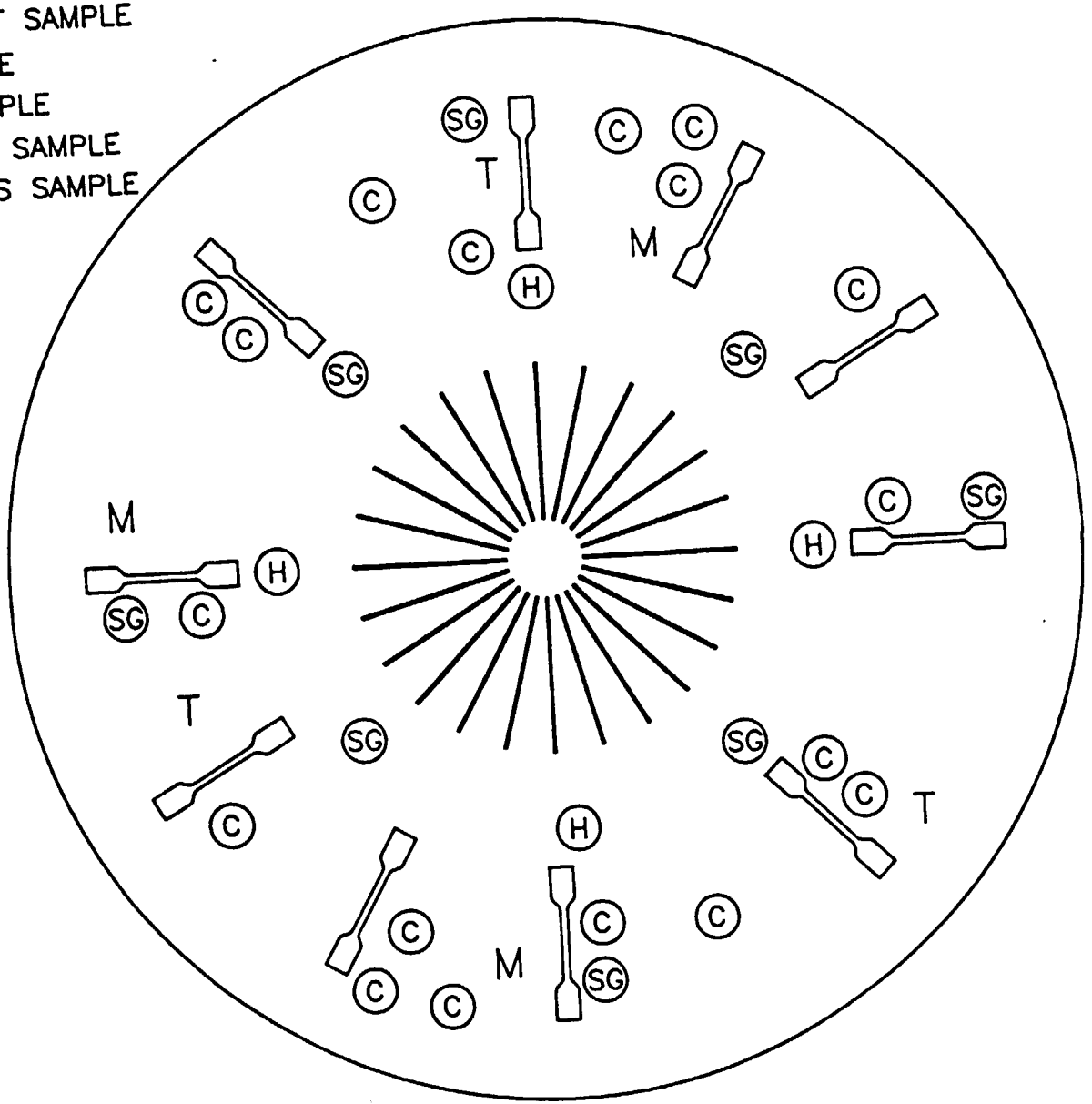

Figure A-1
APU Tank Diaphragm Samples Location

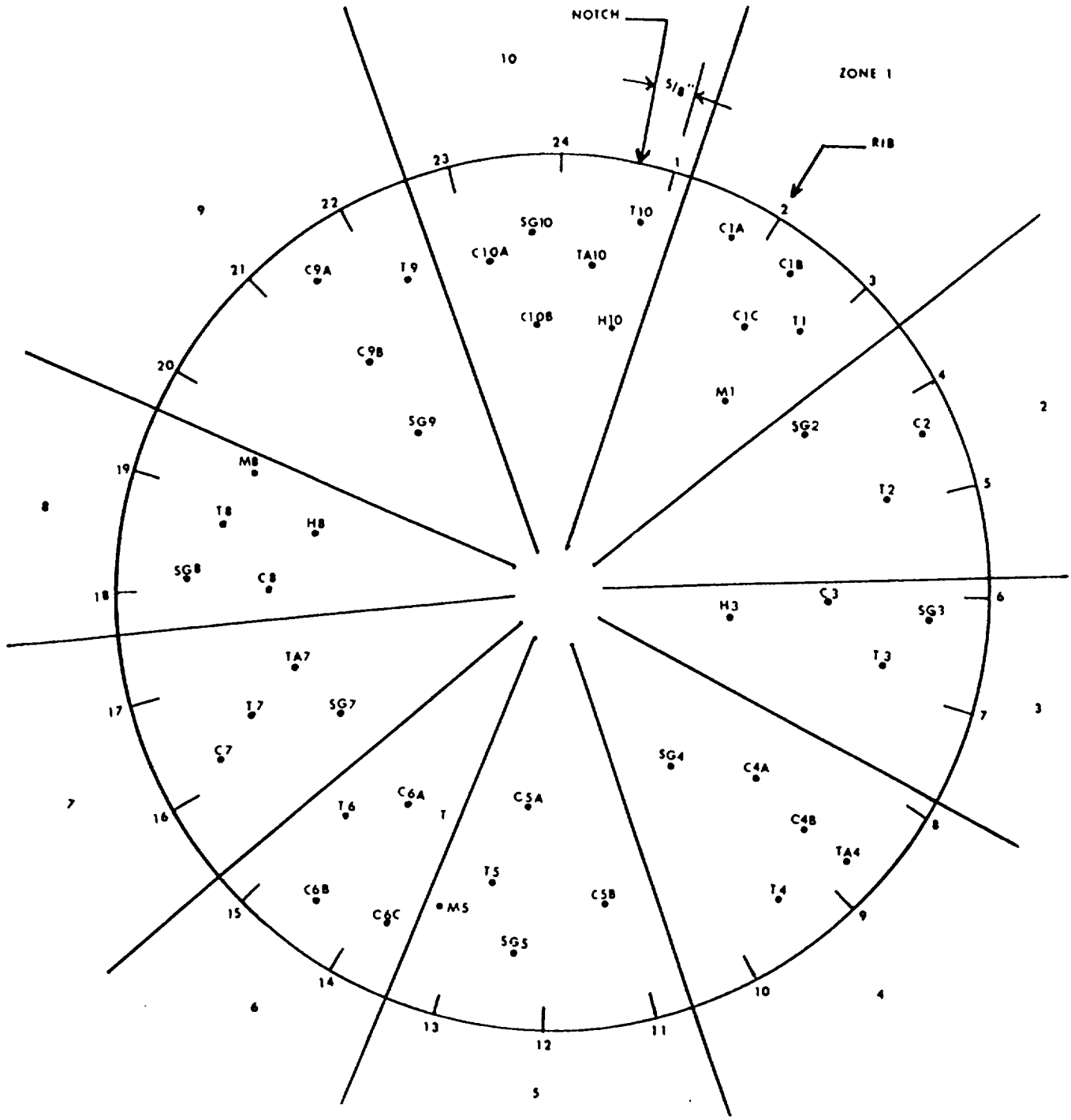

SAMPLE DESIGNATION

C = Compression Set
H = Hardness
M = Micro
SG = Specific Gravity
T = Tensile
TA = Thermal Analysis

SAMPLE DESIGNATION ZONE A,B,C, Etc.

C 4 B

(Sample Code)

Figure A-2
Samples Location on Entire EPR Diaphragm

UNEXPOSED DIAPHRAGM MATERIAL

CS = Compression Set
M = Microscopy
T = Thermal Analysis

H = Hardness
SG = Specific Gravity
Tensile = As Shown

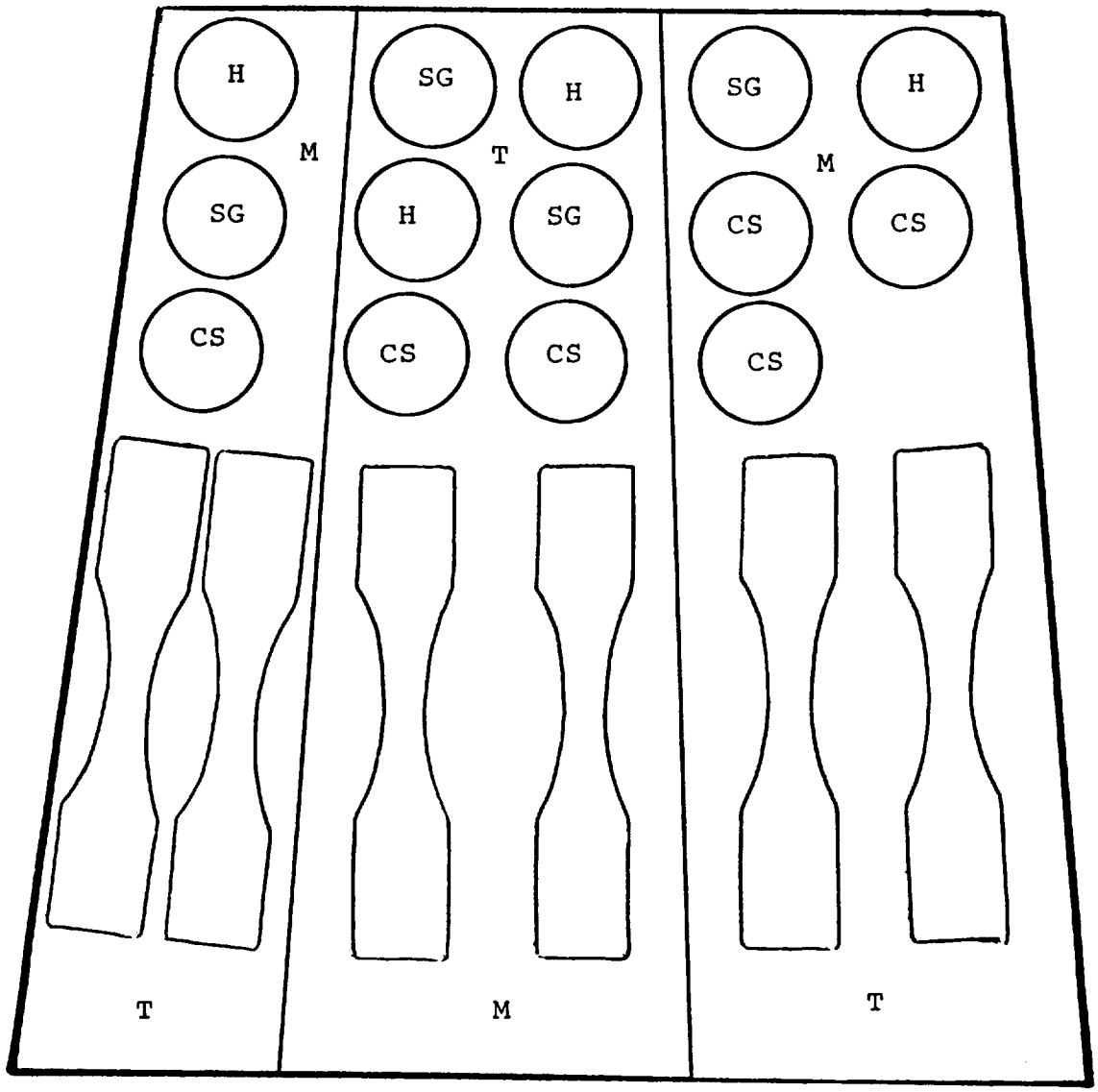

Figure A-3
AFE-332 Sheet (WSTF # 91-25434)
A-5

UNEXPOSED DIAPHRAGM MATERIAL

CS = Compression Set
M = Microscopy
T = Thermal Analysis
H = Hardness
SG = Specific Gravity
Tensile = As Shown

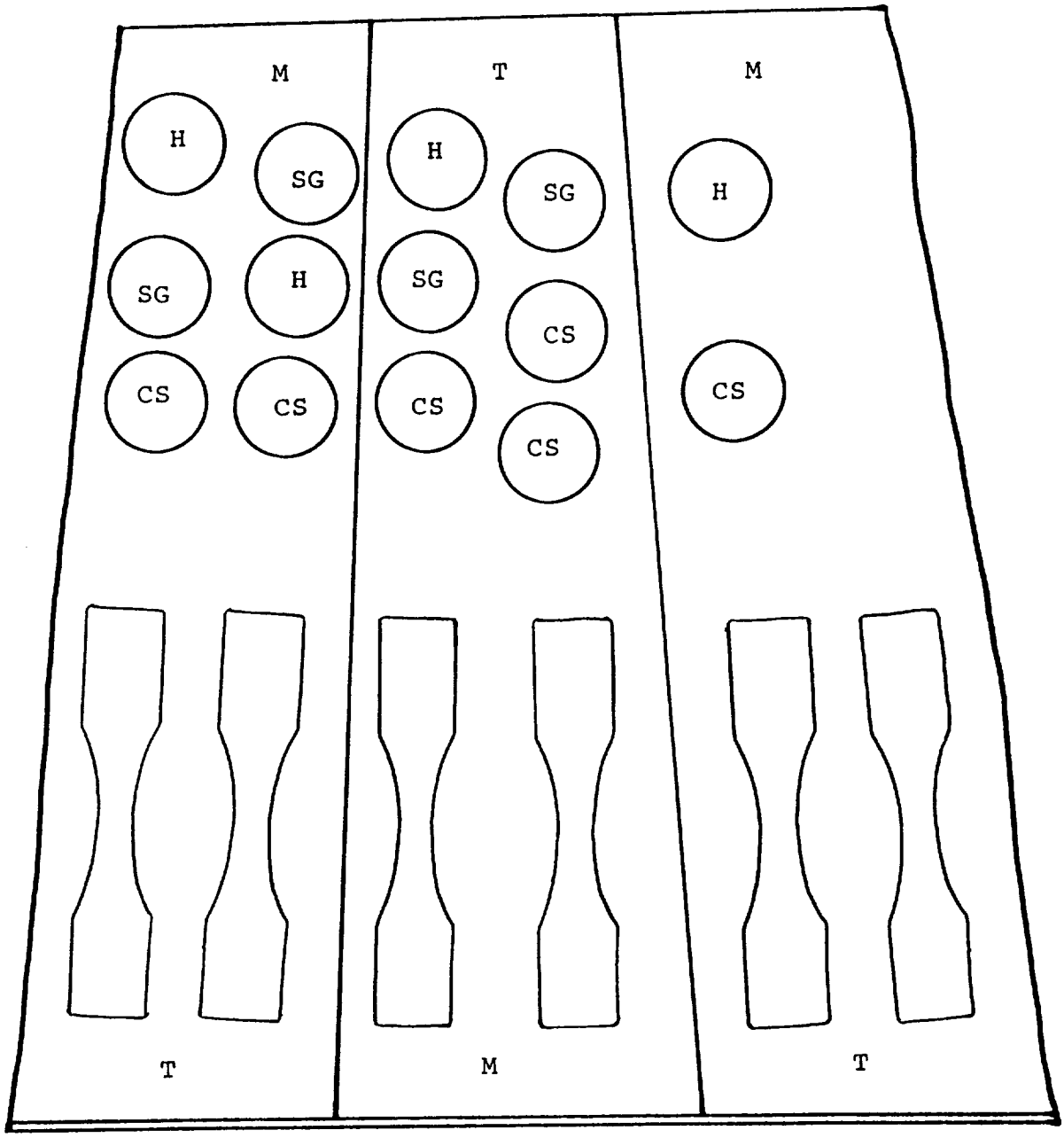

Figure A-4
AFE-332 Sheet (WSTF # 91-25136)
A-6

Appendix B
Detailed EPR Hardness Data

Table B-1
Durometer Hardness Test Data, WSTF No. 91-25361
EPR diaphragm samples plied atop reference samples

Specimen ID	Fuel-Side Hardness, Shore A	Gas-Side Hardness, Shore A	Specimen ID	Fuel-Side Hardness, Shore A	Gas-Side Hardnes Shore A
H1A	86	88	H5C	90	88
H1B	87	86	H6A	86	87
H1C	88	88	H6B	89	90
H2A	87	87	H7A	87	87
H2B	88	88	H7B	89	89
H3A	89	90	H8A	89	90
H3B	86	88	H8B	88	88
H4A	87	87	H8C	88	88
H4B	86	86	H9A	89	88
H4C	89	90	H9B	87	87
H5A	88	87	H10A	86	88
H5B	87	87	H10B	89	88
Median	88	88		N/A	N/A
Mean	88	88		N/A	N/A
Std Dev	1	1		N/A	N/A

Table B-2
Durometer Hardness Test Data, WSTF # 91-25134

Specimen ID	Fuel-Side Hardness Shore A	Gas-Side Hardness Shore A
H1	91*	90
H2	91*	89
H3	90	89
H4	90	88
Residual Material**	88	88
Median	88	89
Mean	88	88
St. Dev.	2	1

* ASTM D2240 recommends that measurements be made with the type D durometer when values above 90 are obtained with the type A durometer.
**Arithmetic mean of 11 data points obtained at various locations around the residual sample material

Table B-3
Durometer Hardness Test Data, APU Diaphragm, WSTF # 91-25136

Specimen ID	Fuel-Side Hardness Shore A	Gas-Side Hardness Shore A
H5	90	89
H6	89	87
H7	87	88
H8	89	89
Residual Material*	87	87
Median	87	87
Mean	87	87
St. Dev.	1	2

*Arithmetic mean of 11 data points obtained at various locations around the residual sample material

Appendix C
Detailed EPR Tensile Data

Table C-1
Tensile Results for WSTF # 91-25134

Specimen	Ultimate Tensile Strength, MPa	Elongation at Break (%)	100% Modulus, MPa
T1	14.3	230	10.2
T2	13.3	210	10.2
T3	15.0	260	10.1
T4	15.3	250	10.1
T5	15.0	250	10.4
T6	14.2	240	10.2
MEDIAN	14.7	245	10.2
MEAN	14.5	240	10.2

Table C-2
Tensile Results for WSTF # 91-25436

Specimen	Ultimate Tensile Strength, MPa	Elongation at Break, %	100-percent Modulus, MPa
T7	15.5	250	10.1
T8	15.4	240	10.0
T9	15.4	260	9.7
T10	12.7	180	10.1
T11	15.3	250	9.6
T12	14.2	220	9.7
MEDIAN	15.4	245	9.9
MEAN	14.8	233	9.9

Table C-3
Tensile Results for WSTF # 91-25316

Specimen	Ultimate Tensile Strength, MPa	Elongation at Break, percent	100-percent Modulus, MPa
T1	11.3	190	8.8
T2	9.7	140	9.0
T3	12.0	240	7.9
T4	12.9	260	9.0
T5	7.9	90	N/A
T6	11.0	230	7.9
T7	11.7	240	8.0
T8	11.3	190	9.2
T9	12.4	240	9.0
T10	10.3	170	8.4
MEDIAN	11.3	210	9.0
MEAN	11.1	199	8.6

Appendix D
EPR FTIR Spectra

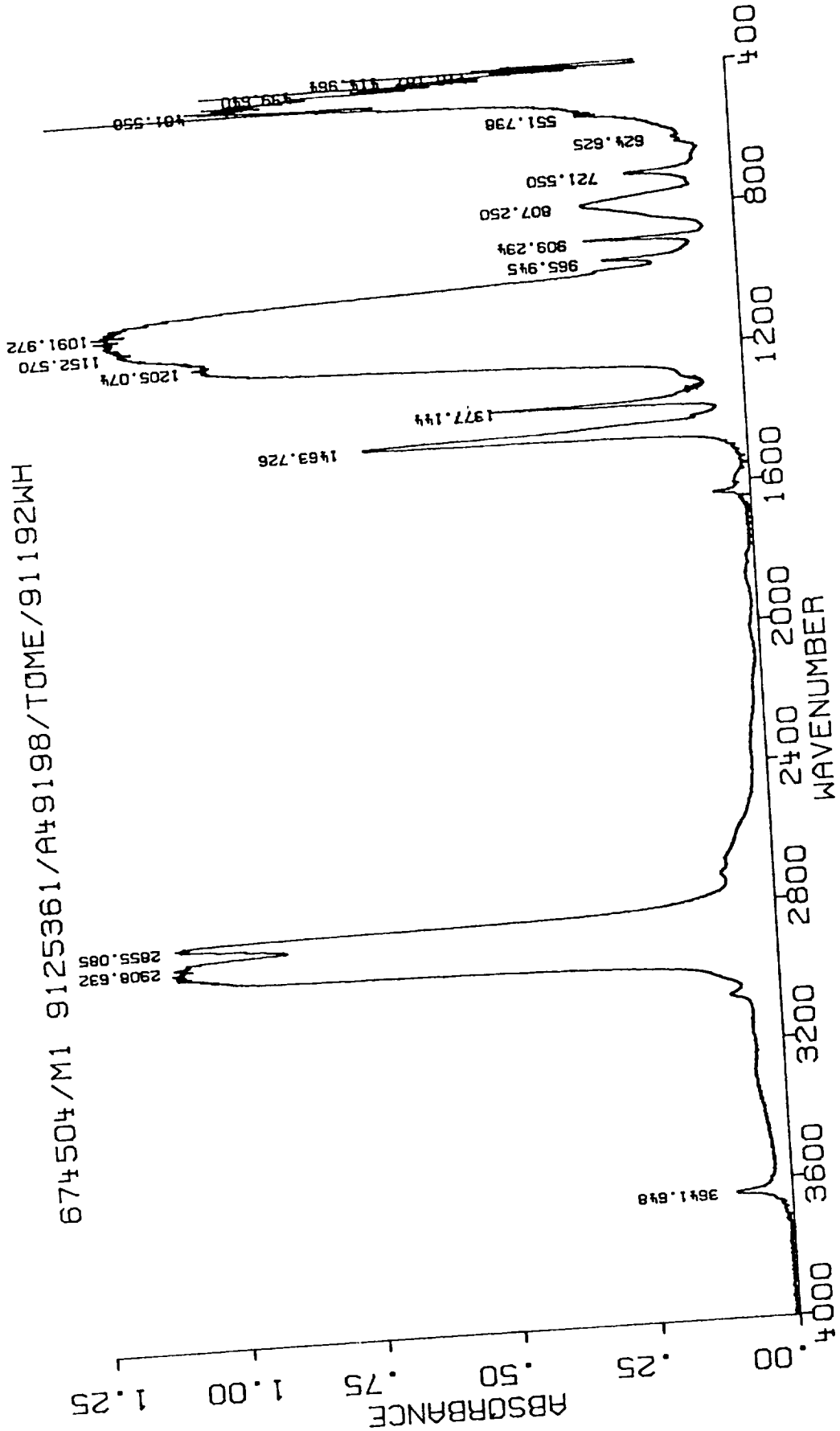

Figure D-1
FTIR Spectra for Exposed EPR Sample M1

D-2 INTENTIONALLY

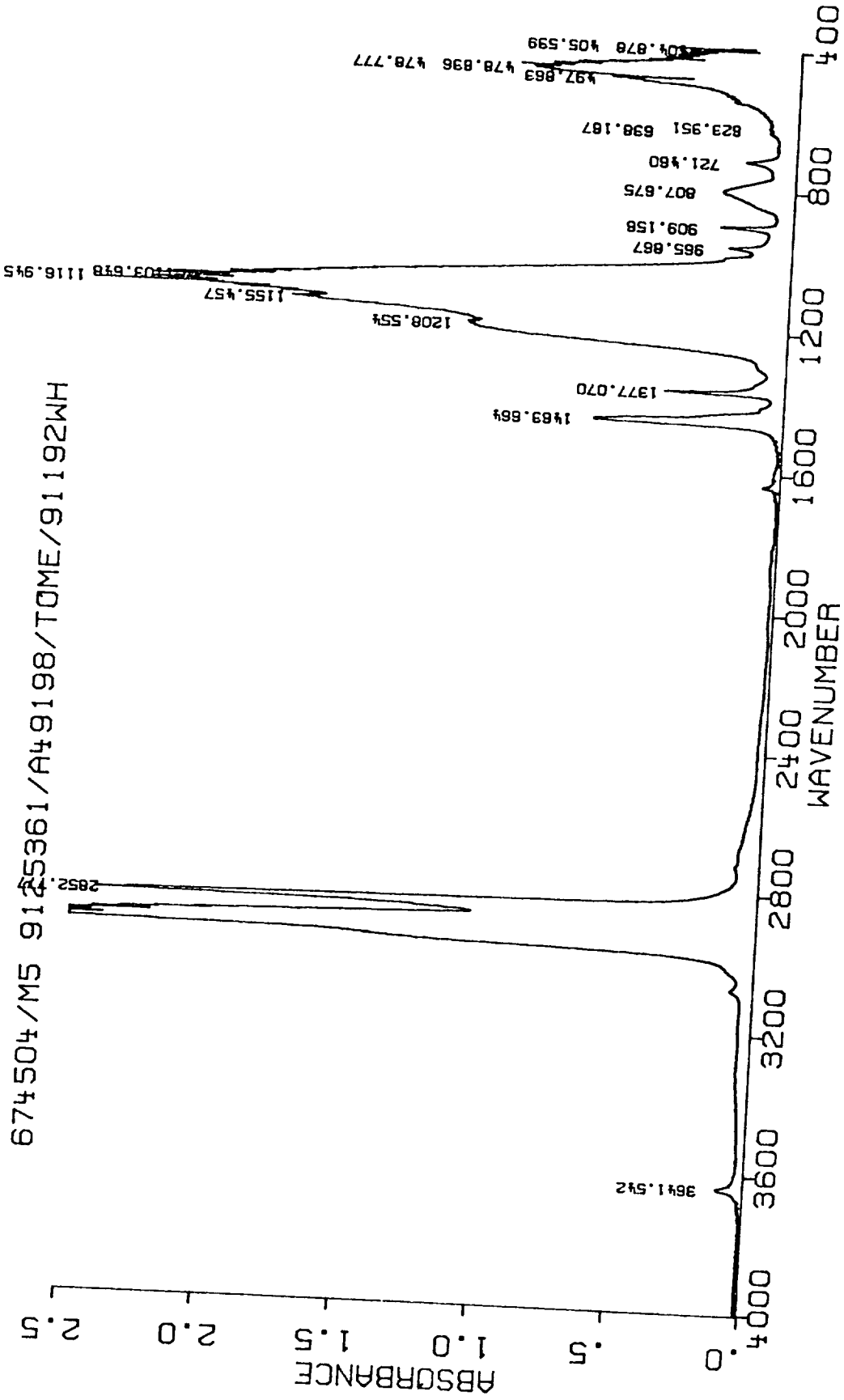

Figure D-2
FTIR Spectra for Exposed EPR Sample M5

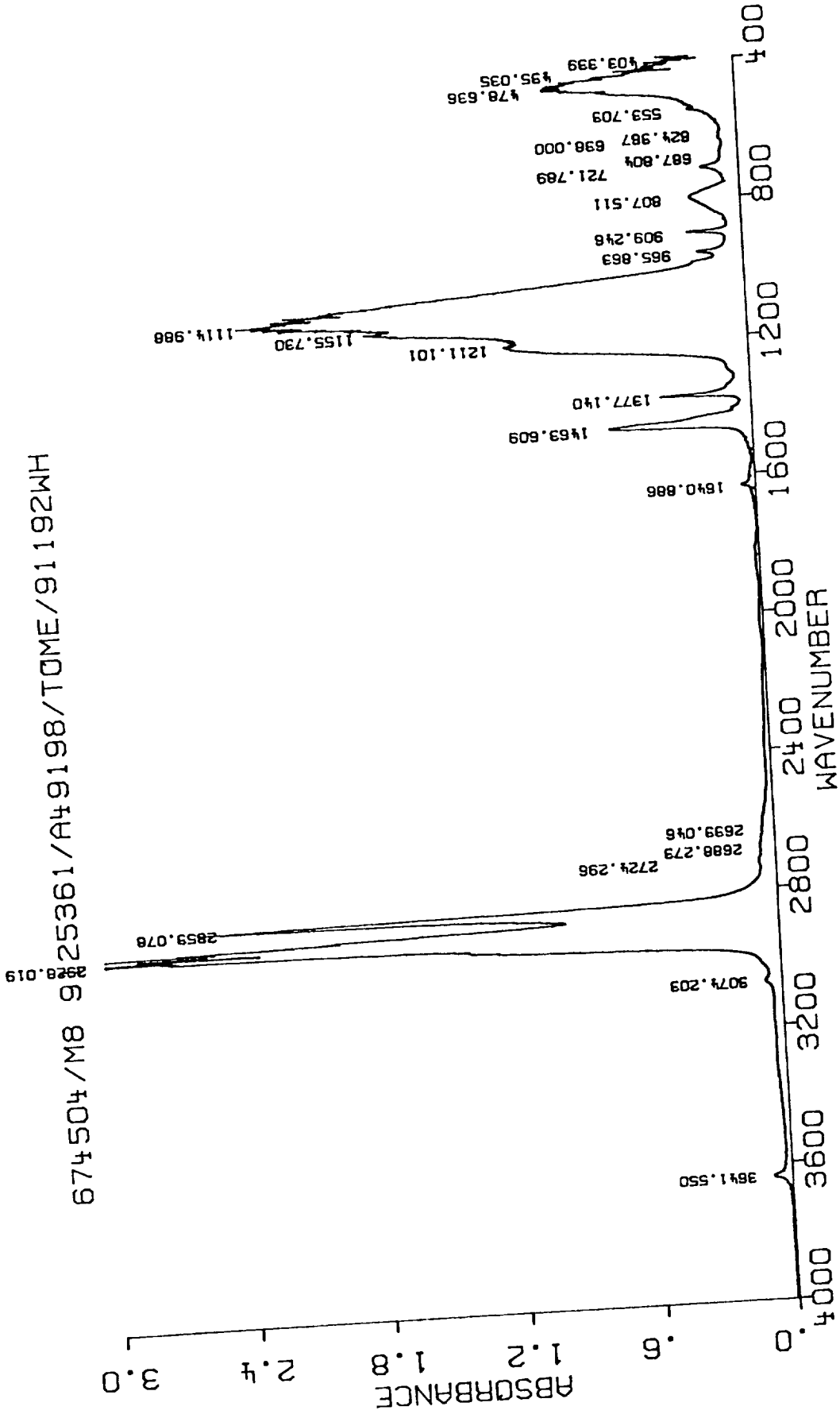

Figure D-3
FTIR Spectra for Exposed EPR Sample M8

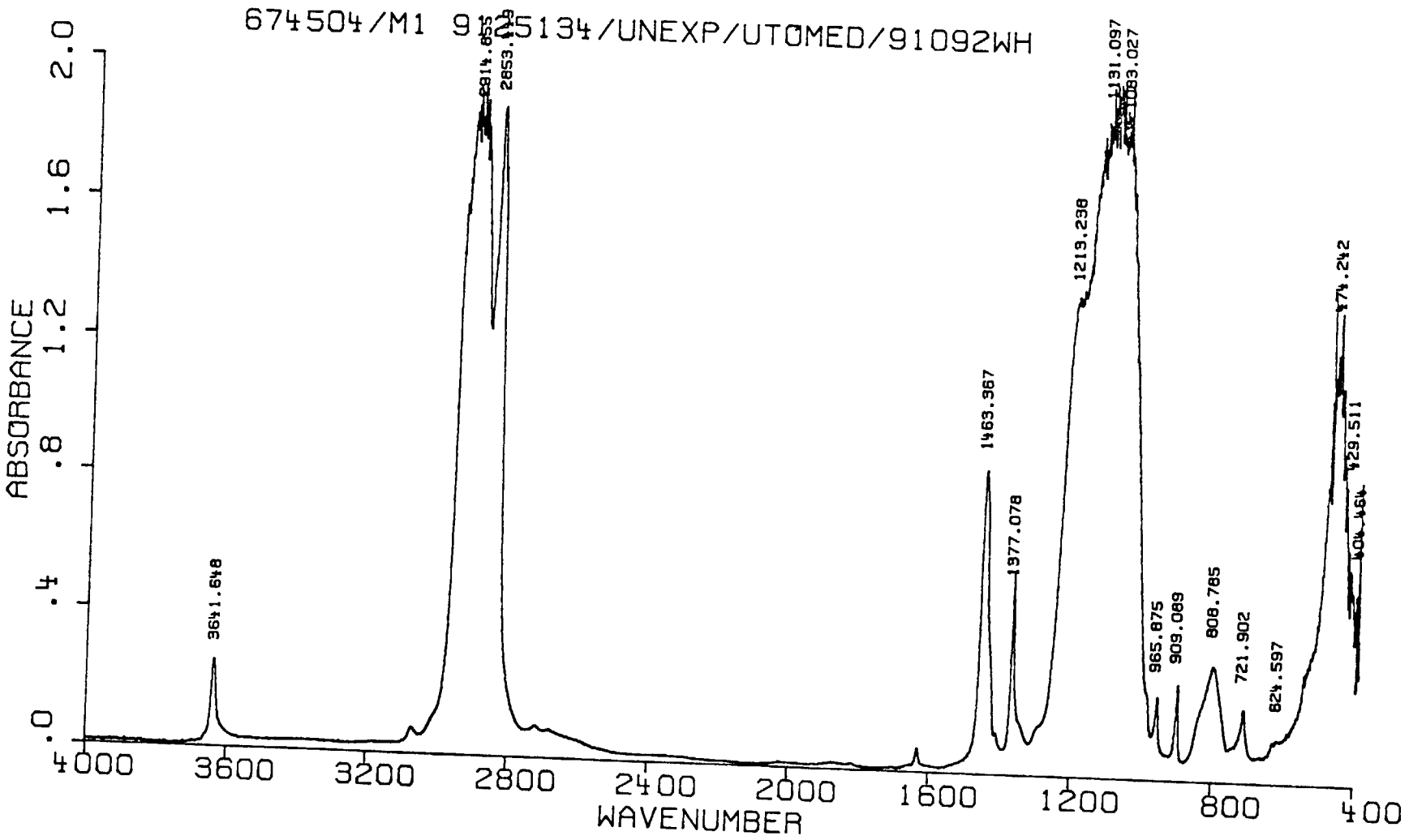

Figure D-4
FTIR Spectra for Unexposed EPR Sample M1

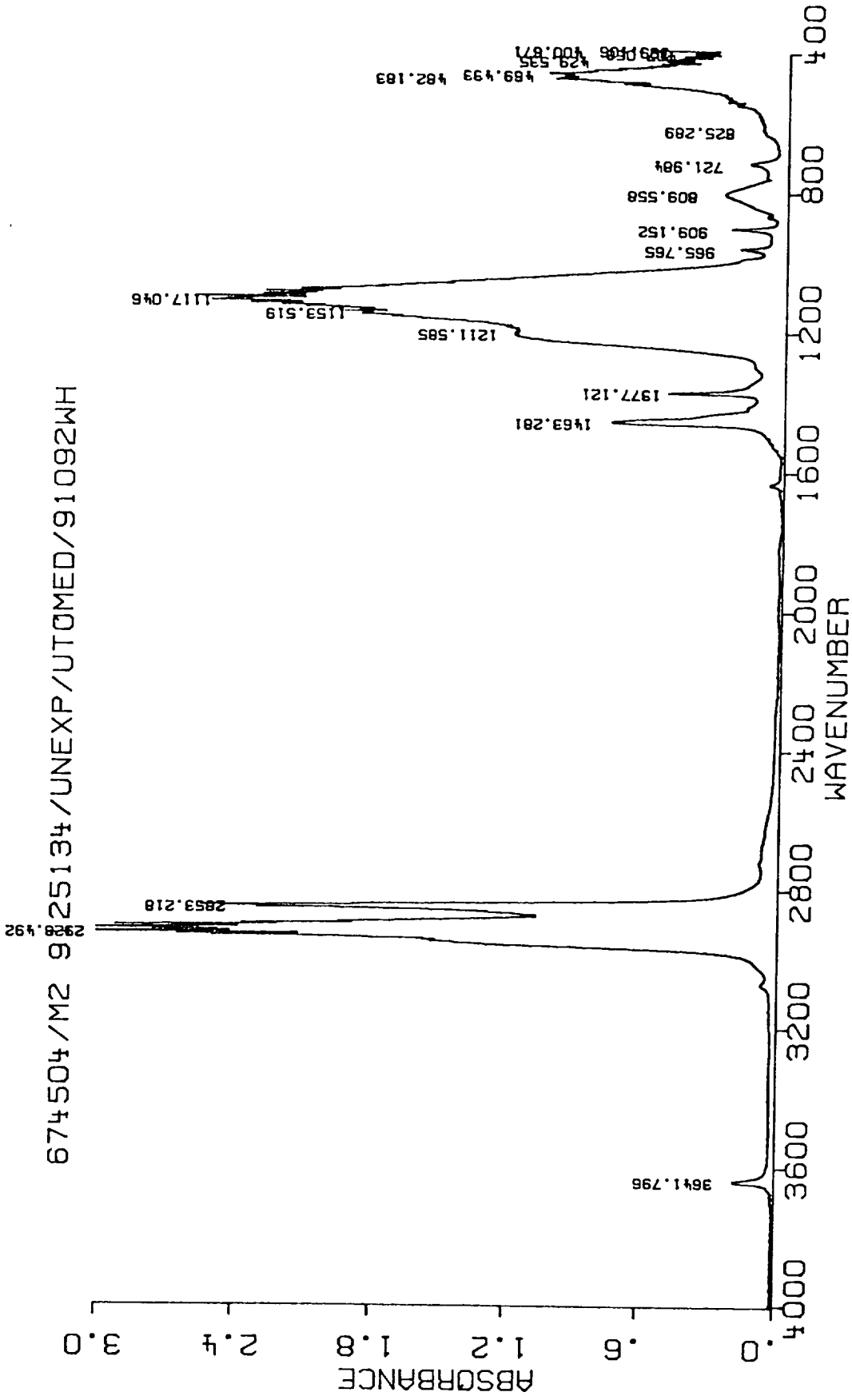

Figure D-5
FTIR Spectra for Unexposed EPR Sample M2

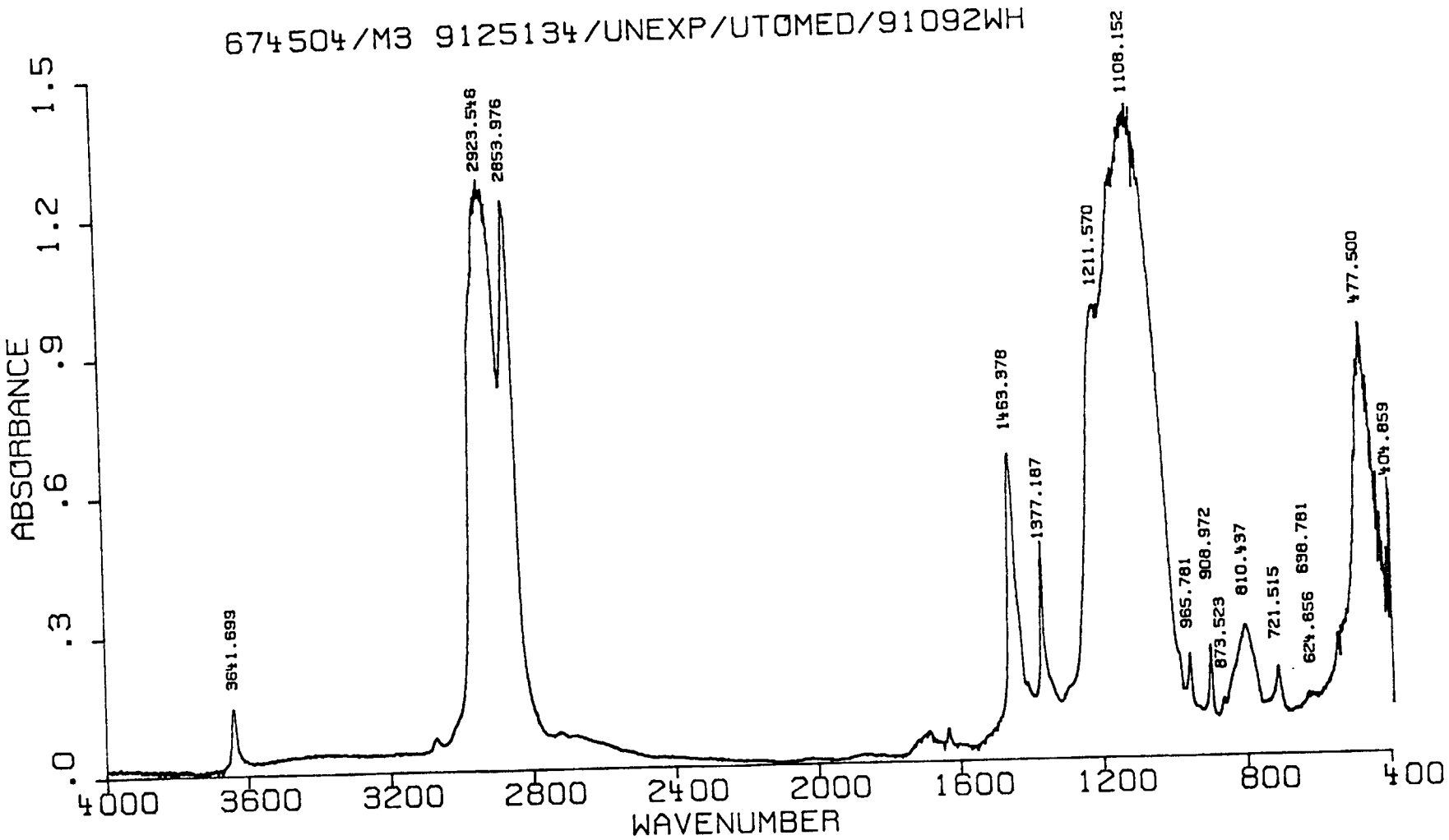

Figure D-6
FTIR Spectra for Unexposed EPR Sample M3

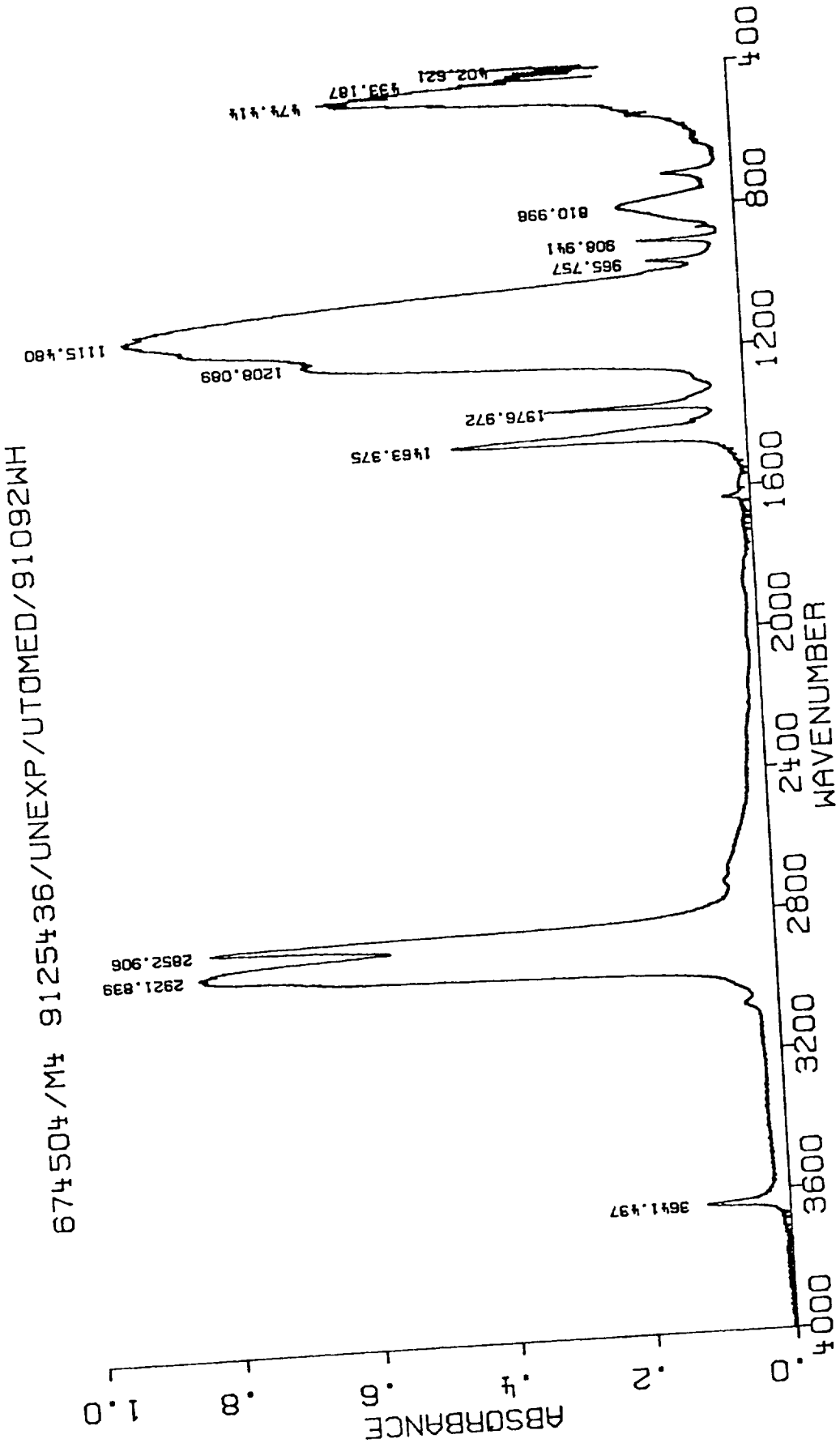

Figure D-7
FTIR Spectra for Unexposed EPR Sample M4

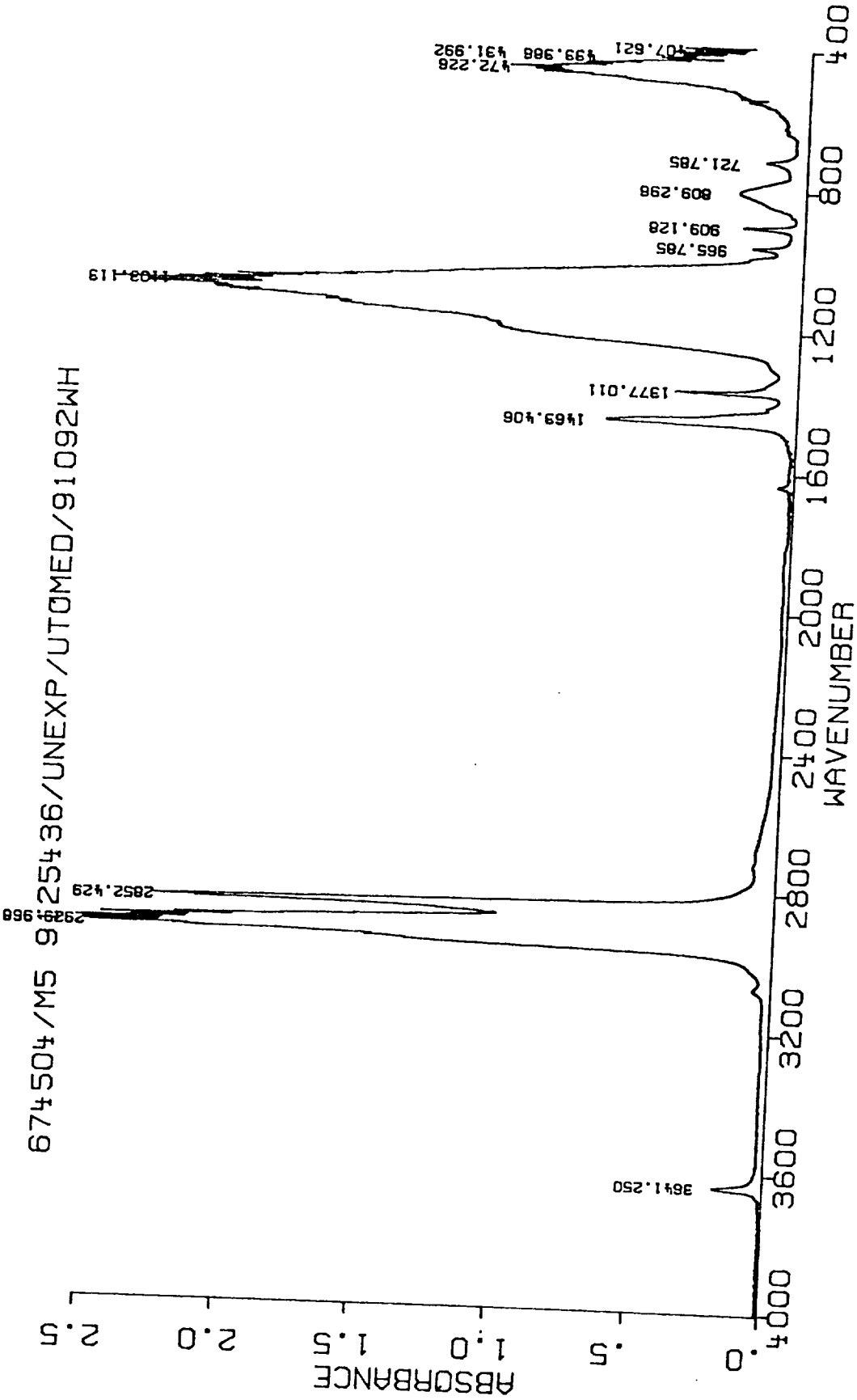

Figure D-8
FTIR Spectra for Unexposed EPR Sample M5

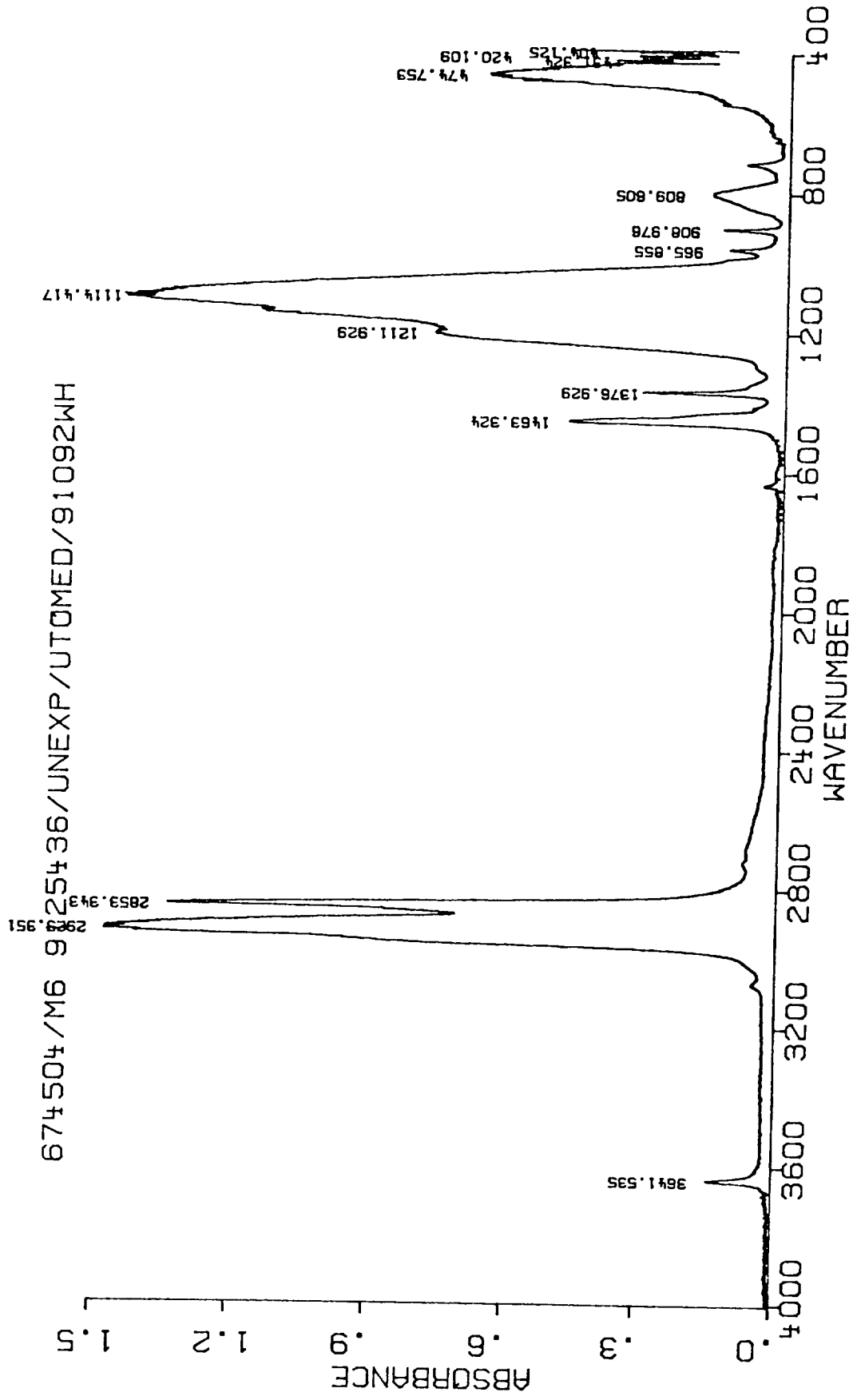

Figure D-9
FTIR Spectra for Unexposed EPR Sample M6

Appendix E
Detailed EPR TGA Data

Table E-1
Detailed EPR TGA Data

Sample	WSTF #	Percent EPR and Poly-butene	Percent PTFE	Total Inorganic Residue	Percent SiO_2	Percent CaO	Percent ZnO
TA4	91-25361	68.5	6.2	25.3	20.6	1.8	2.9
TA7	91-25361	69.7	4.1	26.2	22.0	1.7	2.5
TA10	91-25361	69.6	4.7	25.7	21.4	1.7	2.6
T1	91-25134	69.9	6.0	24.1	19.9	2.0	2.2
T2	91-25134	70.0	5.9	24.1	19.5	2.2	2.4
T3	91-25134	72.4	4.4	23.2	19.2	1.9	2.1
T4	91-25436	70.9	4.4	24.7	20.5	2.0	2.2
T5	91-25436	69.5	4.2	26.3	21.5	2.2	2.6
T6	91-25436	70.2	4.7	25.1	20.2	2.2	2.7

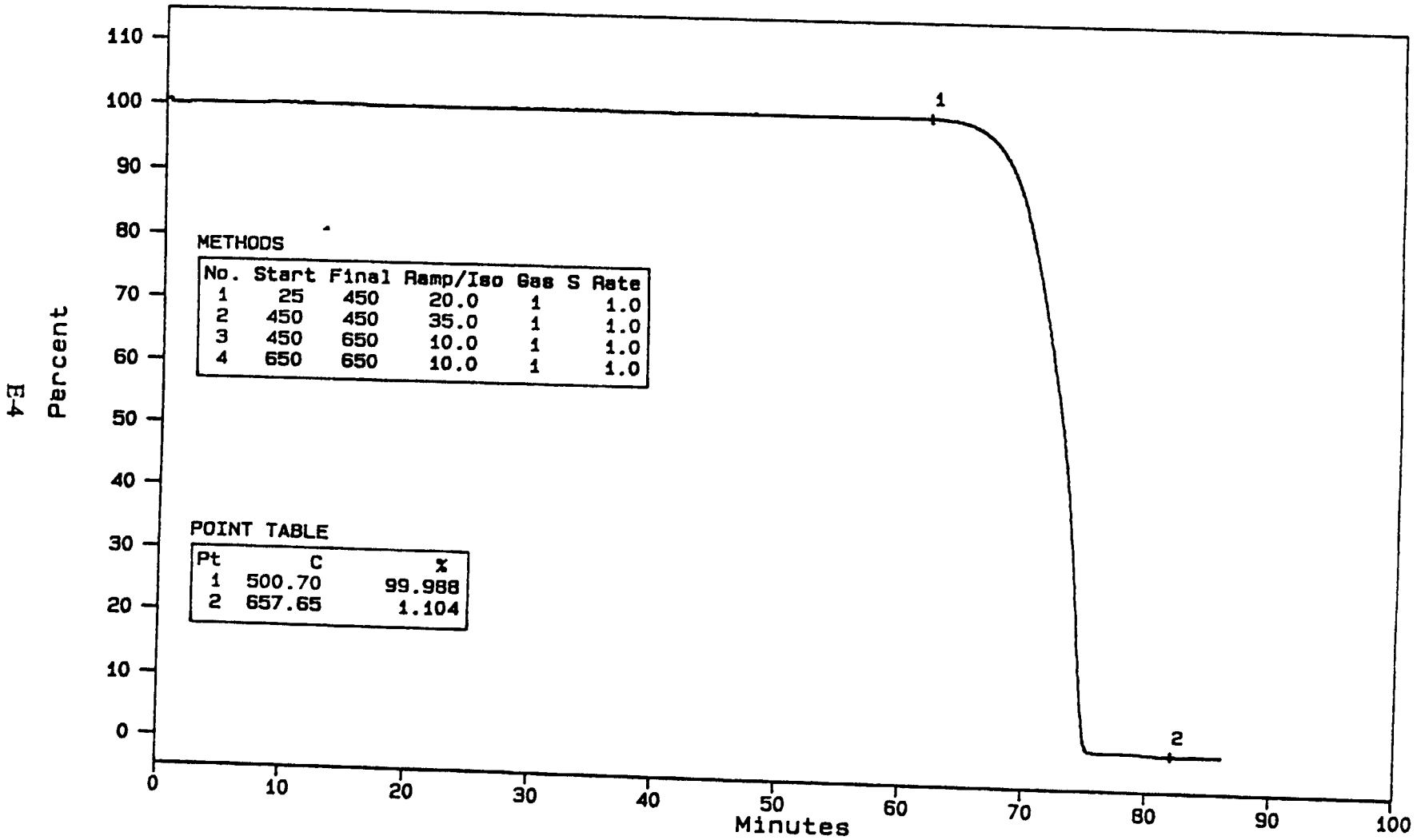

Figure E-1
TGA Calibration Curve

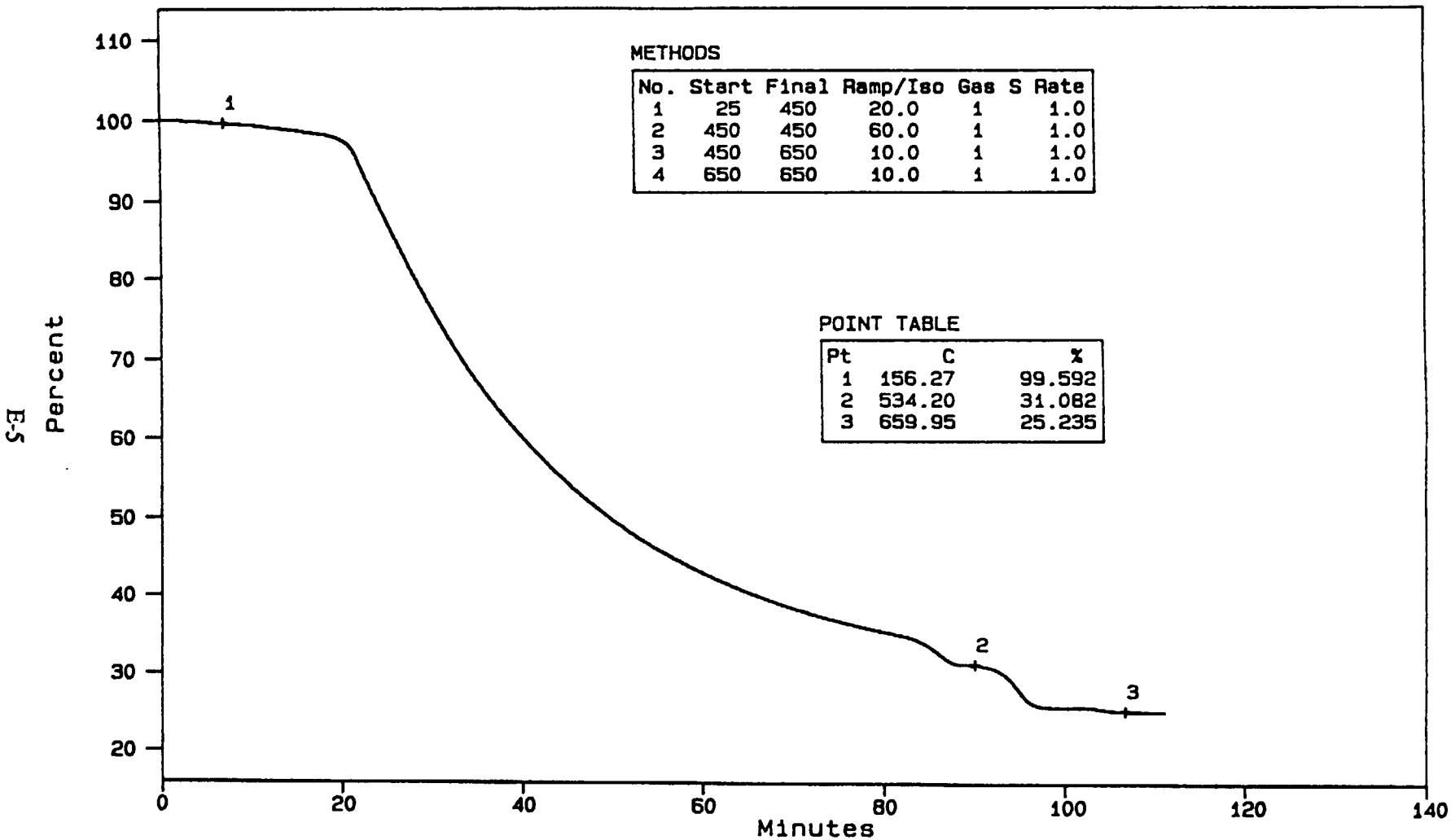

Figure E-2
TGA Curve for Exposed EPR Sample TA4

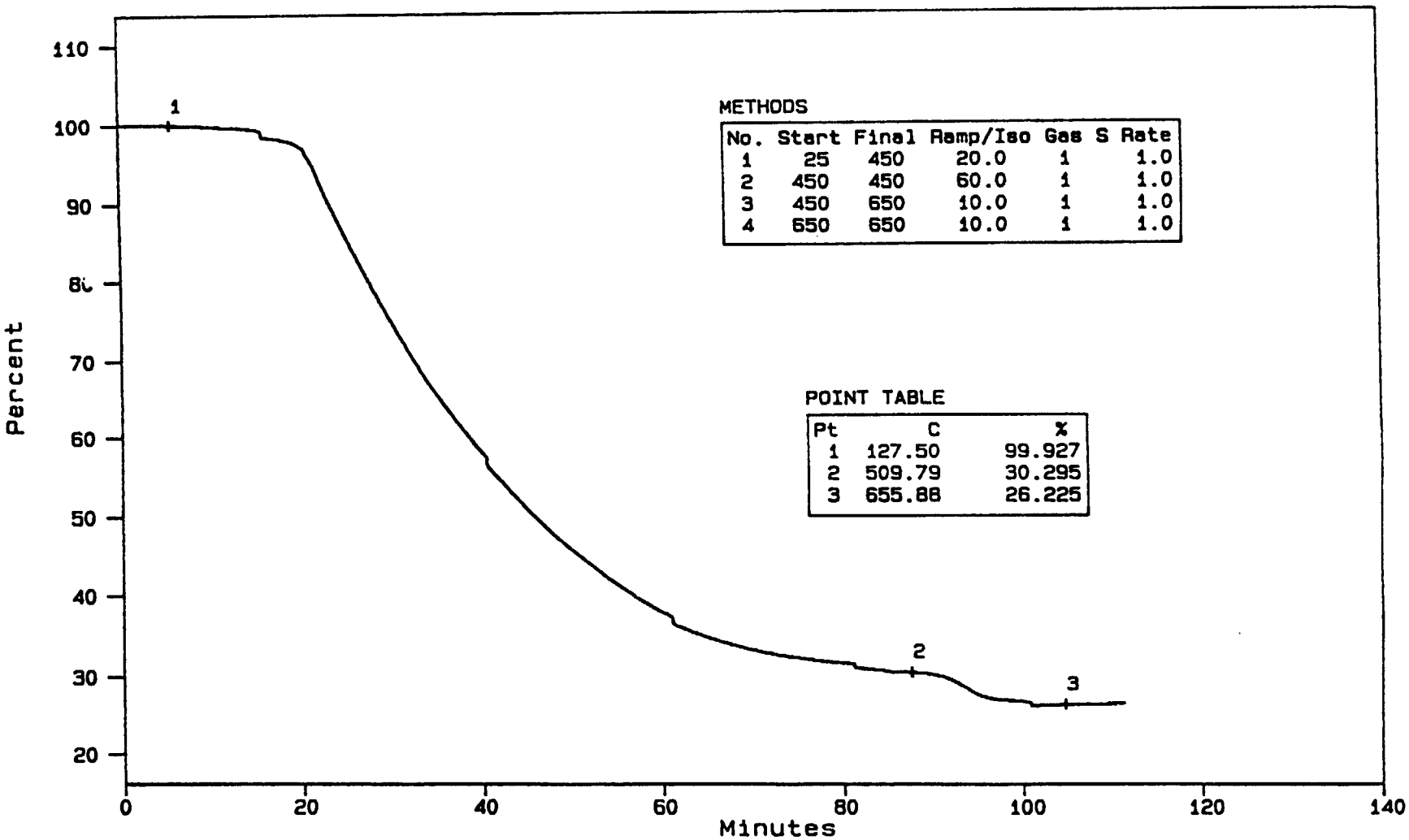

Figure E-3
TGA Curve for Exposed EPR Sample TA7

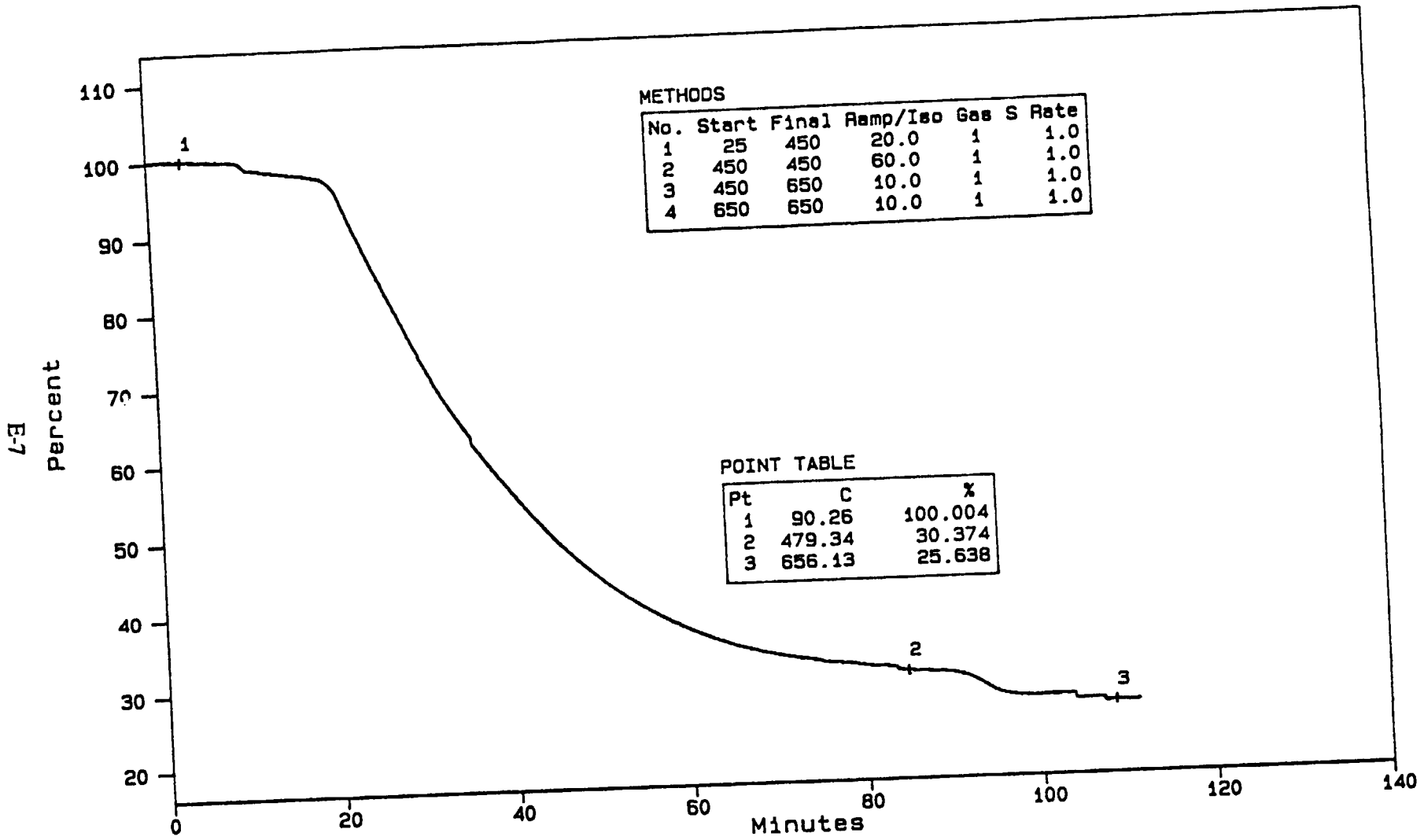

Figure E-4
TGA Curve for Exposed EPR Sample TA10

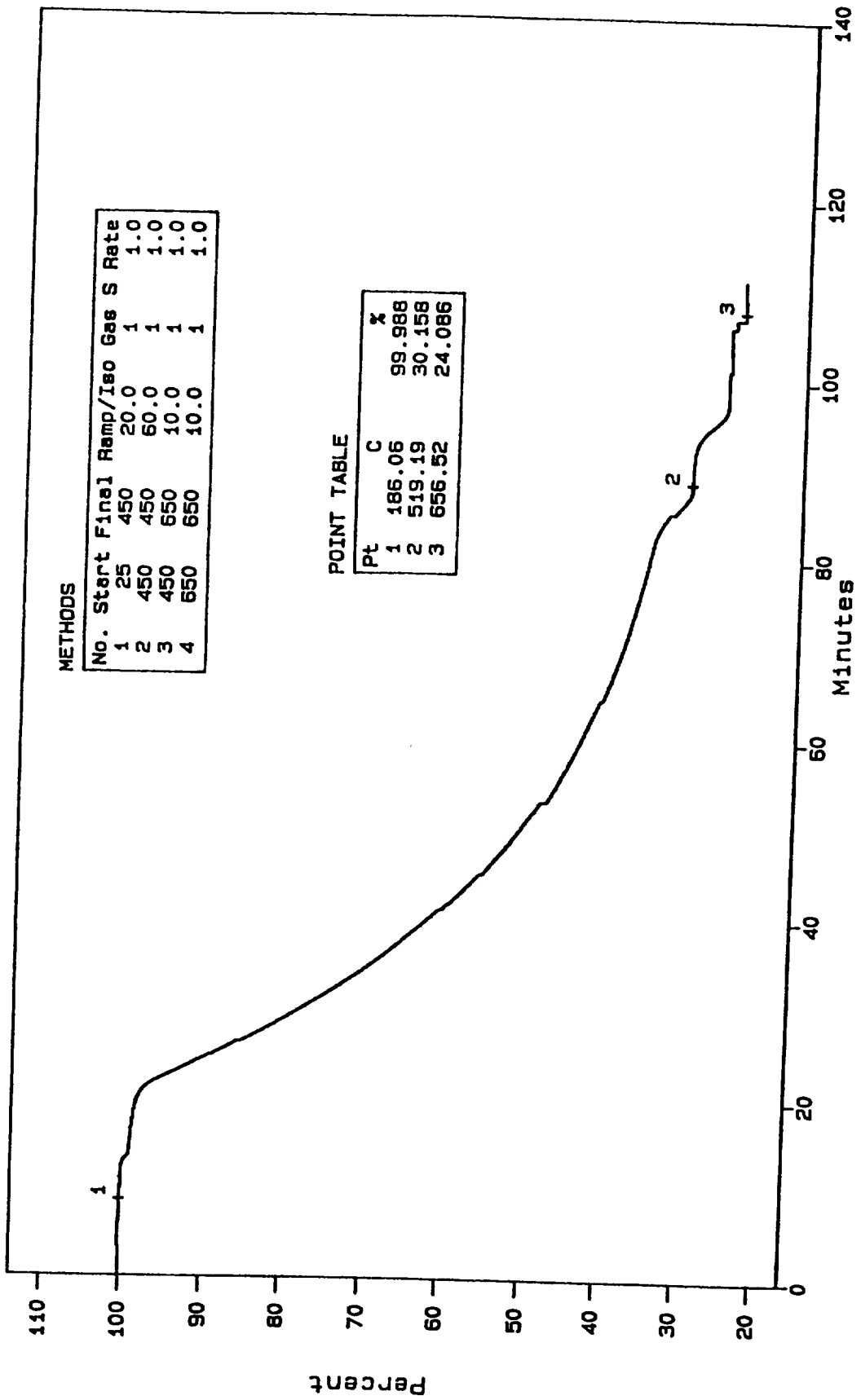

Figure E-5
TGA Curve for Exposed EPR Sample T1

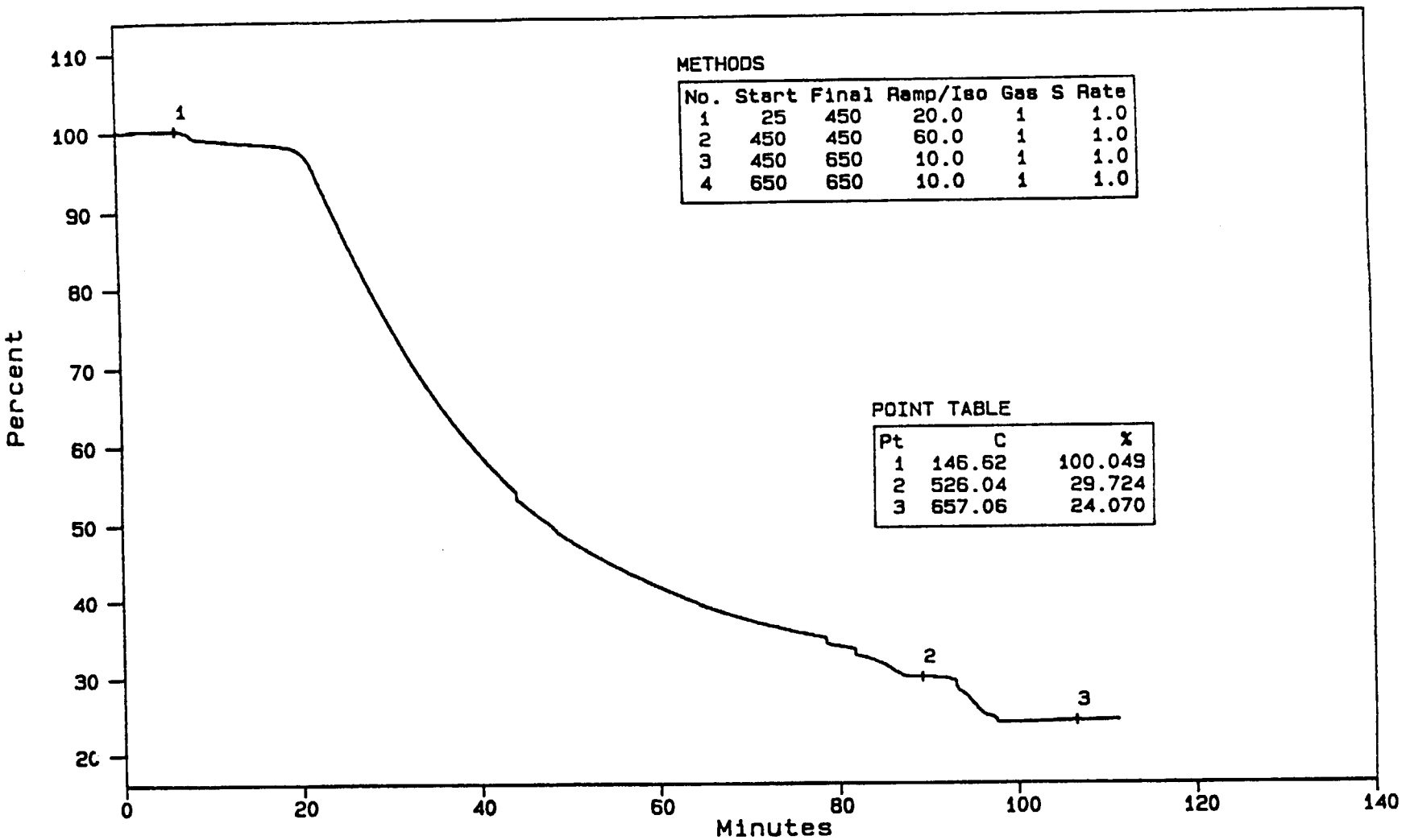

Figure E-6
TGA Curve for Exposed EPR Sample T2

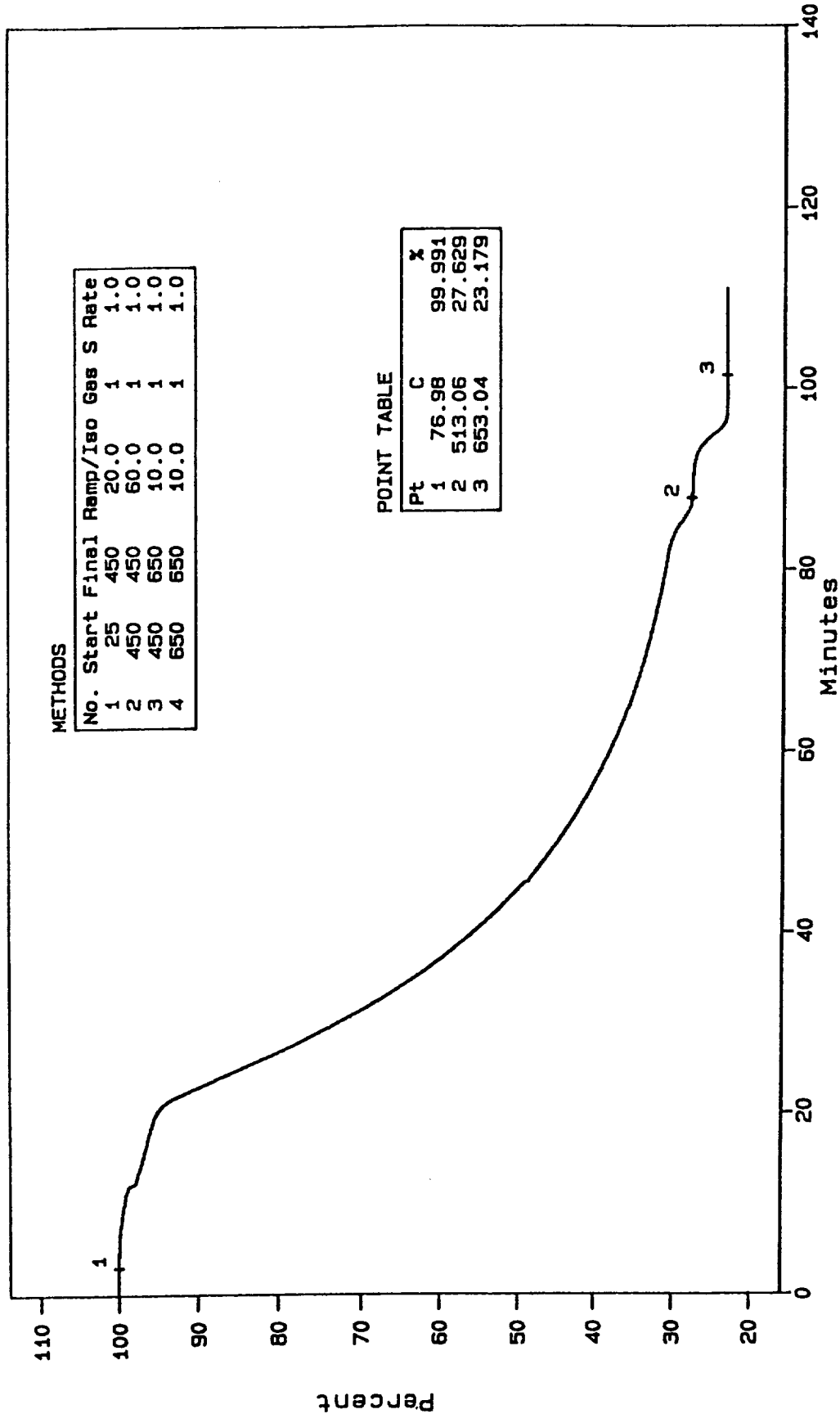

Figure E-7
TGA Curve for Exposed EPR Sample T3

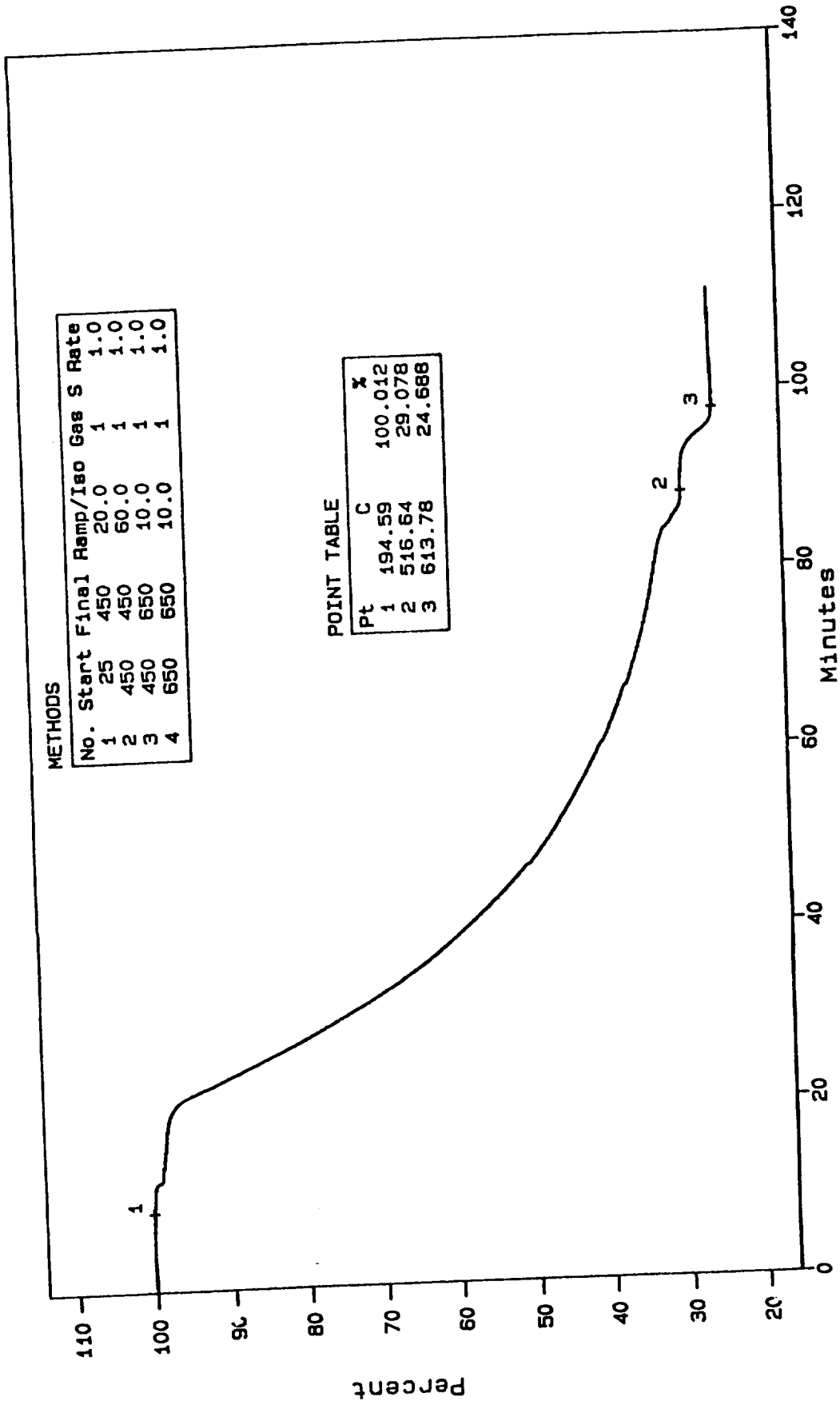

Figure E-8
TGA Curve for Exposed EPR Sample T4

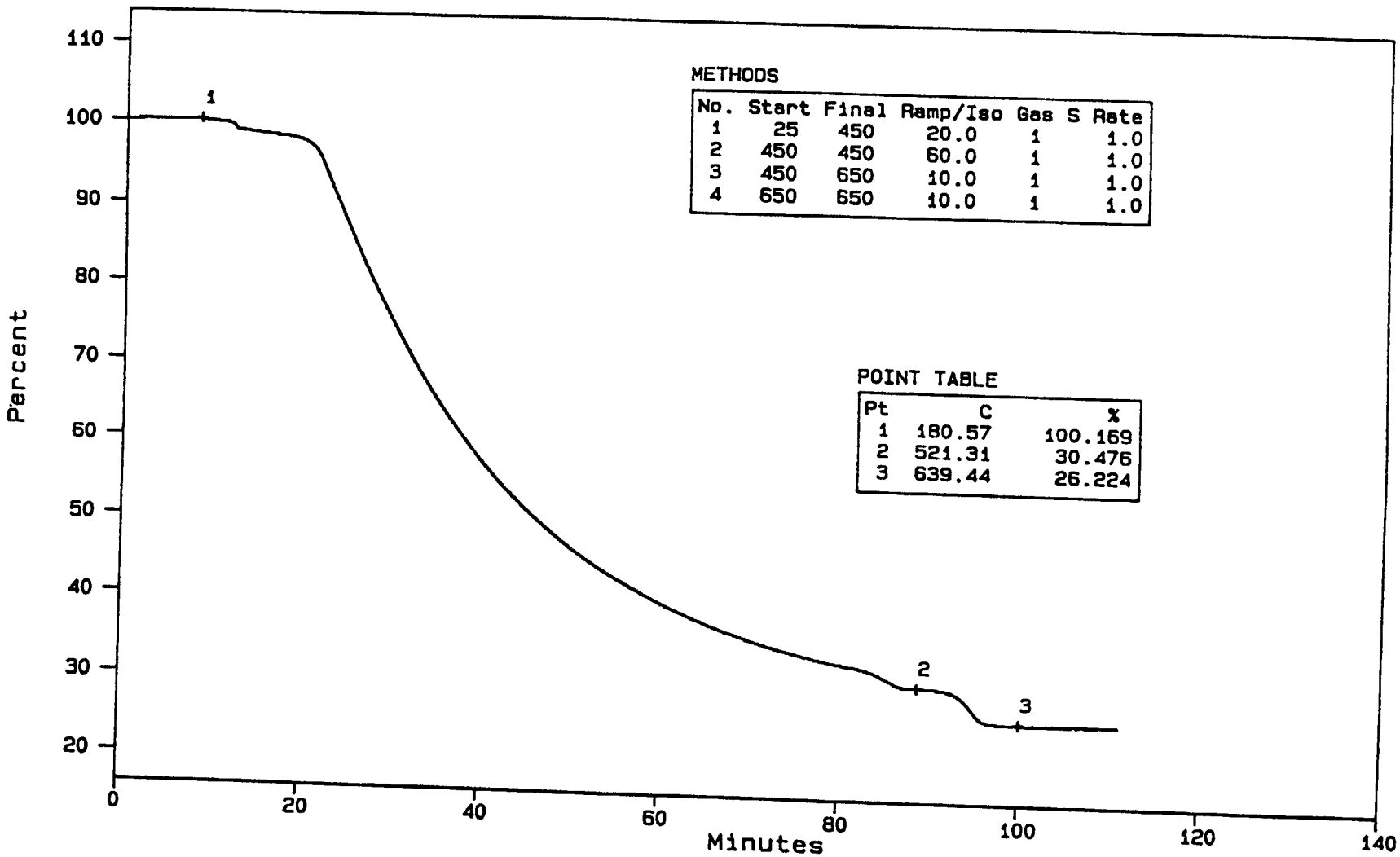

Figure E-9
TGA Curve for Exposed EPR Sample T5

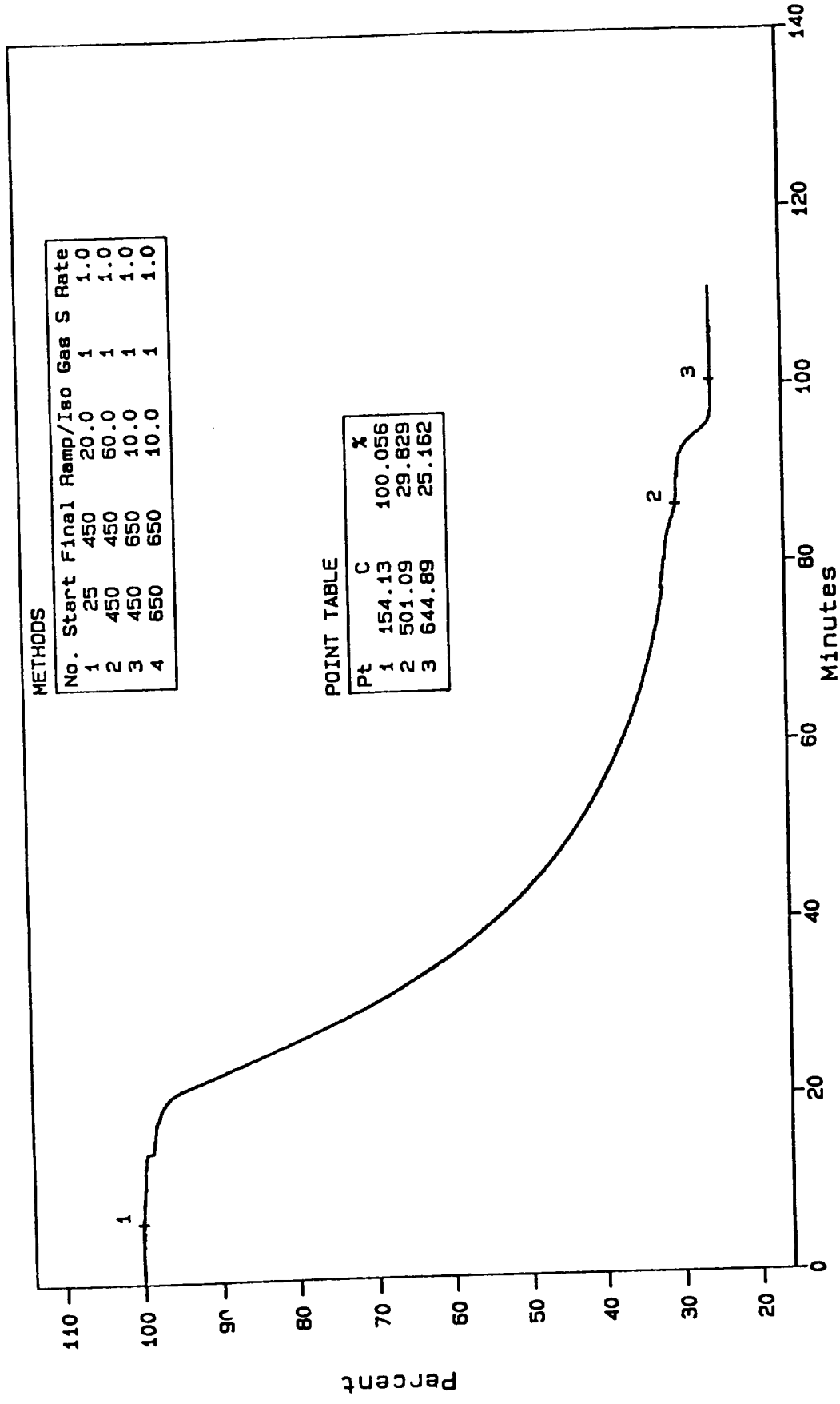

Figure E-10
TGA Curve for Exposed EPR Sample T6

Appendix F
Detailed EPR TMA Data

Table F-1
Detailed EPR TMA Results

Sample	WSTF #	Tan δ Onset (T_{g1}), °C	Temperature of Modulus Curve Drop (T_{g2}), °C	Storage Modulus (T_{g2}), MPa	Storage Modulus at 20 °C, MPa	Sample Thickness (mm)
T1	91-25134	-55.1	-50.6	38.9	2.9	2.435
T2	91-25134	-56.6	-51.3	12.3	1.1	1.745
T3	91-25134	-51.8	-49.1	19.3	2.2	2.230
T4	91-25436	-55.5	-51.1	21.2	2.6	2.210
T5	91-25436	-53.9	-52.1	13.5	0.7	1.465
T6	91-25436	-55.6	-49.5	20.1	1.7	2.290
TA4	91-25361	-54.5	-48.2	24.9	2.4	2.040
TA7	91-25361	-55.4	-50.1	18.4	1.5	2.105
TA10	91-25361	-57.5	-50.5	20.9	1.7	1.805

Dependence of TMA Results on Sample Thickness Regression Output

The results for modulus as a function of thickness (see Figure F-1) at T_g and 20 °C were fitted according to the following equation (see Table F-2 also).

$$MODULUS = CONSTANT + A*X1 + B*X2 + C*X3 + D*X4$$

where X1 = thickness (mm), X2 = shape factor (3/(2X1), X3 = $X1^2$, X4 = $X2^2$ and the results are in MPa.

Table F-2
Coefficients to Modulus Equation

Thermal Analysis Measurement	Constant	A	B	C	D	R squared/ N, DF
Modulus, T_g	93680.52	-32746.2	-78555.5	4252.947	24429.43	0.955588
Standard Error	2.303830	6607.645	16267.41	845.5477	5118.432	9,4
Modulus, 20 °C	4647.578	-1610.71	-3924.99	207.3723	1227.175	0.767639
Standard Error	0.490401	1406.525	3462.737	179.9861	1089.526	9,4

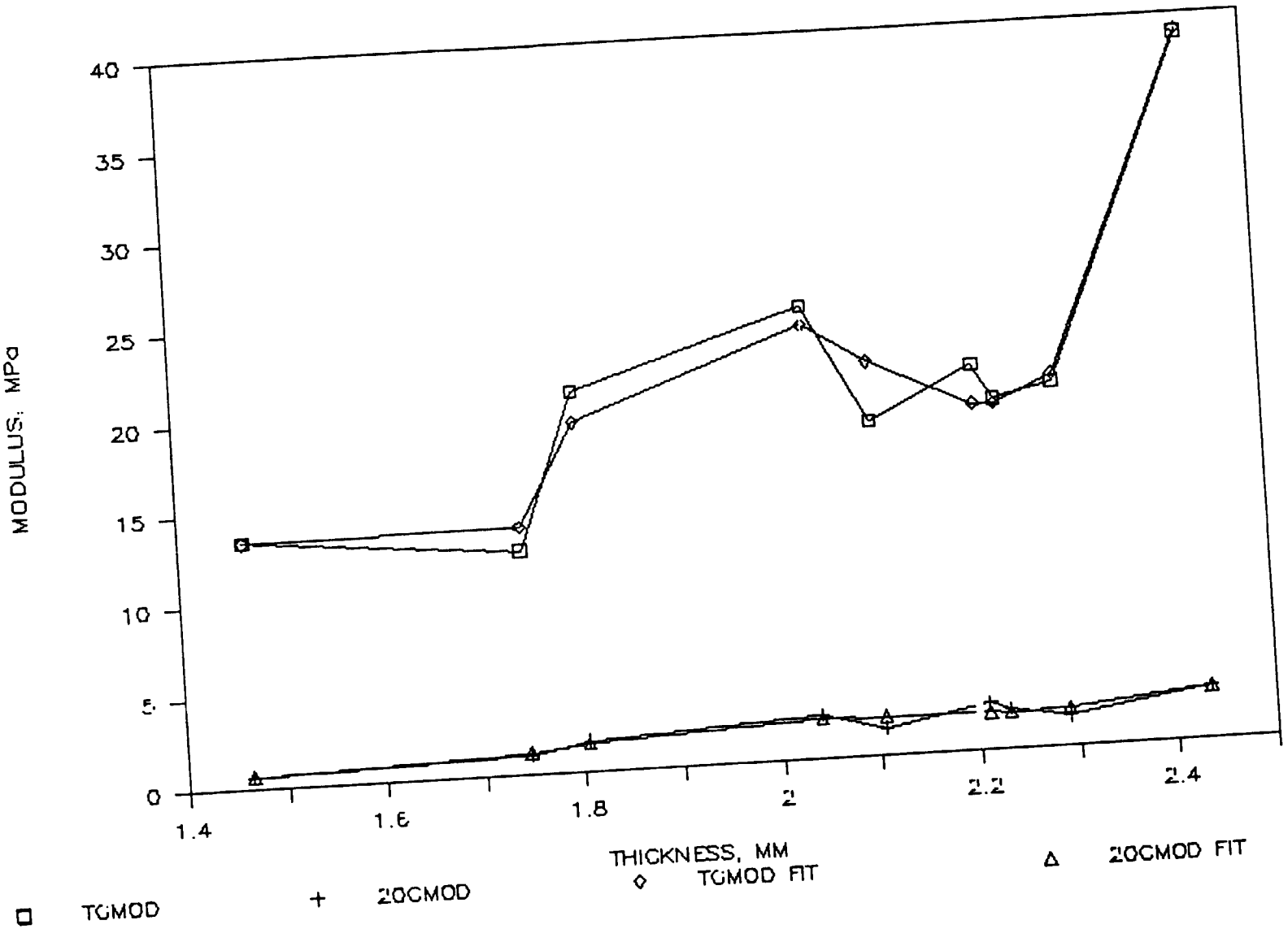

Figure F-1
Effect of Sample Thickness on Modulus

Appendix G
Metal Casing Samples Location

BASELINE SAMPLING REQUIREMENT: Reference Step 05

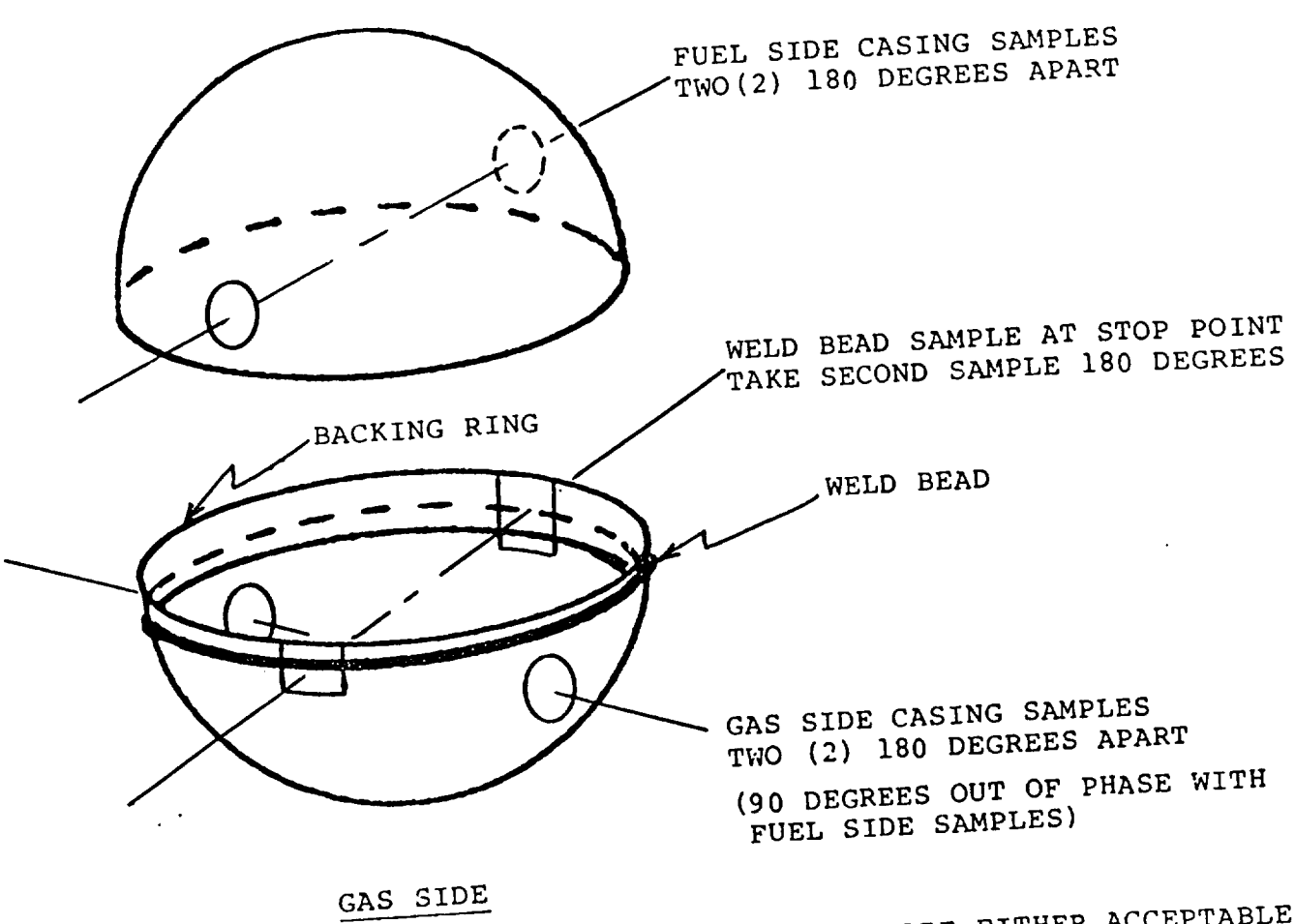

NOTE: SAMPLE SIZE TYPICALLY 1 INCH DIAMETER OR SQUARE,EITHER ACCEPTABLE.

Figure G-1
General Metal Casing Samples Location

APU TANK THICKNESS DATA

All location codes shown were referenced clockwise (C) from the reference punch marks on the outer metal shell and down (D) from the cut edge(s). All measurements were taken with a Krautkramer-Branson digital thickness monitor which was calibrated on the Ti-6Al-4V APU Tank wall at two (2) locations near the circumferential cut edge(s).

FUEL SIDE

LOCATION CODE			THICKNESS (IN.)
A	C0	D1.25	0.151
B	C0	D6	0.052
C	C18	D18	0.212
D	C75	D11	0.051
E	C47	D6	0.051
F	C22	D6	0.051
G	C67	D6	0.052

GAS SIDE

LOCATION CODE			THICKNESS (IN.)
A	C6	D6	0.050
B	C0	D5.5	0.049
C	C0	D16.5	0.068
D	C20	D5.5	0.049
E	C20	D15.5	0.055
F	C41	D5.5	0.049
G	C41	D15.5	0.054
H	C64	D5.5	0.049
I	C64	D15.5	0.055

LAYOUT SHEET: Reference Step 04

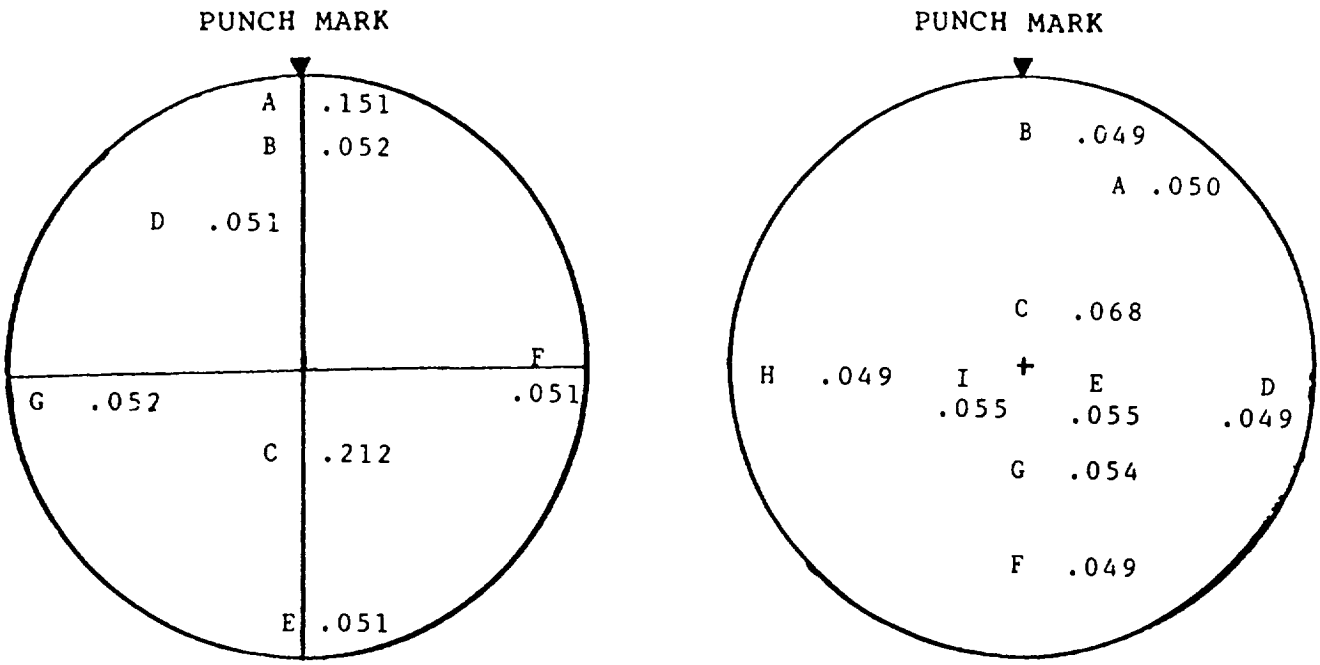

(INTERIOR VIEW)

FUEL SIDE

GAS SIDE

Figure G-2
Metal Casing Samples Code Location

Appendix H
Figures

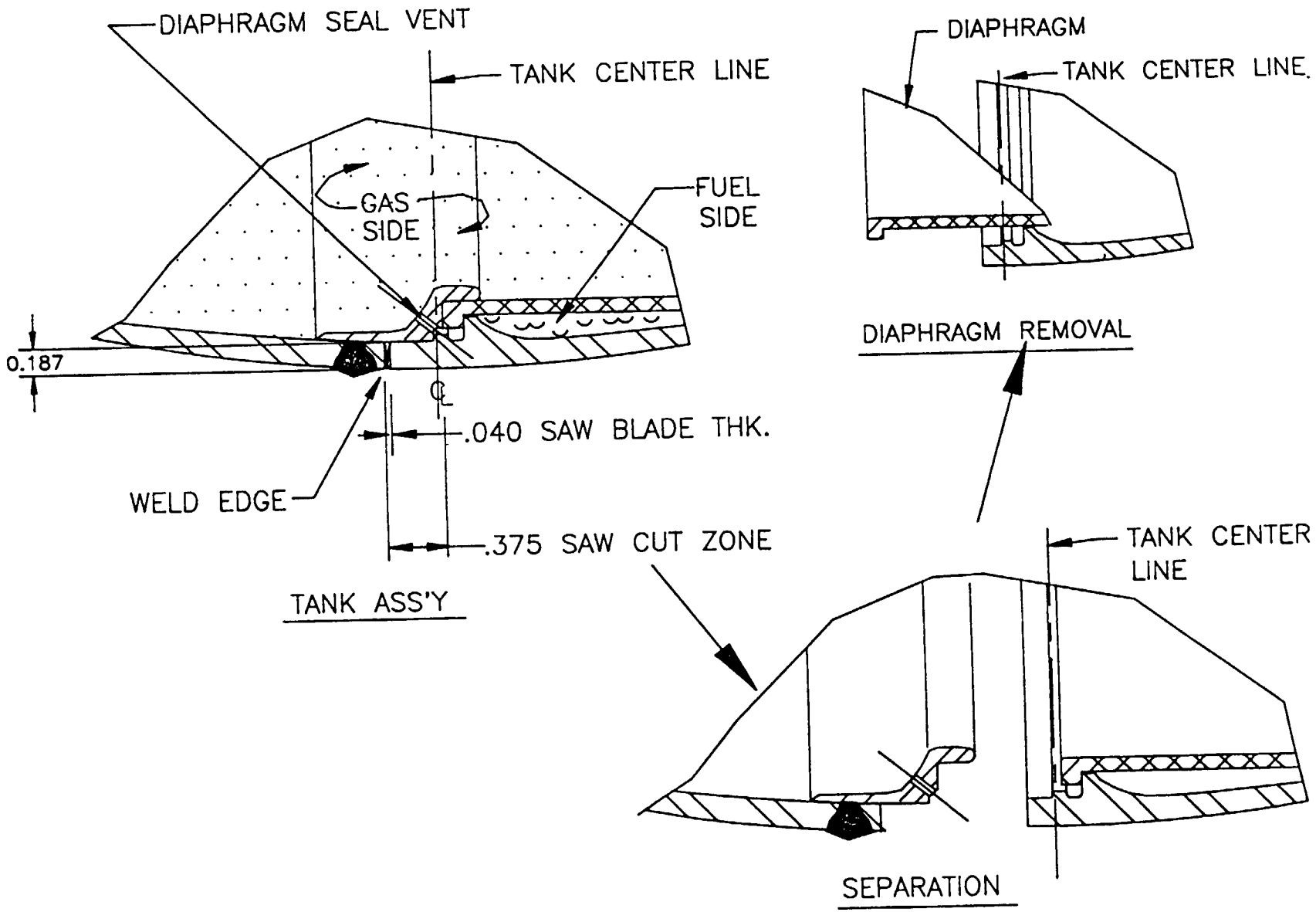

Figure H-1
Tank Assembly Construction

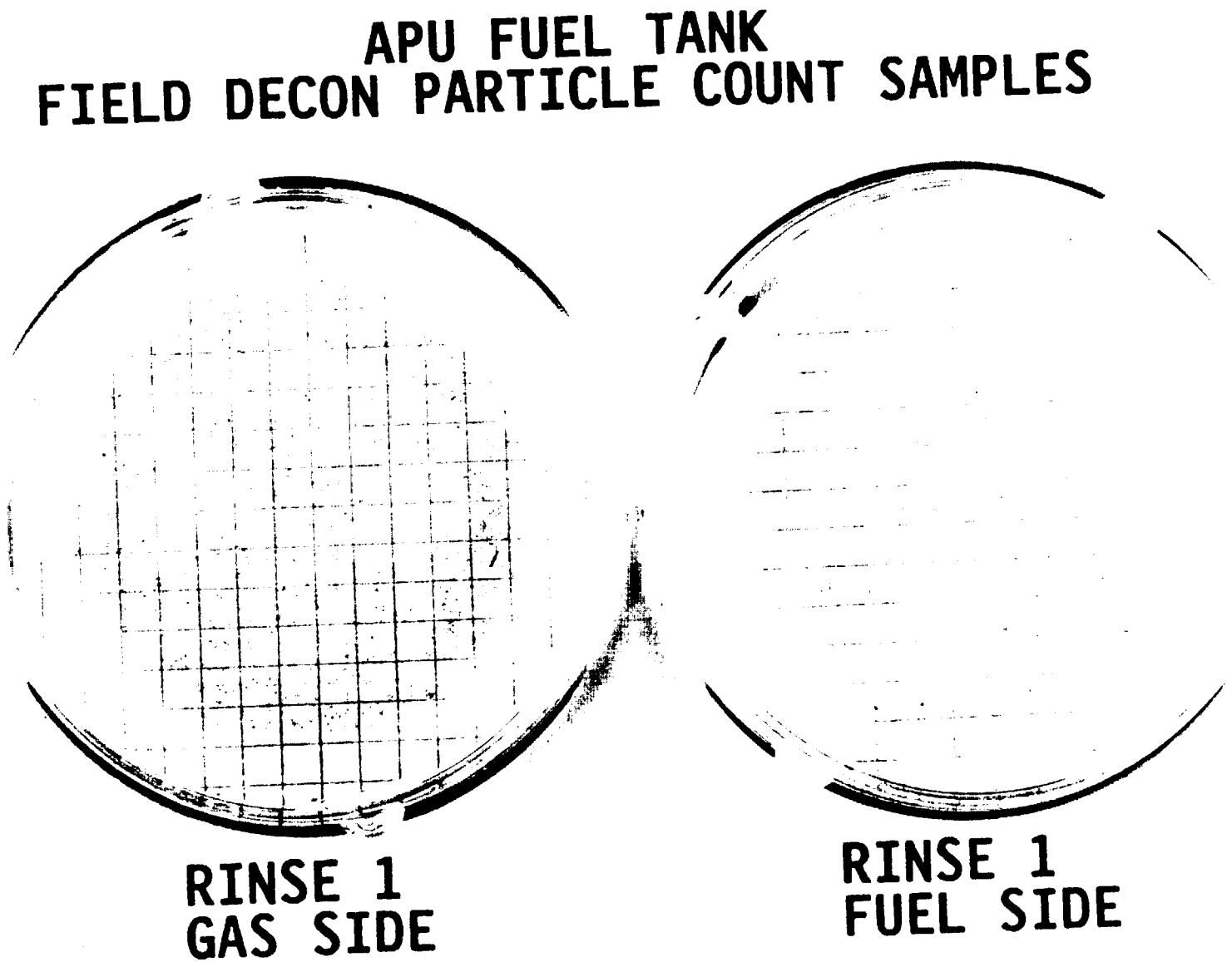

Figure H-2
APU Fuel Tank Particle Count Samples

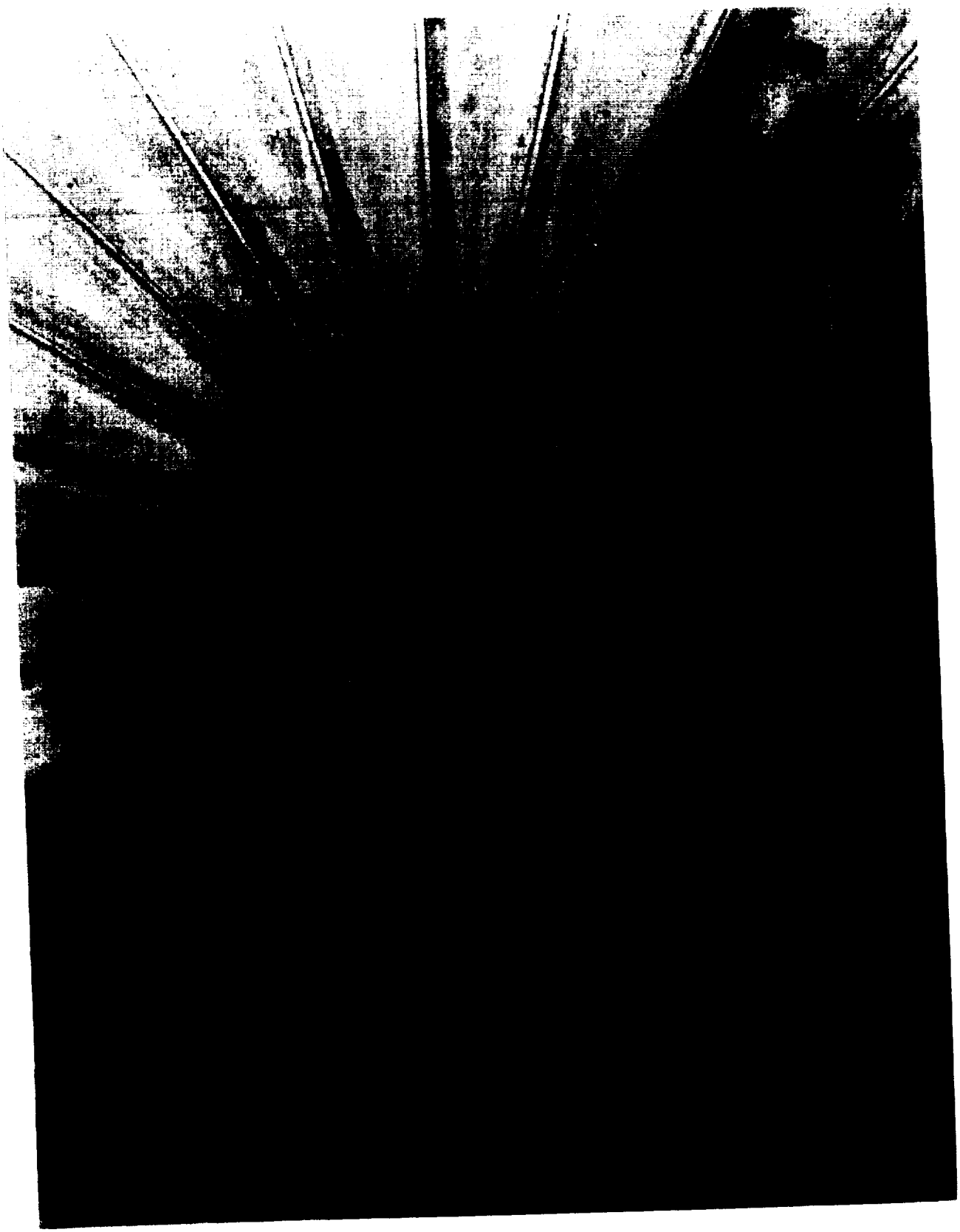

Figure H-3
Close-up of Fuel Side, Center of EPR Diaphragm

ORIGINAL PAGE
COLOR PHOTOGRAPH

ORIGINAL PAGE
COLOR PHOTOGRAPH

Figure H-4
Light/Dark Transition on EPR Diaphragm, First View

ORIGINAL PAGE
COLOR PHOTOGRAPH

Figure H-5
Light/Dark Transition on EPR Diaphragm, 180° from First View

ORIGINAL PAGE
COLOR PHOTOGRAPH

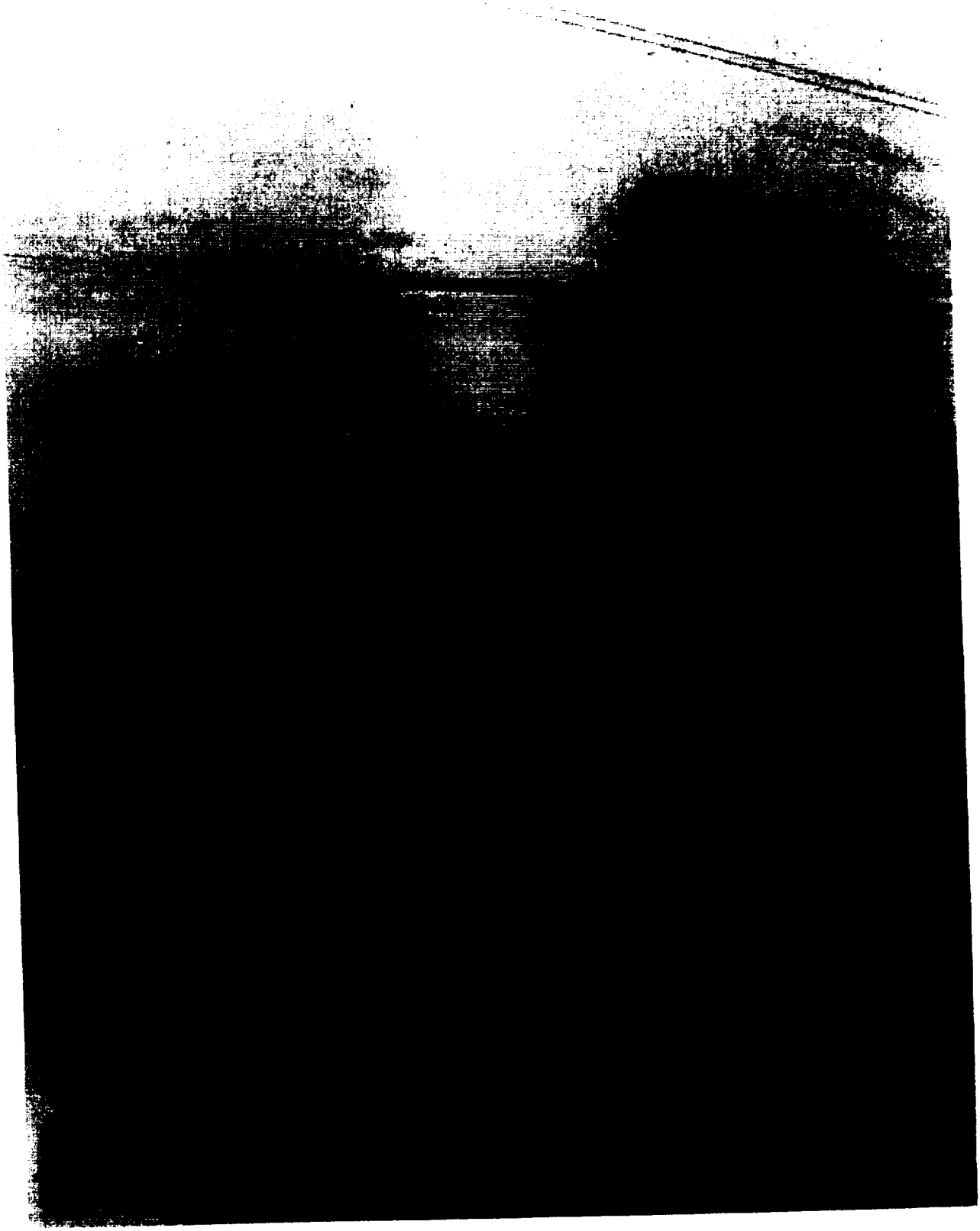

Figure H-6
Close-up of Typical Stains on EPR Diaphragm

ORIGINAL PAGE
COLOR PHOTOGRAPH

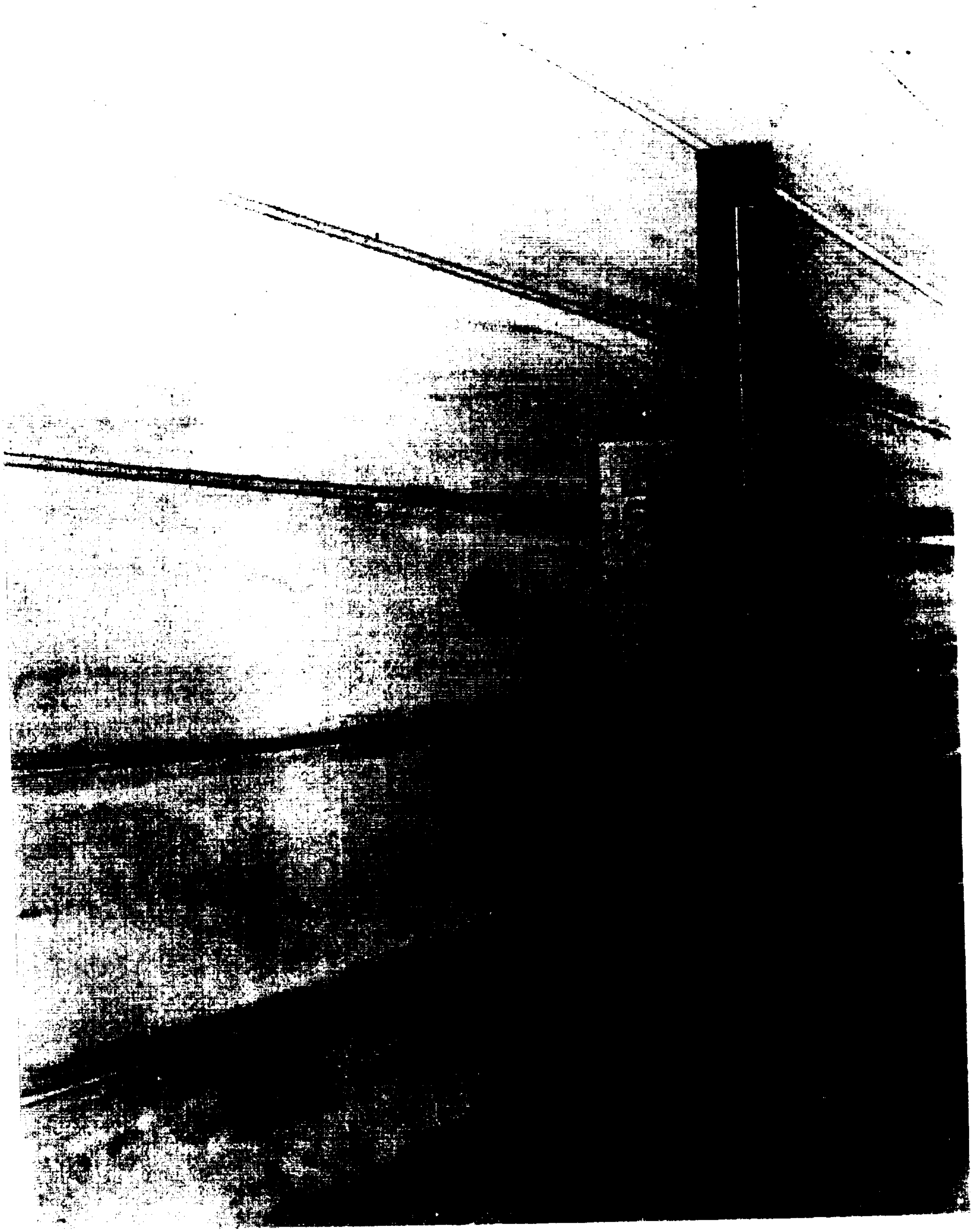

Figure H-7
Close-up of One Typical Stain on EPR Diaphragm

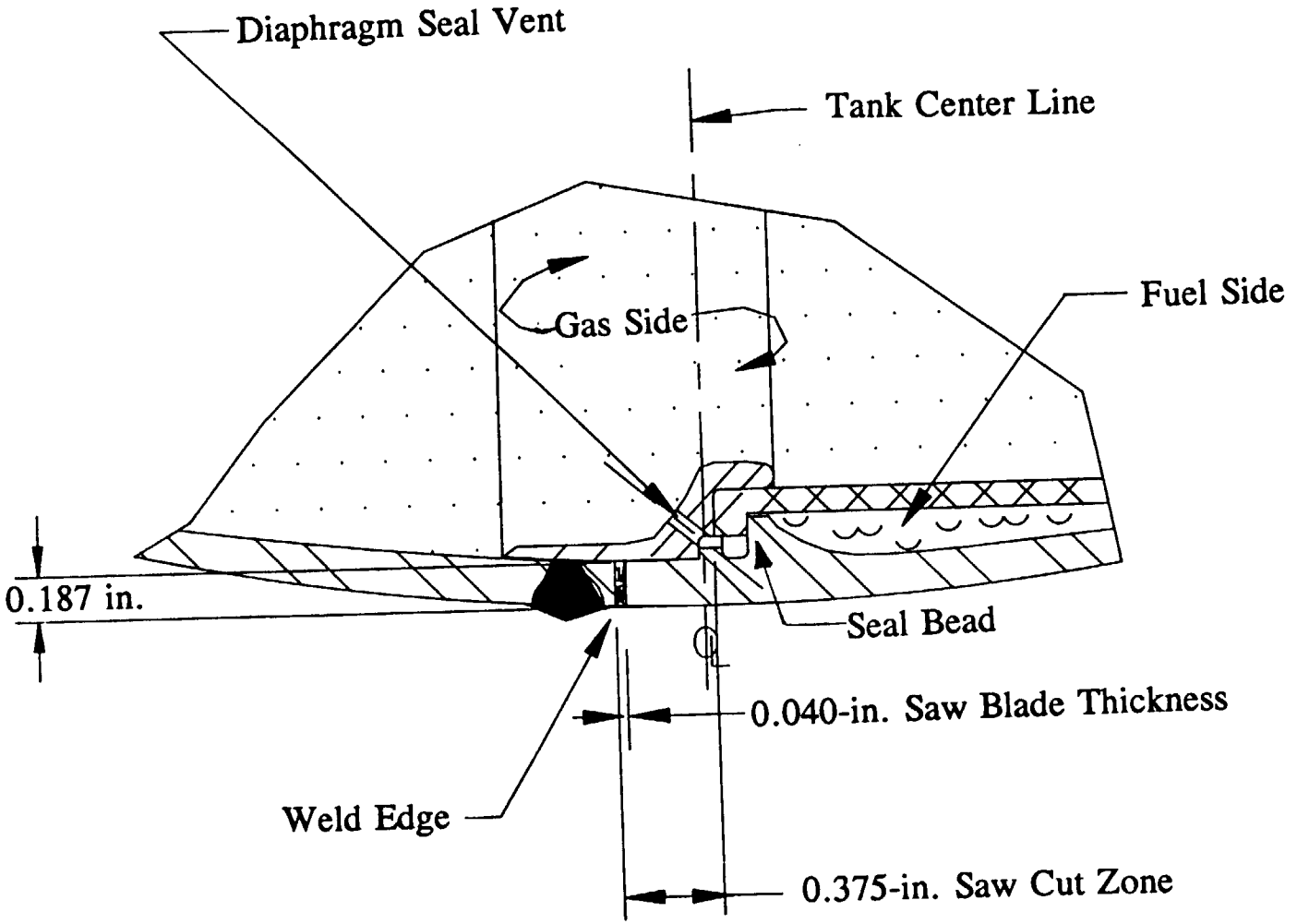

Figure H-8
Dissection of Elastomer Diaphragm

ORIGINAL PAGE
COLOR PHOTOGRAPH

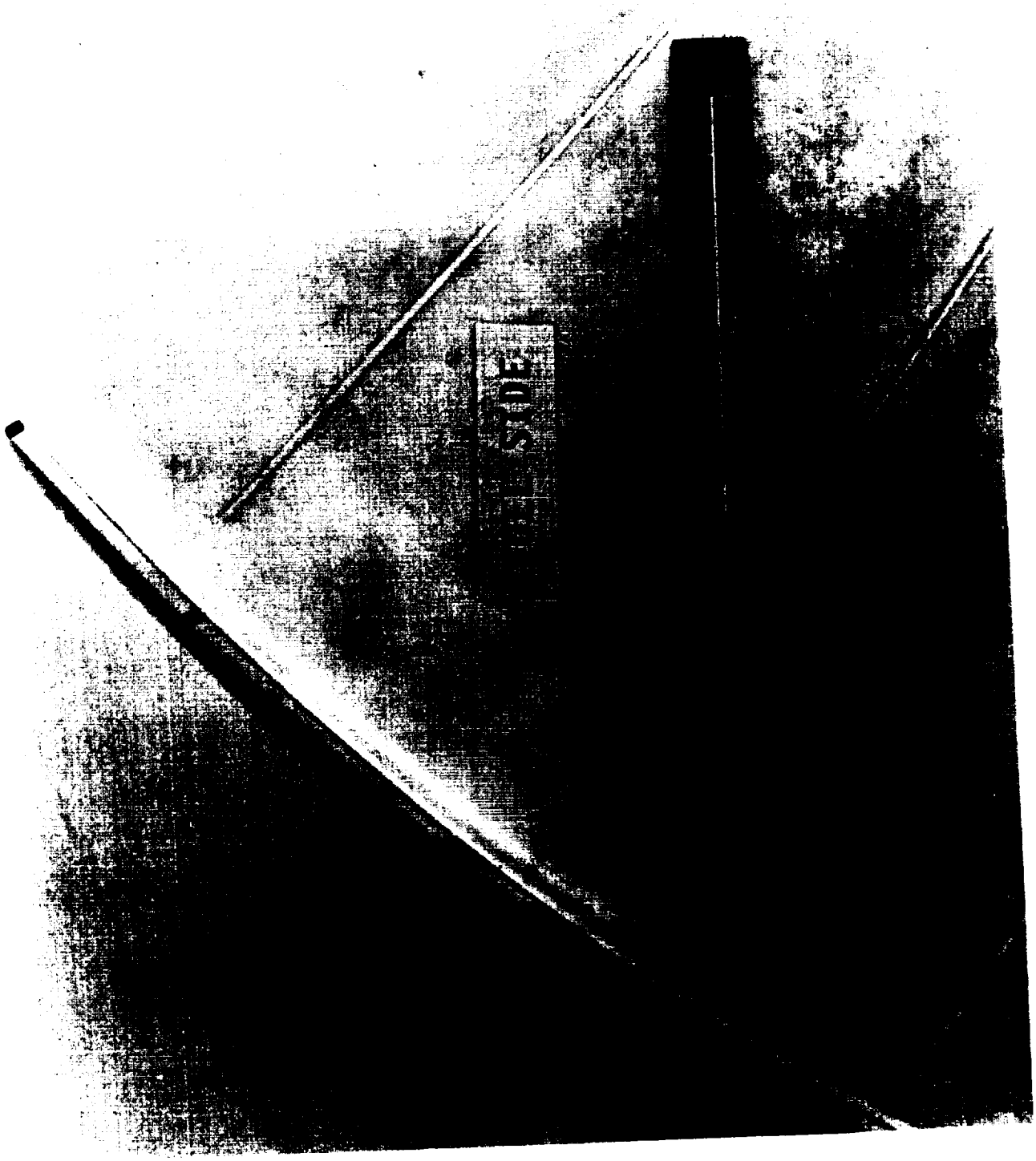

Figure H-9
Close-up of EPR Diaphragm Lip

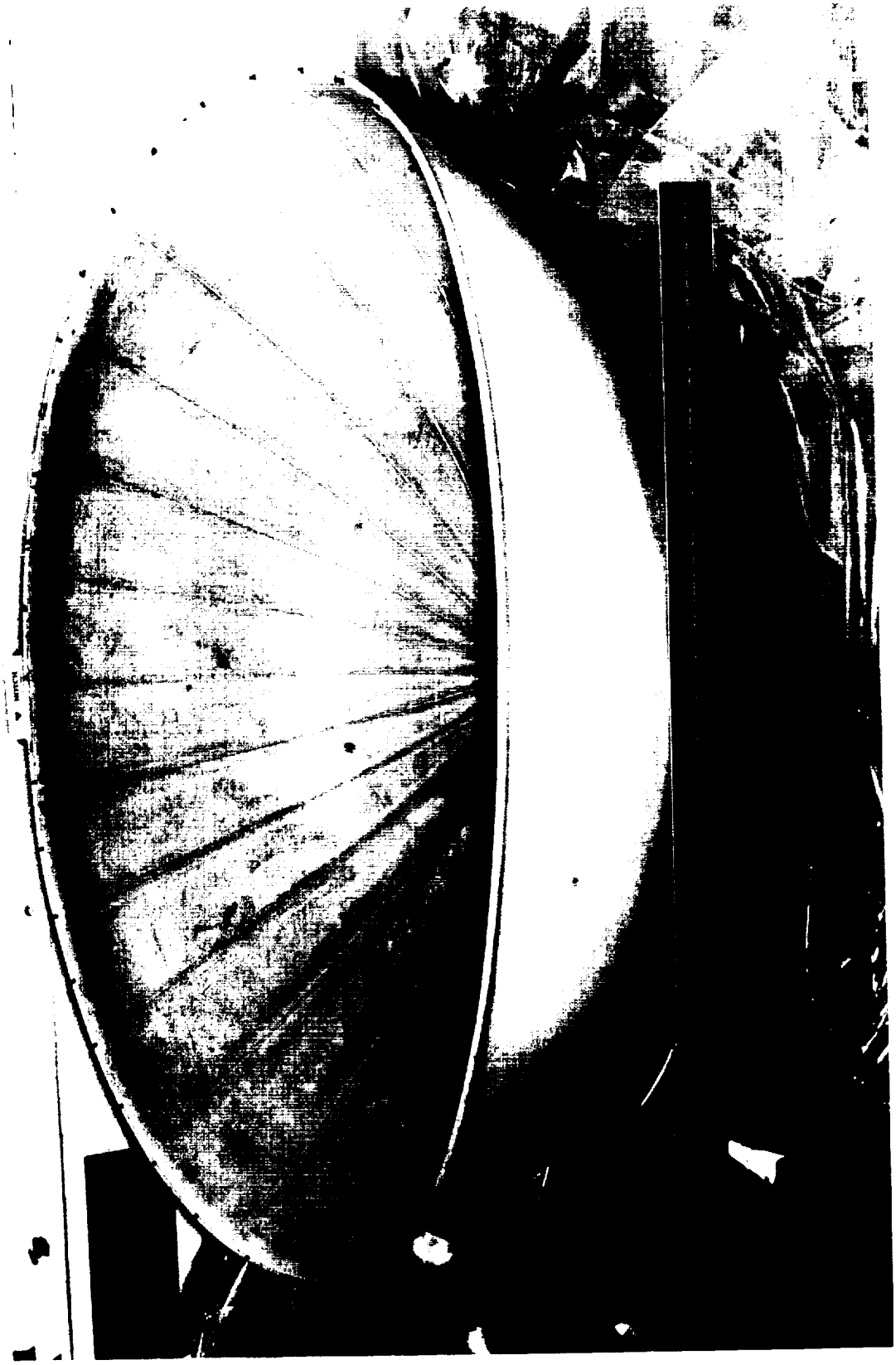

Figure H-10
Fuel Side View of EPR Diaphragm
Marks Indicate Lip Thickness Measure Points

ORIGINAL PAGE
COLOR PHOTOGRAPH

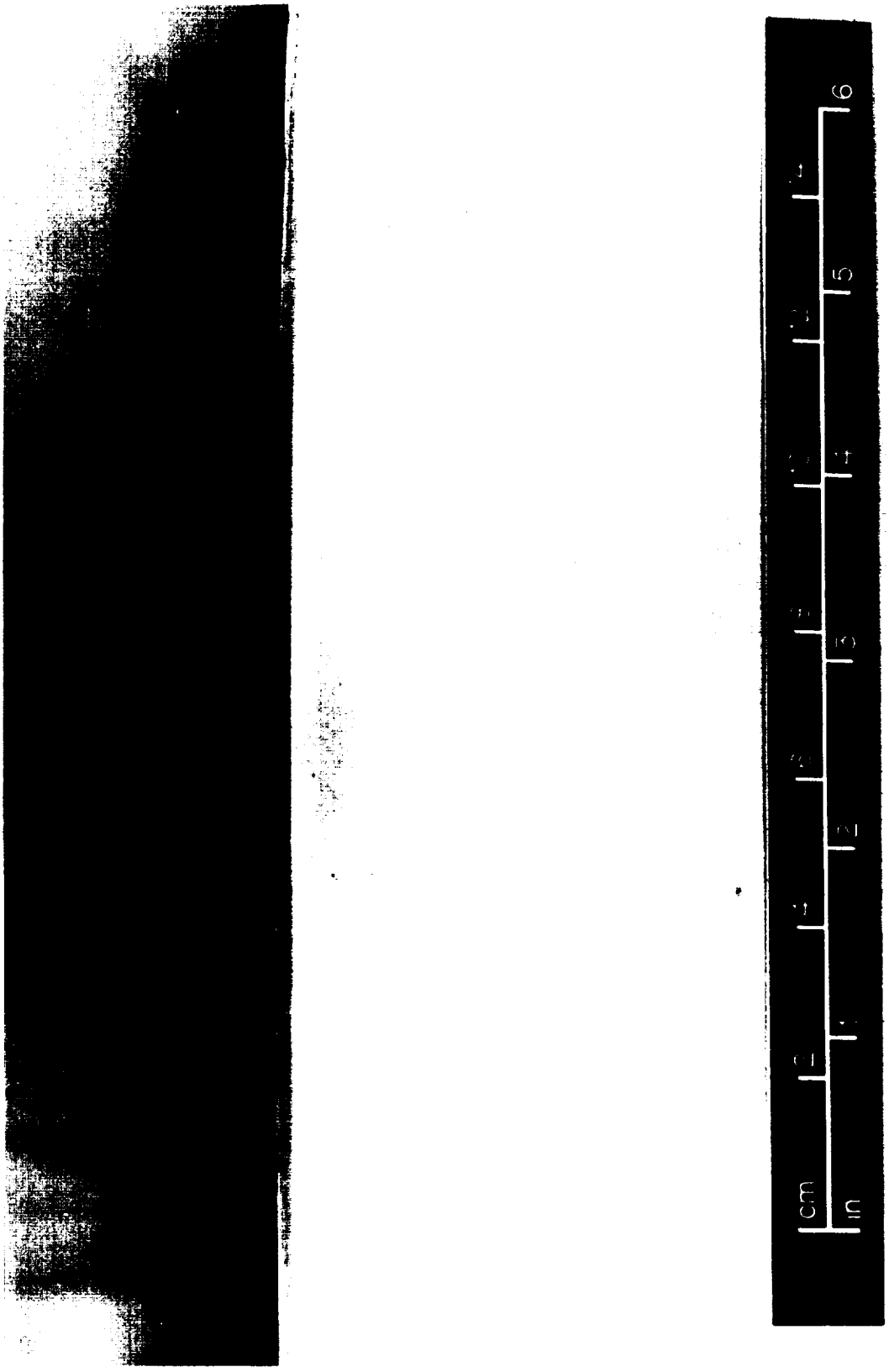

Figure H-11
Back Side of EPR Diaphragm Lip

ORIGINAL PAGE
COLOR PHOTOGRAPH

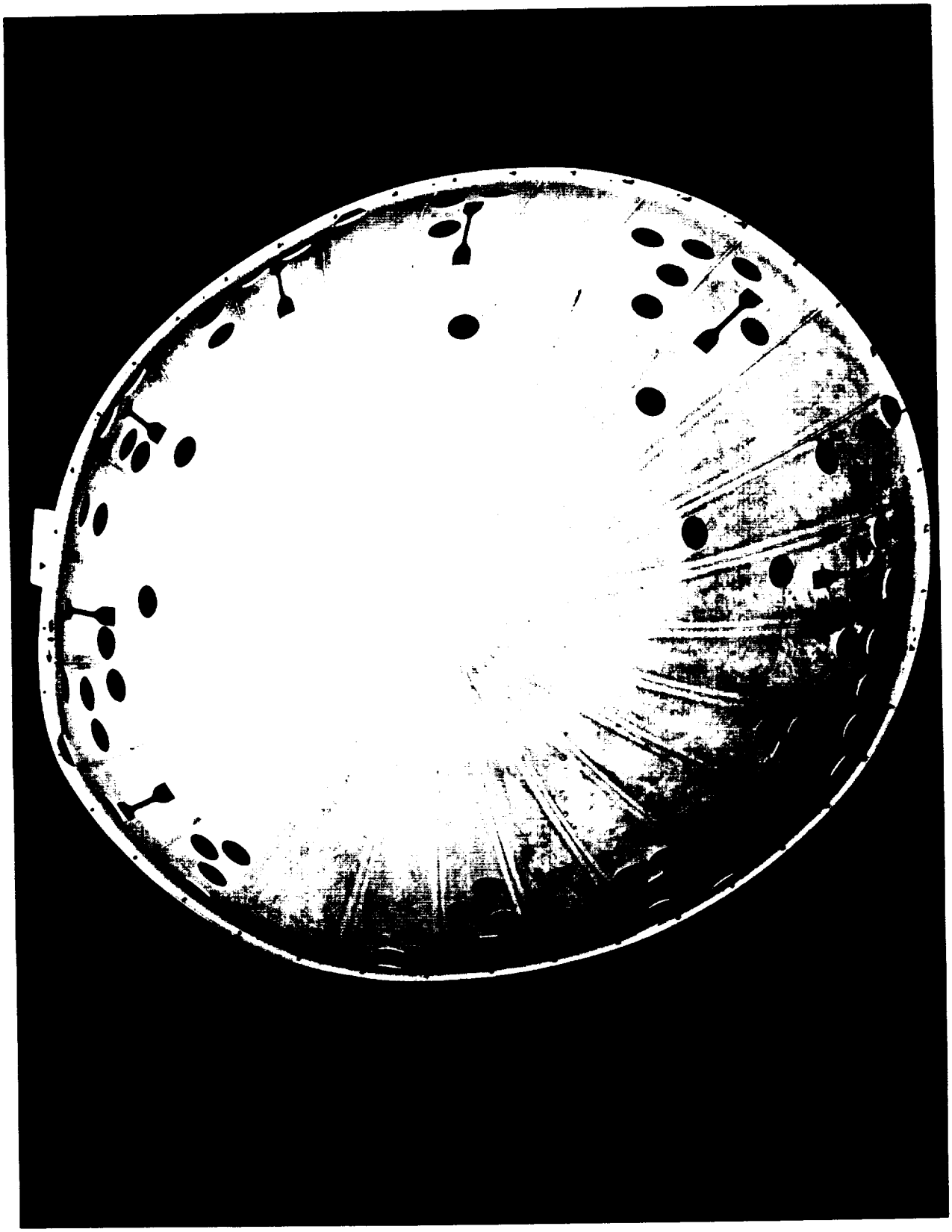

Figure H-12
Exposed Material Samples Location (WSTF # 91-25361)

ORIGINAL PAGE
COLOR PHOTOGRAPH

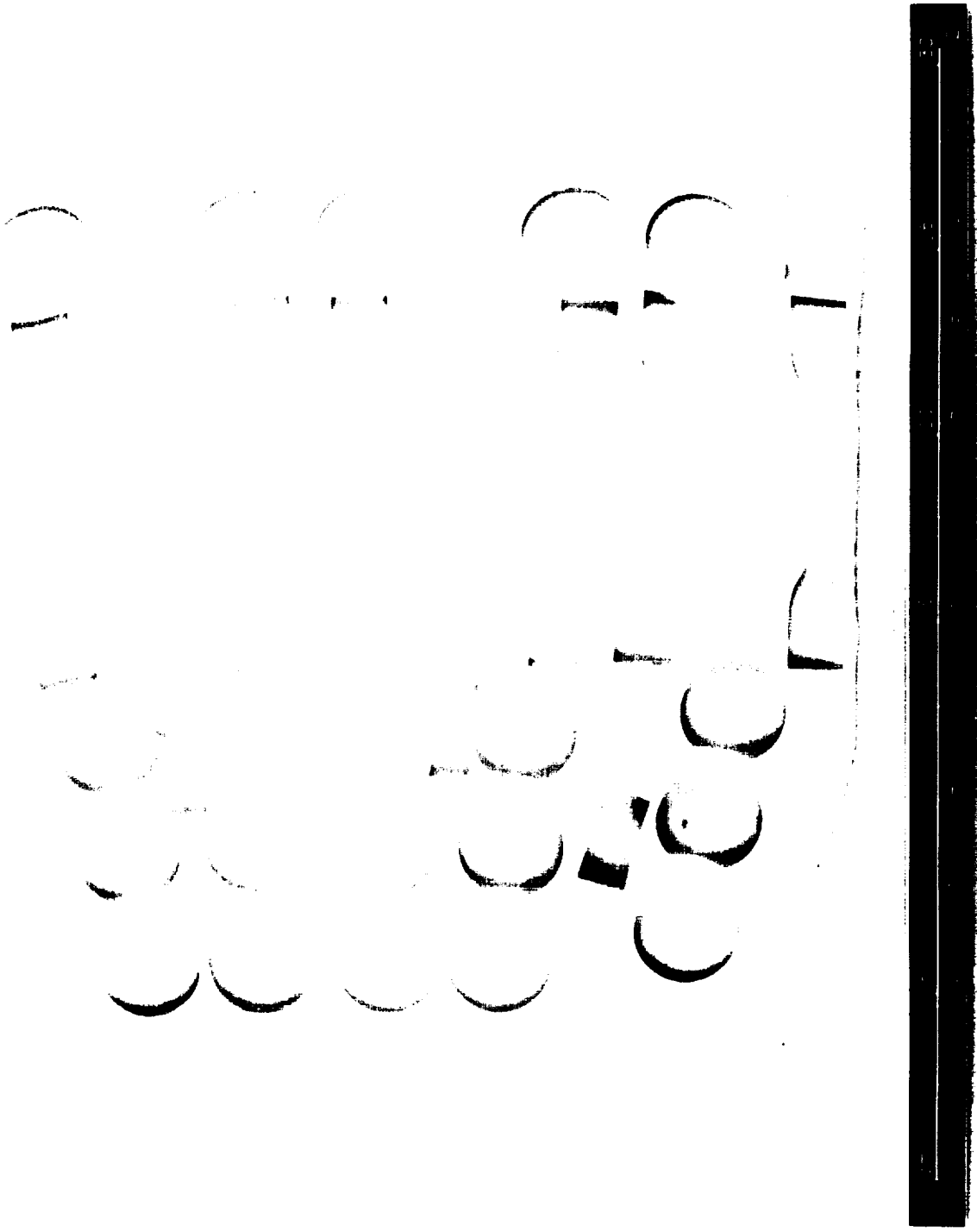

Figure II-13
Unexposed Material Samples Location (WSTF # 91-25134)

0792-1790

ORIGINAL PAGE
COLOR PHOTOGRAPH

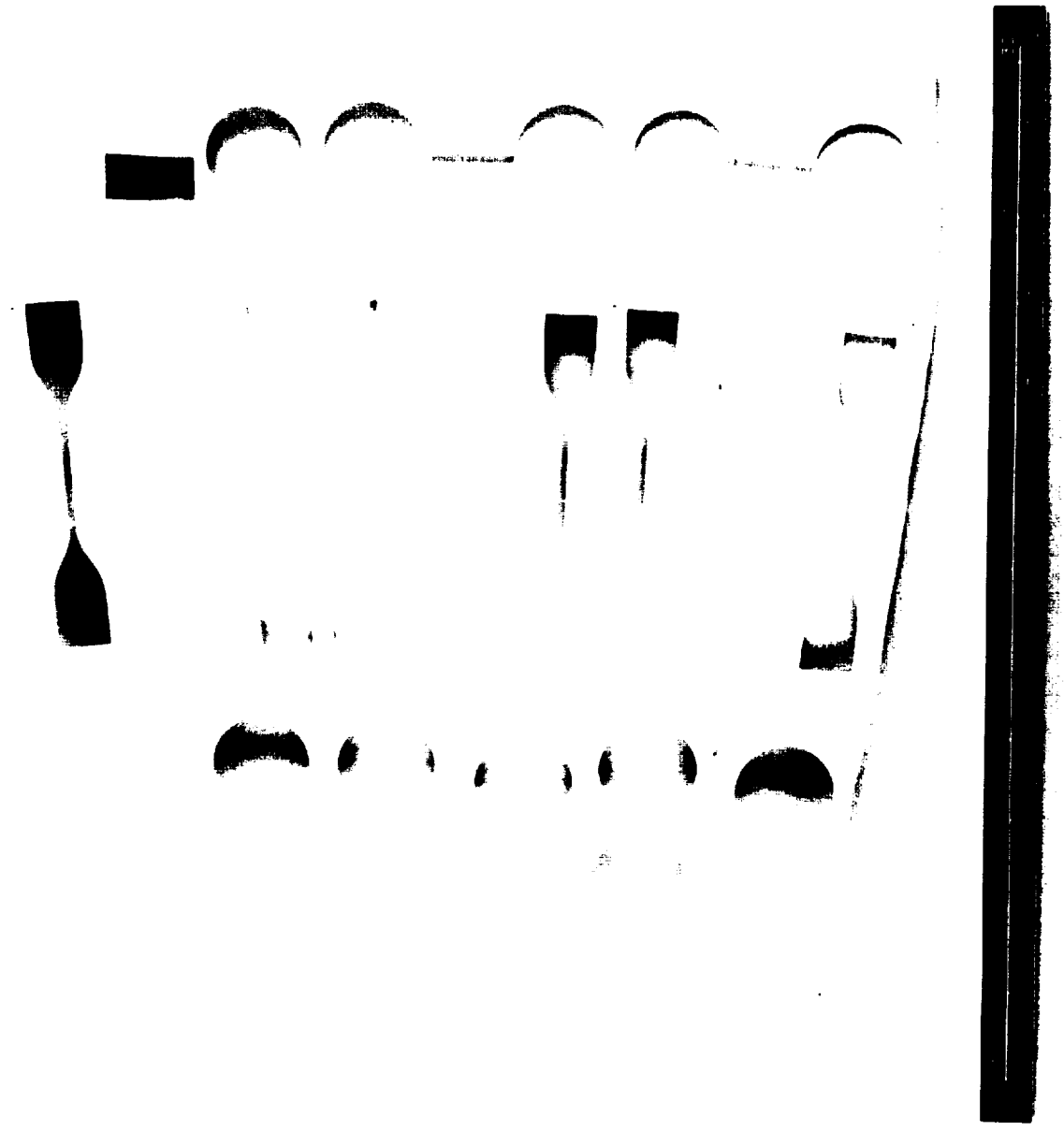

Figure H-14
Unexposed Material Samples Location (WSTF # 91-25136)

0792-1791

ORIGINAL PAGE
COLOR PHOTOGRAPH

Figure H-15
Typical Label on Metal Casing

1191-3140

ORIGINAL PAGE
COLOR PHOTOGRAPH

Figure H-16
Typical PSI Etch Anodized Label on Metal Casing

1191-5149

Figure II-17
Gas Inlet End of Metal Casing

ORIGINAL PAGE
COLOR PHOTOGRAPH

Figure H-18
Typical Heater Arrangement on Metal Casing

1191-3163

ORIGINAL PAGE
COLOR PHOTOGRAPH

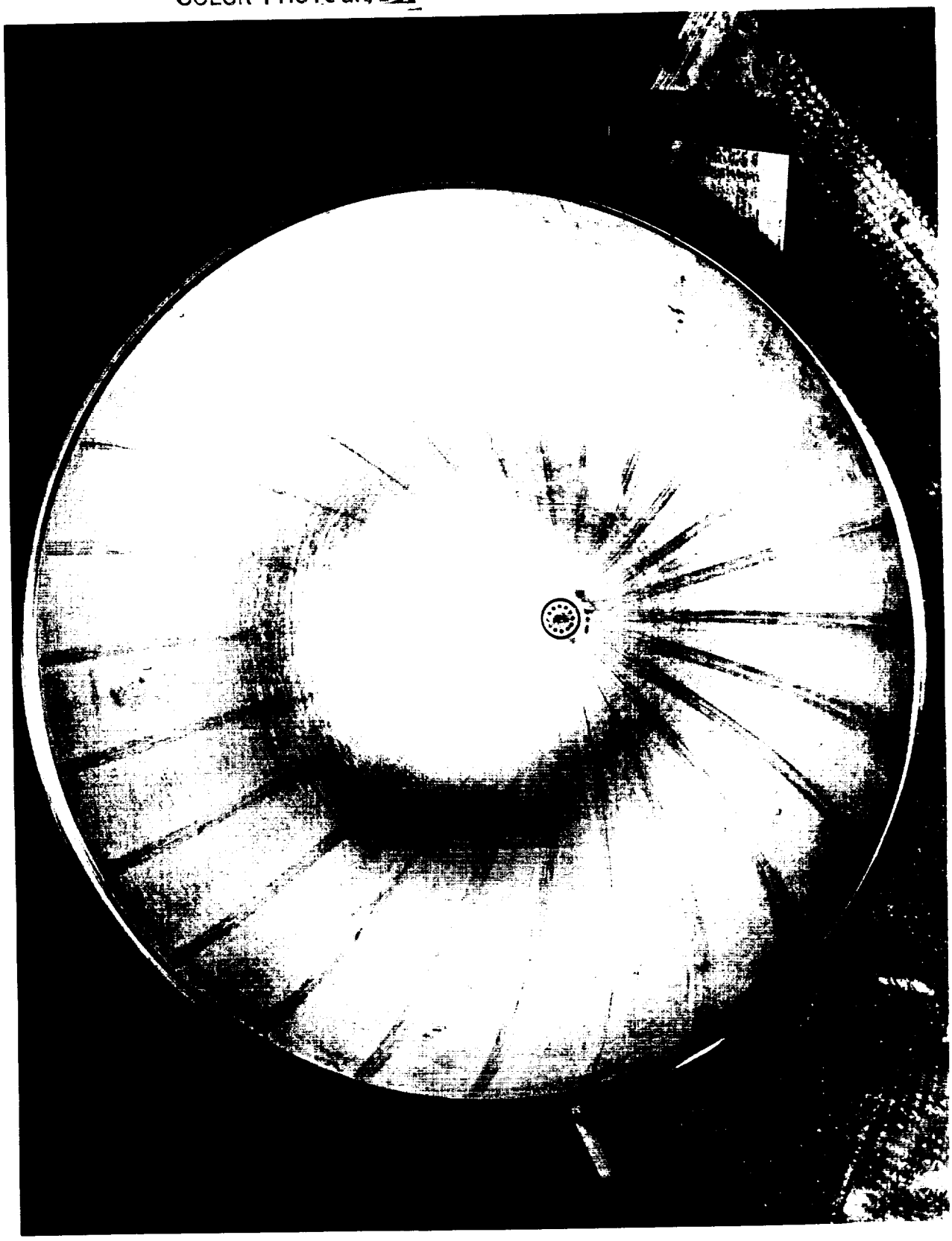

Figure H-19
Interior View of Metal Casing Fuel Side

Figure H-20
Interior View of Metal Casing Gas Side

ORIGINAL PAGE
COLOR PHOTOGRAPH

Figure H-21
Circumferential Butt Weld Start/Stop Point on Metal Casing

C-2

H-42

ORIGINAL PAGE
COLOR PHOTOGRAPH

Figure H-22
Deep Grind Marks on Gas Side of Metal Casing

ORIGINAL PAGE
COLOR PHOTOGRAPH

Figure H-23
Typical Interior Stains on Gas Side of Metal Casing

A-46 INTENTIONALLY

ORIGINAL PAGE
COLOR PHOTOGRAPH

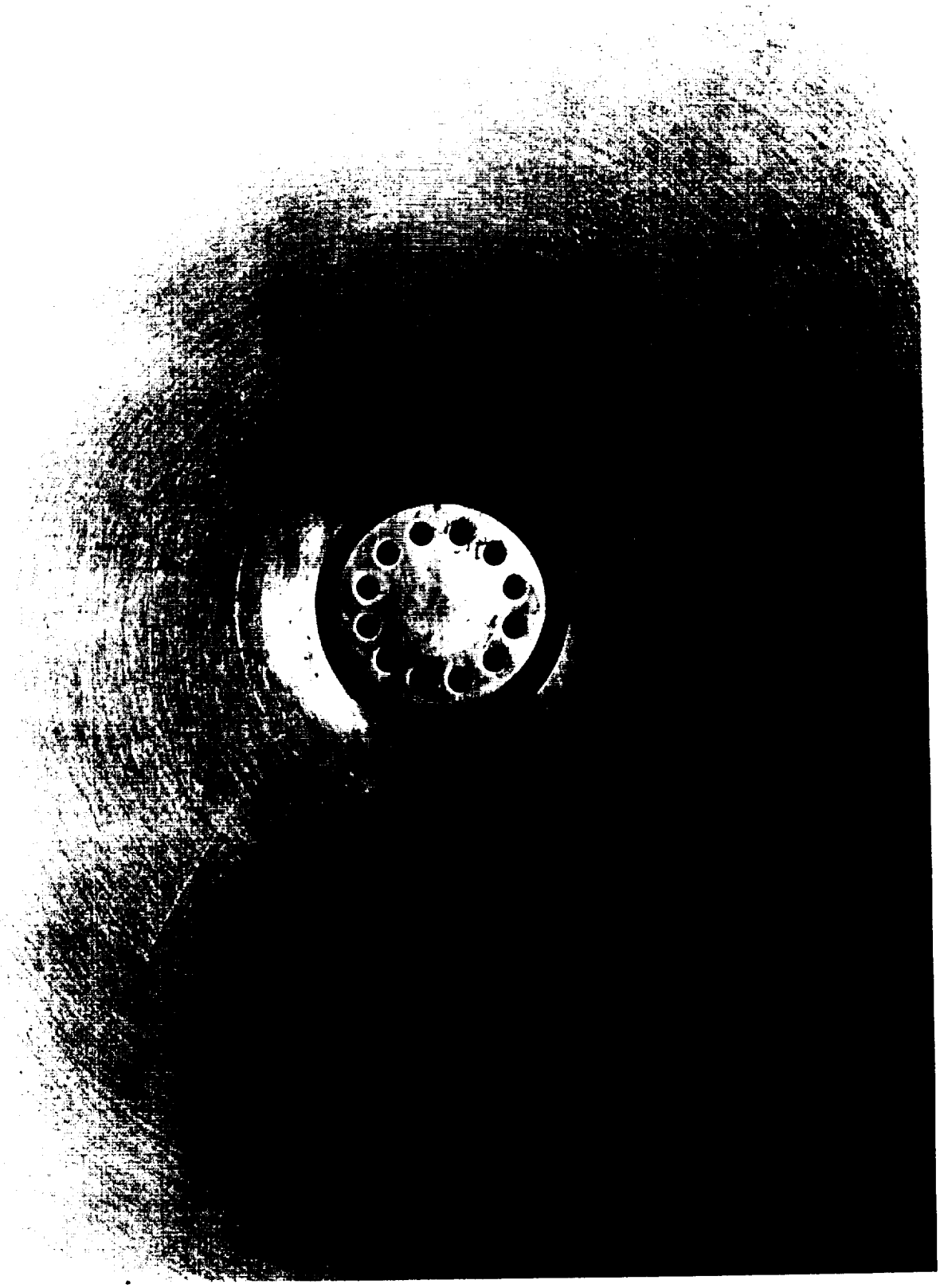

Figure H-24
Close-up of Gas Side Interior Inlet/Outlet of Metal Casing

H-48

ORIGINAL PAGE
COLOR PHOTOGRAPH

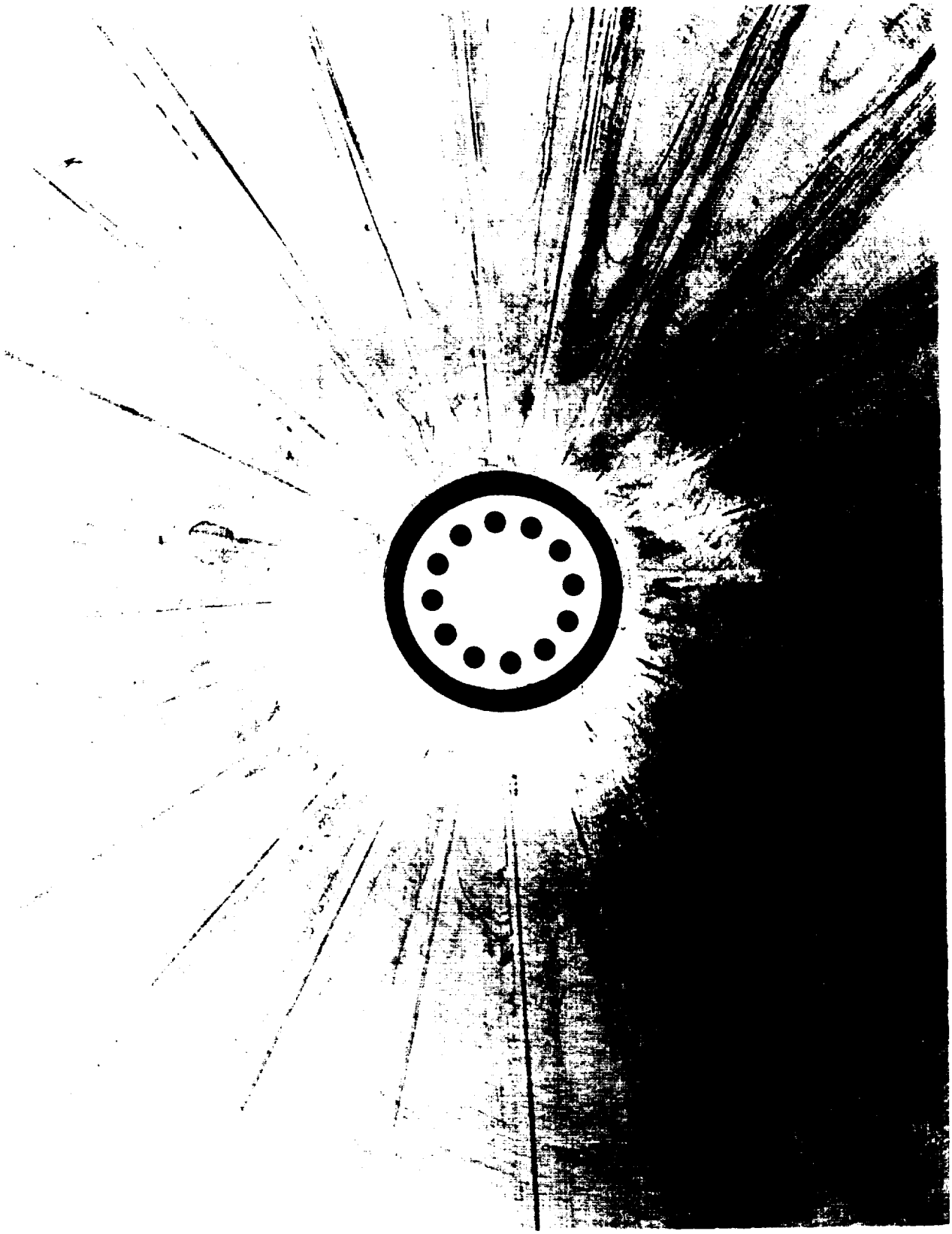

Figure H-25
Close-up of Fuel Side Interior Inlet/Outlet of Metal Casing

CV-1-346

ORIGINAL PAGE
COLOR PHOTOGRAPH

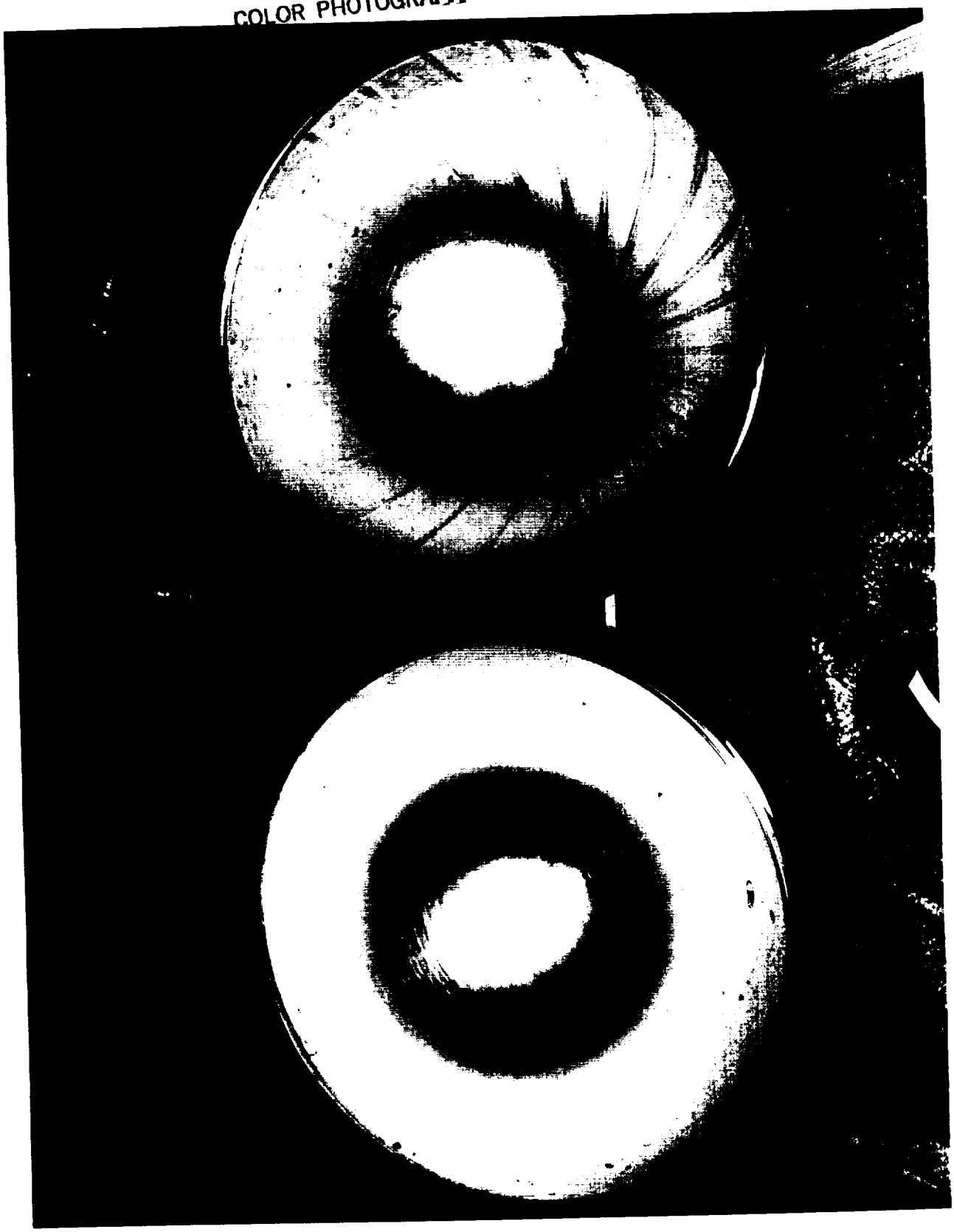

Figure H-26
Interior View of Metal Casing After Cutting

0592-1343

H-52 INTENTIONALLY

ORIGINAL PAGE
COLOR PHOTOGRAPH

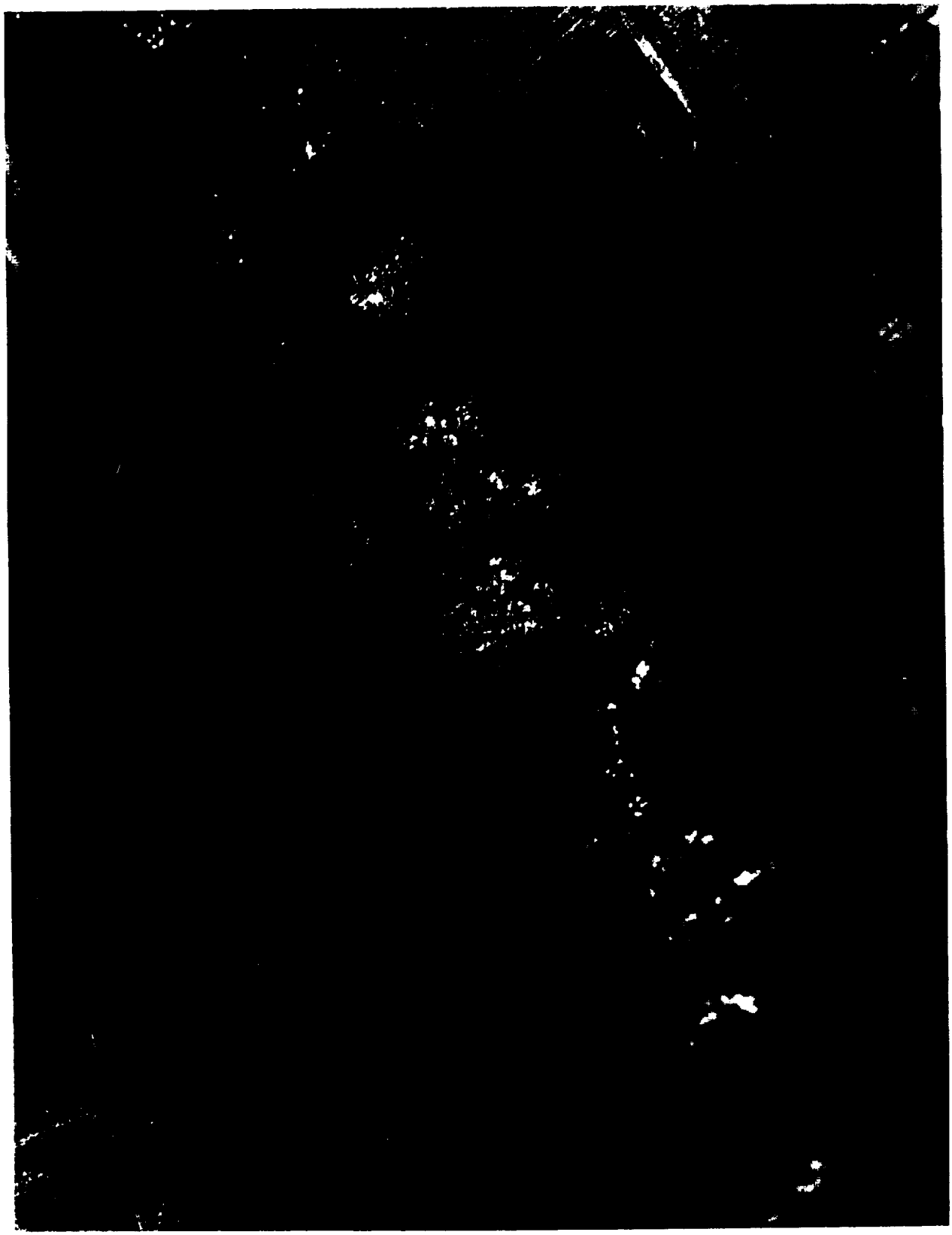

Figure II-27
Stained Area on Metal Casing
(Note Rib Marks)

U5Y6-1344

H-54

ORIGINAL PAGE
COLOR PHOTOGRAPH

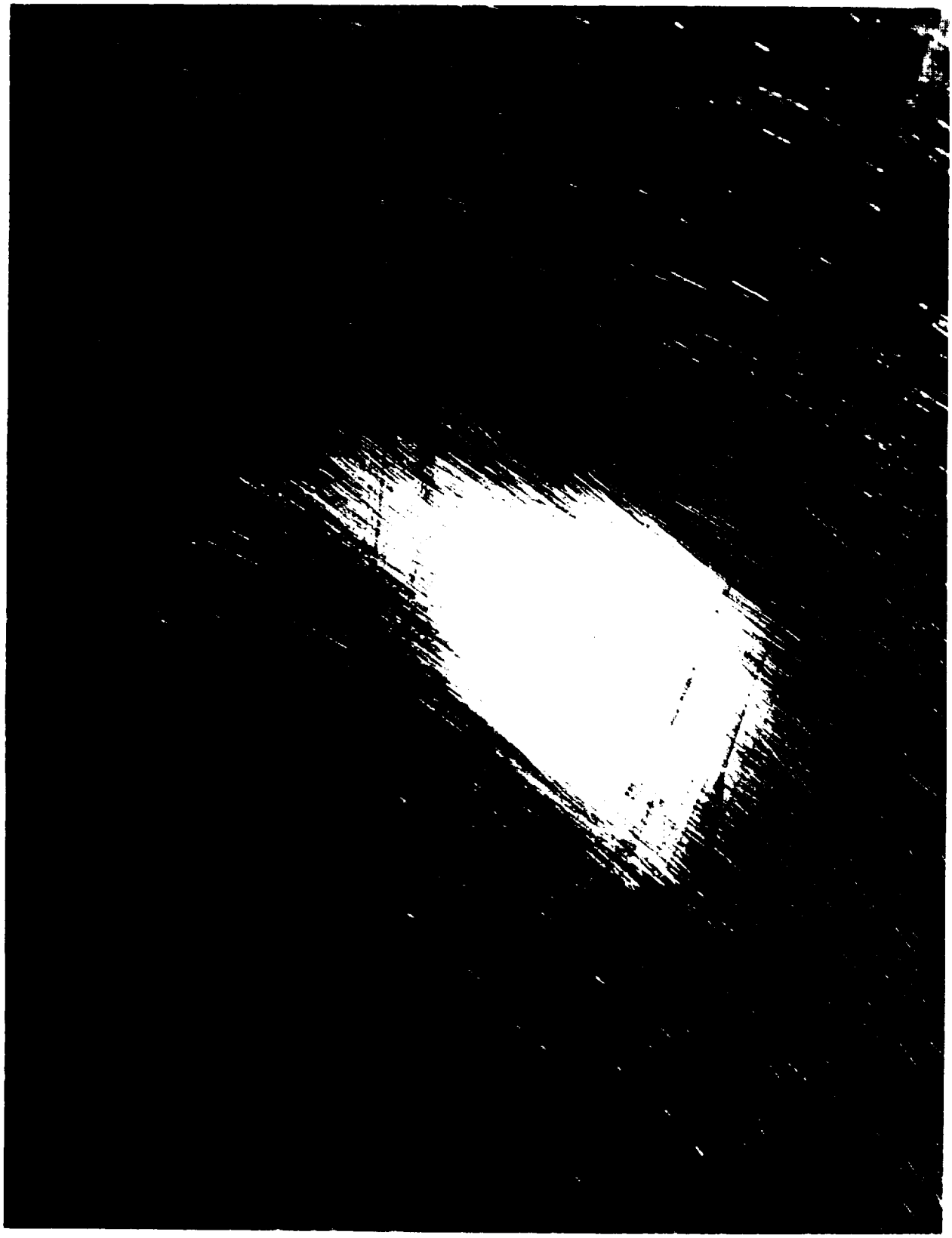

Figure H-28
Polish/Grind Marks on Metal Casing
(Note Rib Marks)

ORIGINAL PAGE
COLOR PHOTOGRAPH

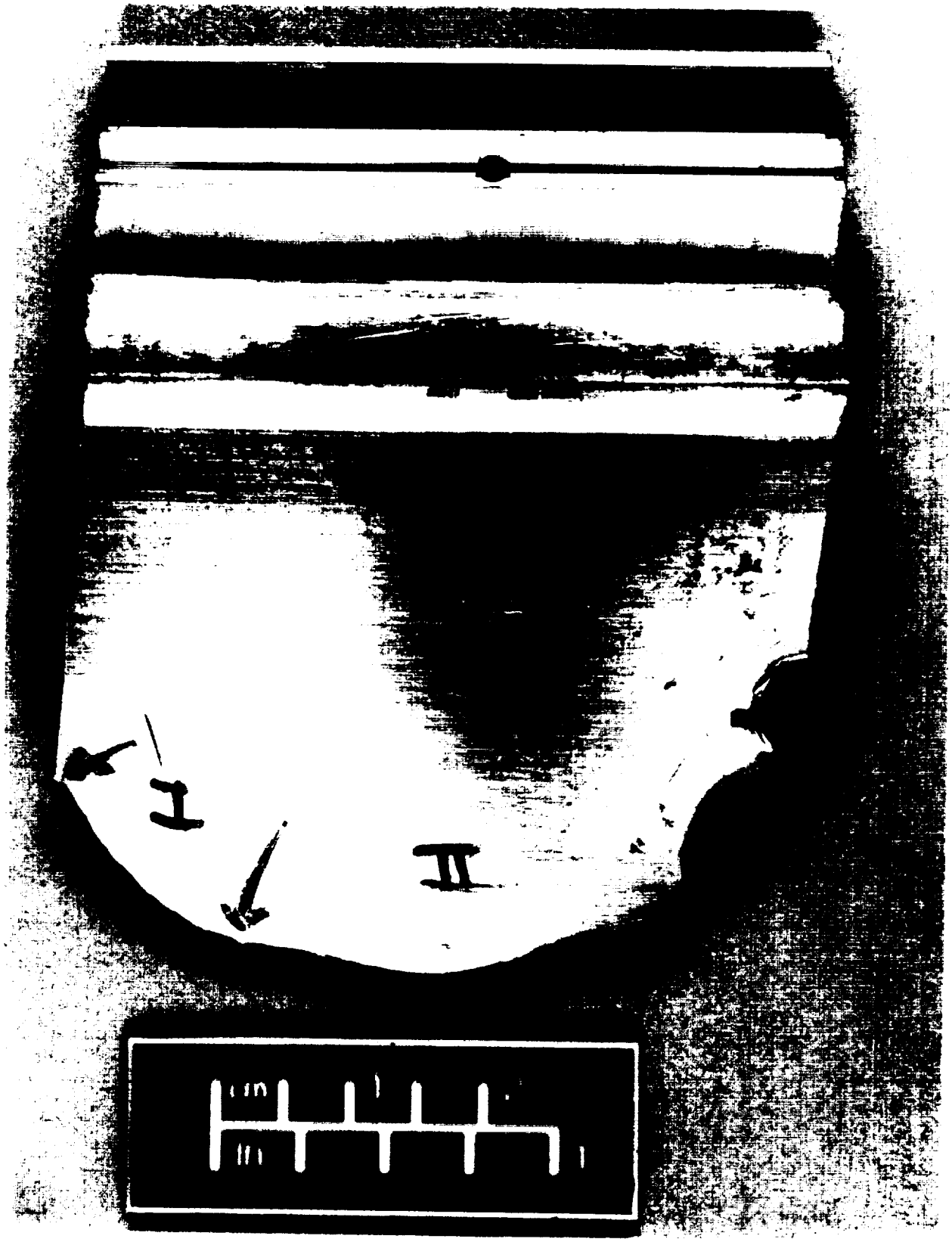

Figure II-29
180° Weld Sample, Gas Side of Metal Casing

ORIGINAL PAGE
COLOR PHOTOGRAPH

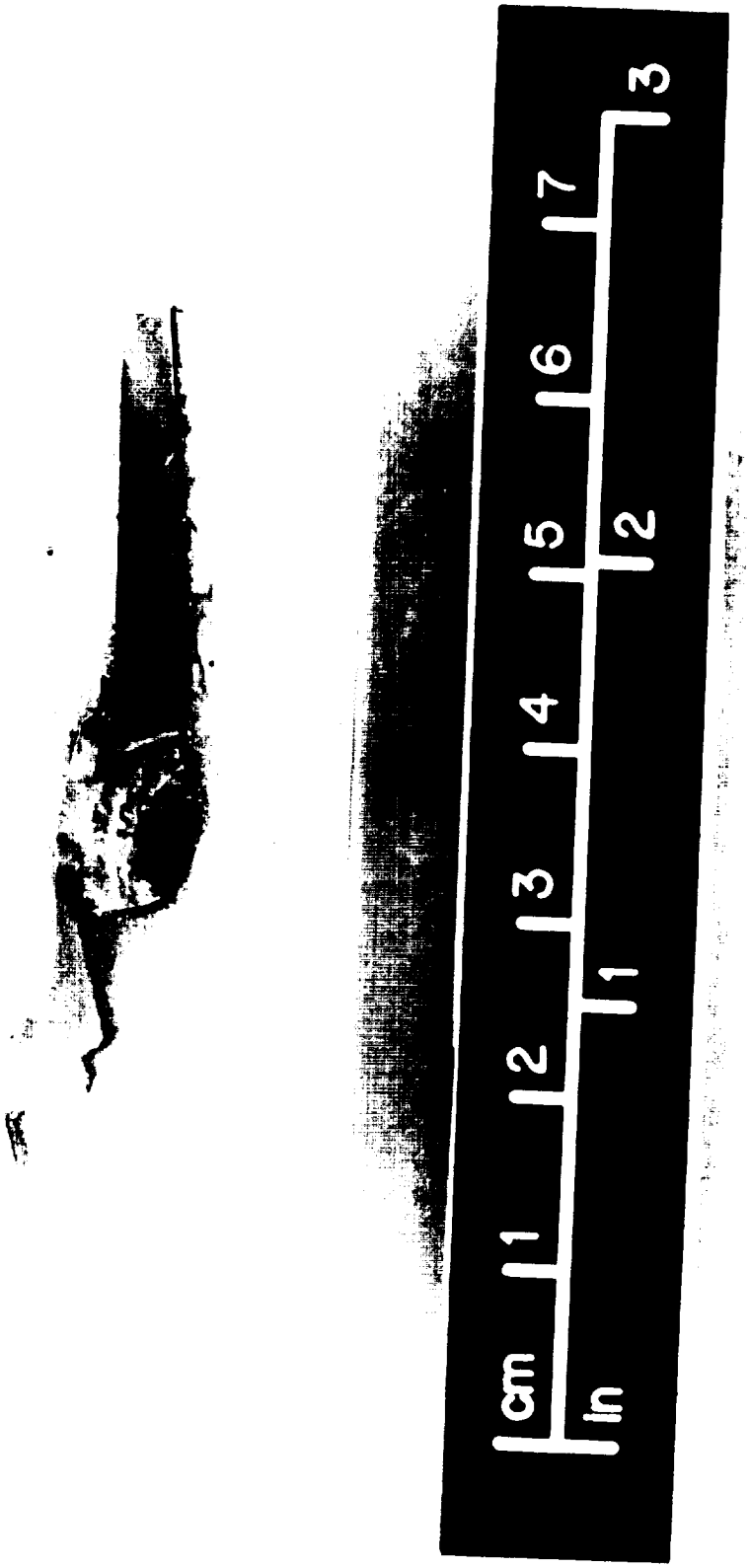

Figure H-30
Cross Section of Weld Start/Stop Point from Metal Casing

H-60 INTENTIONALLY

ORIGINAL PAGE
COLOR PHOTOGRAPH

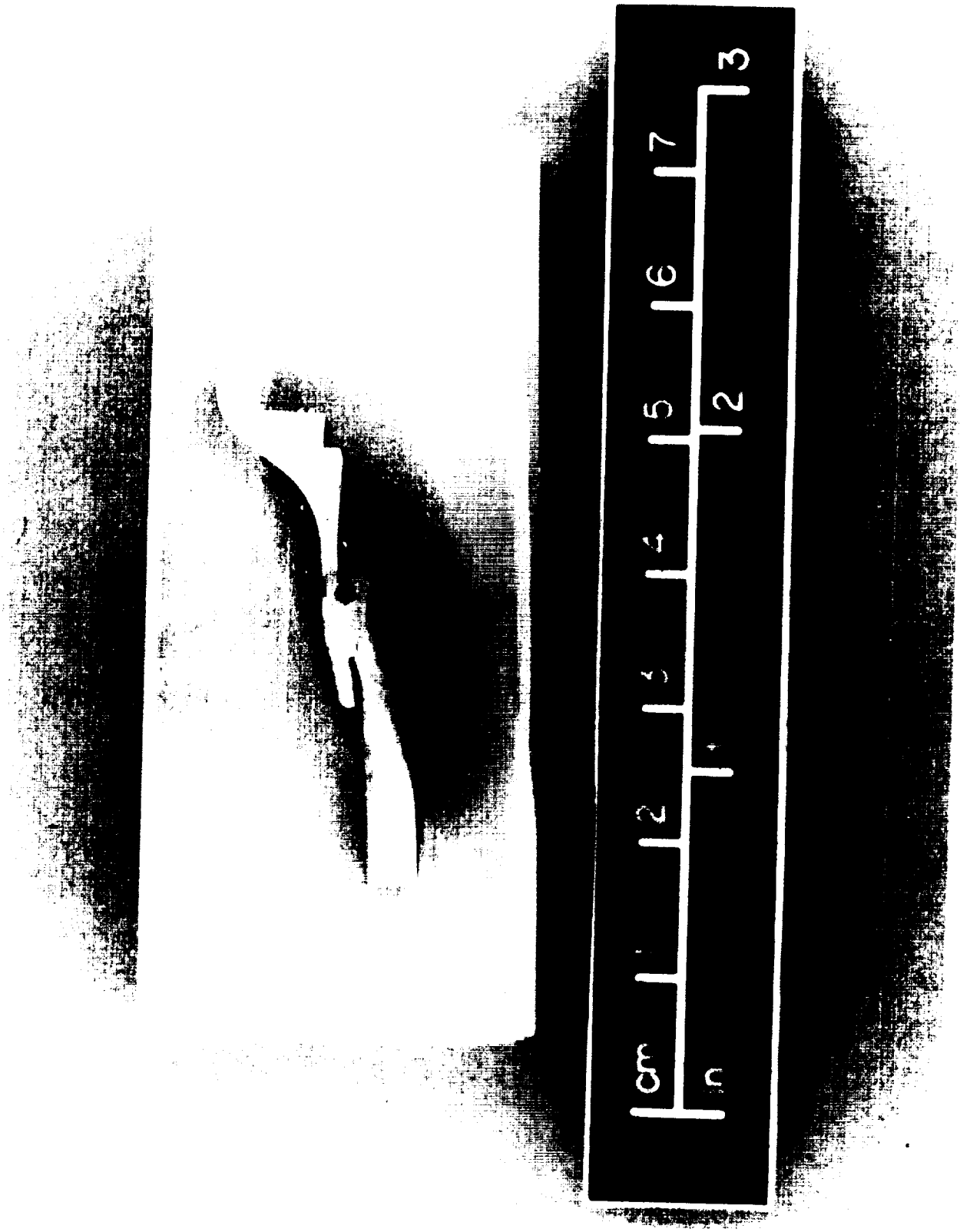

Figure H-31
Cross Section of 180° Weld Sample from Metal Casing

Distribution

Organization	No. of Copies
NASA Johnson Space Center	
Propulsion and Power Division	3
Materials Branch	2
Rockwell International	
Space Systems Division	3
NASA, White Sands Test Facility	
Laboratories Office	4
Lockheed-ESC White Sands Test Facility	
Laboratory Programs Section	2
Laboratory Services Section	1
Publications Office	2
Technical Library	3